AD NUMBER
AD006723
CLASSIFICATION CHANGES
TO: unclassified
FROM: confidential
LIMITATION CHANGES
TO: Approved for public release, distribution unlimited
FROM: Distribution authorized to U.S. Gov't. agencies and their contractors; Administrative/Operational Use; 13 APR 1953. Other requests shall be referred to National Aeronautics and Space Administration, Washington, DC.
AUTHORITY
NACA reclass notice no. 97 dtd 24 Feb 1956; NASA TR Server website

AD-

6723

CONFIDENTIAL

Copy 73

RM A53B06

NACA

RESEARCH MEMORANDUM

AN INVESTIGATION OF A FOUR-BLADE SINGLE-ROTATION PROPELLER IN COMBINATION WITH AN NACA 1-SERIES D-TYPE COWLING AT MACH NUMBERS UP TO 0.83

By Robert M. Reynolds, Robert I. Sammonds,
and George C. Kenyon

Ames Aeronautical Laboratory
Moffett Field, Calif.

NATIONAL ADVISORY COMMITTEE
FOR AERONAUTICS

WASHINGTON
April 13, 1953

NATIONAL ADVISORY COMMITTEE FOR AERONAUTICS

RESEARCH MEMORANDUM

AN INVESTIGATION OF A FOUR-BLADE SINGLE-ROTATION PROPELLER IN COMBINATION WITH AN NACA 1-SERIES D-TYPE COWLING AT MACH NUMBERS UP TO 0.83

By Robert M. Reynolds, Robert I. Sammonds,
and George C. Kenyon

SUMMARY

An investigation has been made of a four-blade single-rotation propeller in combination with an NACA 1-series D-type spinner-cowling combination at Mach numbers up to 0.83. Characteristics of the propeller operating in the presence of the cowling are compared with the characteristics of the propeller with the spinner. Pressure distributions on the surfaces of the cowling with the propeller operating are compared with the pressure distributions on the cowling with the propeller removed. The data were obtained at a Reynolds number of 1.5 million per foot based on the wind-tunnel datum velocity.

Variation of cowling inlet-velocity ratio and change in type of propeller-spinner juncture (ideal and platform) had no significant effects on the characteristics of the propeller operating in the presence of the cowling. The maximum apparent efficiency of the propeller with the spinner-cowling combination was higher, at all Mach numbers, than the efficiency of the propeller with the spinner.

With the propeller removed, the static-pressure distributions on the surfaces of the cowling were affected by compressibility and inlet-velocity ratio in a manner typical for the 1-series profile. For the design inlet-velocity ratio, the measured critical Mach number 0.79 was somewhat higher than the predicted critical Mach number.

Operation of the propeller resulted in more positive pressure coefficients on the external surface of the cowling, as compared with the distributions obtained with the propeller removed, at all inlet-velocity ratios and Mach numbers. The pressure distributions were unaffected, at least for the inlet-velocity ratios of these tests, by the change from ideal to platform propeller-spinner junctures.

INTRODUCTION

Current interest in the turbine-propeller type of power plant for moderately high-speed long-range airplanes has led to a need for data concerning the high-speed characteristics of propeller-spinner-cowling combinations suitable for use with large turbine engines. To provide data useful for design purposes, an investigation was undertaken in the Ames 12-foot pressure wind tunnel to determine the characteristics of a representative propeller-spinner-cowling combination, employing the NACA 4-(5)(05)-041 four-blade single-rotation propeller with the NACA 1-46.5-047 1-series spinner and the NACA 1-62.8-070 cowling. One phase of the investigation, the determination of the characteristics of the propeller-spinner combination in the absence of the cowling, has been reported in reference 1. A second phase of the investigation, the effects of propeller operation and propeller-spinner juncture on the pressure-recovery characteristics of the propeller-spinner-cowling combination, has been reported in reference 2.

Presented herein are the force-test results for the propeller operating in the presence of the spinner-cowling combination, obtained concurrently with the data presented in reference 2. A comparison is made of the results obtained with the propeller operating in the presence of the cowling with the results presented in reference 1. The static pressures measured on the surfaces of the cowling, with the propeller removed and with the propeller operating, are included.

The tests were made with the propeller-spinner-cowling combination at an angle of attack of 0° for propeller blade angles from 40° to 60°, for inlet-velocity ratios from 0.26 to 1.33, and at Mach numbers from 0.20 to 0.83. The Reynolds number was constant at 1.5 million per foot throughout the tests.

SYMBOLS

a	speed of sound, ft/sec
b	blade width, ft
c_{l_d}	blade section design lift coefficient
C_{P_a}	apparent propeller power coefficient, $\frac{P_a}{\rho n^3 D^5}$
C_{T_a}	apparent propeller thrust coefficient, $\frac{T_a}{\rho n^2 D^4}$

D	propeller diameter, ft
$\frac{b}{D}$	blade width ratio
h	maximum thickness of blade section, ft
$\frac{h}{b}$	blade thickness ratio
J	advance-diameter ratio, $\frac{V_o}{nD}$
M_{cr}	critical Mach number, the free-stream Mach number at which sonic velocity is first attained on the external surface of the cowl
M_d	datum Mach number, $\frac{V}{a}$
M_t	tip Mach number, $M_d\sqrt{1+\left(\frac{\pi}{J}\right)^2}$
n	propeller rotational speed, rps
P	pressure coefficient, $\frac{p-p_o}{q_o}$
P_a	apparent power applied to propeller, ft-lb/sec
P_{cr}	critical pressure coefficient, corresponding to local Mach number of 1.0
p	static pressure, lb/sq ft
q	dynamic pressure, $\frac{\rho V^2}{2}$, lb/sq ft
R	propeller tip radius, ft
r	blade-section radius, ft
T_a	apparent thrust of the propeller-spinner combination in the presence of the cowling, corrected for the drag of the spinner (also in the presence of the cowling), lb
T_{c_a}	apparent propeller thrust coefficient, $\frac{T_a}{\rho V^2 D^2}$
T_s	drag of the spinner expressed as thrust
T_{c_s}	spinner thrust coefficient, $\frac{T_s}{\rho V^2 D^2}$

V datum velocity (wind-tunnel air-stream velocity corrected for solid blockage of cowling but uncorrected for wind-tunnel-wall constraint on the propeller slipstream), ft/sec

V_o equivalent free-air velocity (datum velocity corrected for wind-tunnel-wall constraint on the propeller slipstream), ft/sec

$\frac{V_1}{V}$ inlet-velocity ratio

X total length along the longitudinal axis of any component of the model, such as the cowl, spinner, or inner lip, in.

x distance along the longitudinal axis from any reference, such as the leading edge of the cowl, spinner, or inner lip, in.

β propeller blade angle at 0.75R, deg

β_d design propeller section blade angle, deg

η_a apparent propeller efficiency, $\frac{T_a V_o}{P_a}$ or $\frac{C_{T_a}}{C_{P_a}} J$

ρ mass density of air, slugs/cu ft

Subscripts

o free stream

1 location of rake in cowling inlet

c cowling

i cowling inner lip

max maximum

APPARATUS AND TESTS

A photograph of the propeller-spinner-cowling model on the 1000-horsepower propeller dynamometer is shown in figure 1. A sketch of the general arrangement of the model is presented in figure 2. The design criteria for the propeller, resulting in the blade-form curves shown in figure 3, are given in reference 1. A complete description of the

dynamometer, including typical results of calibrations of the thrust gages and torquemeter, is also given in reference 1. The design information and coordinates for the spinner-cowling combination are given in reference 2. The ideal and platform propeller-spinner junctures, shown in figures 4 and 5, are also described in reference 2.

The cowling model contained 28 flush static-pressure orifices located with respect to the leading edge of the cowl as listed below:

External surface, in.					Inner-lip surface, in.
0	0.59	1.96	5.88	10.80	0.10
.10	.78	2.45	6.86	11.80	.20
.20	.98	2.94	7.84	12.80	.29
.29	1.18	3.92	8.82	13.80	.39
.39	1.57	4.90	9.80	14.80	----

The static- and total-pressure rakes used to measure the flow characteristics in the inlet are described in reference 2.

Tests were made of the spinner-cowling combination with the propeller removed and with the propeller installed. With the propeller removed, static pressures on the external and inner-lip surfaces of the cowl were measured concurrently with the pressure-recovery surveys reported in reference 2. These tests, made at inlet-velocity ratios ranging from 0.26 to 1.33 and for Mach numbers from 0.20 to 0.83, were repeated with the spinner-cowling combination located 2 feet upstream of its normal position on the dynamometer, as shown in figure 6. With the propeller installed, measurements of the propeller thrust, torque, and rotational speed, and static pressures on the external and inner-lip surfaces of the cowl were made concurrently with the pressure-recovery surveys reported in reference 2. These tests were made at the conditions tabulated below:

Datum Mach number, M_d	Propeller blade angle, deg, β	Juncture type	Inlet-velocity ratio, V_1/V	Advance-diameter ratio, J
0.83	60	Ideal	0.31 to 1.00	3.15 to 4.15
.79	60		.31 to 1.02	3.14 to 4.30
.69	60		.31 to 1.10	3.06 to 4.36
.59	60		.42 to 1.27	2.93 to 4.50
.59	50		.39 to 1.29	2.44 to 2.95
.39	50		.39 to 1.28	2.00 to 3.05
.39	40		.37 to 1.26	1.67 to 2.10
.30	40		.36 to 1.26	1.50 to 2.12
.20	40		.37 to 1.24	1.30 to 2.10
.83	60	Platform	.30 to .84	3.13 to 4.16
.79	60		.27 to .80	3.15 to 4.24
.69	60		.30 to .83	3.04 to 4.42
.59	60		.32 to .81	2.95 to 4.44
.59	50		.37 to 1.27	2.36 to 2.96
.39	50		.39 to 1.27	2.06 to 3.00
.39	40		.38 to 1.28	1.68 to 2.10
.30	40		.35 to 1.26	1.50 to 2.15
.20	40		.40 to 1.24	1.30 to 2.10

The range of operation of the propeller was limited by the same factors discussed in reference 1.

All tests were conducted with the model at an angle of attack of 0° and at a Reynolds number of 1.5 million per foot, based on the datum velocity.

REDUCTION OF DATA

Datum Mach Number and Velocity

The datum Mach number was taken as the average Mach number over the propeller disc area (propeller and cowling removed, and extended cylindrical spinner installed), as determined from the air-stream-velocity surveys reported in reference 1. For the tests reported herein, the datum Mach number (and the corresponding dynamic pressure) was corrected for the solid-blockage effects of the cowling. The magnitude of these solid-blockage corrections, estimated by the method of reference 3, was less than 1 percent of the uncorrected Mach number (or uncorrected dynamic pressure). The datum Mach number was not corrected for the

wind-tunnel-wall constraint on the propeller slipstream. The free-air Mach number can be obtained by applying the tunnel-wall corrections (fig. 7) to the datum Mach number. At Mach numbers above 0.59, the correction amounts to less than 1 percent. In the exact use of the data, however, the datum Mach number should be corrected to the free-air Mach number wherever small changes in Mach number produce large changes in the results.

The air-stream velocity (and, consequently, the propeller advance-diameter ratio and efficiency) was corrected for the effects of both solid blockage due to the cowling and the wind-tunnel-wall constraint on the propeller slipstream. The ratio of the free-air velocity to the datum velocity, computed by the method of reference 4, is shown in figure 7. This velocity ratio is the same ratio used in reference 1.

Propeller Thrust and Torque

The propeller thrust as used herein is the algebraic difference between the resultant longitudinal force on the propeller-spinner combination operating in the presence of the cowling and the resultant longitudinal force acting on the spinner (in the presence of the cowling) at the same datum Mach number, Reynolds number, and inlet-velocity ratio.

The longitudinal force on the spinner and the thrust forces due to pressures acting between the floating and fixed members of the dynamometer were measured and treated in the same manner as reported in reference 1. It may be noted here that the resultant longitudinal force acting on the spinner in the presence of the cowling (both with and without the propeller) was adjusted for computational purposes to correspond to a spinner base pressure equal to the static pressure of the free stream. This procedure, the same as employed for the data of reference 1, determined the magnitude of the spinner drag but had no influence on the propeller thrust. The longitudinal force on the spinner in the presence of the cowling, with the spinner base pressure equal to the free-stream static pressure, varied between 3.7 and 31.3 pounds, depending on datum Mach number and inlet-velocity ratio. These forces, reduced to thrust-coefficient form for computational purposes, are shown in figure 8.

The propeller torque was obtained in the same manner as reported in reference 1, using the same variation of the torquemeter calibration constant with rotational speed.

Cowling Pressure Distributions

The results of surveys made to determine the local stream Mach numbers in the vicinity of the dynamometer, without the cowling installed, were reported in reference 1. These data indicated the presence (at radii up to 30 inches from the dynamometer center line) of adverse longitudinal pressure gradients in the region where the cowling was to be located. It was noted in reference 1 that calculations had shown these gradients to be due to the presence of the dynamometer body downstream of the propeller station. It was realized that the flow measured during these surveys would be altered by the introduction of the cowling, and it was anticipated that the dynamometer body aft of the cowling might also affect the flow in the vicinity of the cowl. In order to determine the magnitude of this effect, tests were made with the spinner-cowling combination located 2 feet upstream of its normal position on the dynamometer, as shown in figure 6. Typical differences (ΔP) between the pressure coefficients measured on the external surface of the cowling with the cowling in its normal position (fig. 9(a)) and in the forward position (fig. 9(b)) are shown in figure 9(c). For all subsequent tests of the spinner-cowling combination, both with the propeller removed and with the propeller operating, pressures on the cowling were corrected by the amount of these increments.

Accuracy of Results

As in reference 1, analysis of the accuracy of the separate measurements of thrust, torque, and air-stream velocity indicates that errors in the propeller efficiencies reported herein are probably less than 2 percent, but could be as large as 4 percent if a maximum error in the indicated torque is assumed as a possibility from the torquemeter calibration data.

RESULTS AND DISCUSSION

Propeller Characteristics

The characteristics of the propeller operating in the presence of the spinner-cowling combination are shown in figures 10 and 11 for the ideal and for the platform propeller-spinner junctures, respectively. These data are presented as apparent values, in accord with the discussion in reference 5, since the thrust and torque were measured for the propeller while operating in the presence of the cowling, and no

allowance was made for the increase in drag of the cowling and dynamometer parts within the influence of the propeller slipstream.

Typical effects of cowling inlet-velocity ratio on the characteristics of the propeller are shown in figures 12 and 13. While the measured thrust coefficients and maximum efficiency generally increased with increasing inlet-velocity ratio (for constant advance-diameter ratio), the changes do not appear to be particularly significant in view of the stated accuracy of the results and the scatter in the η_{max} values evident in figures 10 and 11.

As shown in figures 12 and 13, there was little difference between the characteristics of the propeller with ideal and platform junctures. This would be expected in view of the fact that the portion of the blade devoted to the junctures constitutes such a small fraction of the disc area and is designed to operate at near-zero thrust loadings.

Figure 14 presents a comparison of the maximum apparent efficiency of the propeller operating in the presence of the spinner-cowling combination with the maximum efficiency (from ref. 1) of the propeller in combination with the spinner. The maximum apparent efficiency of the propeller with the spinner-cowling combination was higher, at all test Mach numbers, than the efficiency of the propeller in combination with the spinner. At datum Mach numbers of 0.20 (β,40°) and 0.83 (β,60°), the maximum apparent efficiency of the propeller with the spinner-cowling combination was about 0.91 and 0.75, respectively, as compared to maximum efficiencies of about 0.86 and 0.55, respectively, for the propeller in combination with the spinner. This trend would be expected, considering the reduction in air-stream velocities in the region of the propeller resulting from the interference effects of the cowling. At a given free-stream Mach number and rotational speed, this reduction in velocity results in an increase of both propeller thrust and torque. Since the useful work done by the propeller is defined as the product of the thrust and the free-stream velocity, the apparent efficiency of the propeller will be increased when it is operating in the region of reduced velocity ahead of the cowl. That the apparent efficiency of a propeller operating in the presence of a body will be greater than the efficiency of the isolated propeller (for equal advance-diameter ratios) has long been recognized, and the reasons noted for this behavior have been discussed in many works, such as references 5 and 6.

A word of caution is in order regarding indiscriminate use of the spinner thrust coefficients presented in figure 8 in calculating the thrust and efficiency of the propeller-spinner combination in the presence of the cowling. The method used in treating the spinner-drag term was dictated by the dynamometer configuration, which, because of the pressure-seal arrangement (ref. 1), required that some reference pressure be assumed to act on the base of the spinner in order to obtain

a value for the spinner-drag tare. The choice of any particular reference pressure would have served equally well as far as the propeller thrust was concerned since, in applying the spinner-drag correction to the apparent thrust, the reference pressure appears in both terms but of opposite sign and, hence, is eliminated. Free-stream static pressure was assumed as the spinner base pressure primarily for computational convenience. However, it should be stressed that any efficiencies computed for the propeller-spinner combination, with the spinner base pressure assumed to be equal to the free-stream static pressure, would be purely ficticious and of no practical significance for an actual airplane installation.

It may be mentioned that, even though the propeller thrust has been corrected for the drag of the spinner, the interference effects of the spinner on the characteristics of the propeller in combination with the spinner and cowling have not been eliminated from these data.

Spinner-Cowling Characteristics

Spinner-cowling combination with propeller removed.- The effects of compressibility and variation of inlet-velocity ratio on the static-pressure distributions on the external and inner-lip surfaces of the cowling with the propeller removed are shown in figures 15 to 19. These data show the same general characteristics as reported for other inlets employing the 1-series coordinates, references 7 to 9 for example.

The effect of inlet-velocity ratio on the critical Mach number of the spinner-cowling combination is shown in figure 20. At the design inlet-velocity ratio of 0.42, the measured critical Mach number 0.79 was somewhat higher than the predicted critical Mach number 0.75 (ref. 7).

Spinner-cowling combination with propeller operating.- For the propeller with ideal and platform junctures, the effects of compressibility and variation of inlet-velocity ratio on the static-pressure distributions on the external and inner-lip surfaces of the cowling with the propeller operating are shown in figures 21 to 26. Again, these data show characteristics typical for the 1-series profile. Study of these figures and additional cross plots of the pressure distributions as a function of inlet-velocity ratio indicates that operation of the propeller resulted in more positive pressure coefficients on the external surface of the cowling at all inlet-velocity ratios and Mach numbers, as compared with the distributions obtained with the propeller removed. The pressure distributions were unaffected, at least for the inlet-velocity ratios of these tests, by the change from ideal to platform propeller-spinner junctures.

Apparent Efficiency With Allowance for the Increase in Pressure Drag of the Cowling Due to Operation of the Propeller

In the discussion of propeller-body interference in references 5 and 6, it is noted that when a propeller is located such that its operation causes an increase in the drag of a body behind it, the thrust available for propulsion is not simply the apparent thrust of the propeller in the presence of the body, but rather this apparent thrust less the increase in drag of the body due to operation of the propeller. In the tests reported herein it was not possible to determine the increase in drag of the dynamometer and cowling parts within the influence of the propeller slipstream, except for one term, namely, the increase in pressure drag of the cowling. In order to gain some idea as to the magnitude of this term and its influence on the apparent efficiency of the propeller, integrations of the pressure distributions over the cowling surface were made for the cowling with the propeller removed (M_d, 0.79) and with the propeller operating (β, 60°; M_d, 0.79; J, 3.60). Pressure-drag coefficients were calculated from the relationship

$$C_D = \frac{\pi}{144\ S} \int_{(4.320)^2}^{(7.000)^2} P\ dr^2$$

where S is the maximum frontal area (sq ft) of the cowling. The difference between the pressure drag of the cowling, propeller removed, and the pressure drag of the cowling, propeller operating, was obtained as

$$\Delta D = q_o S \left(C_{D_{\substack{\text{propeller} \\ \text{operating}}}} - C_{D_{\substack{\text{propeller} \\ \text{removed}}}} \right)$$

where the cowling pressure-drag coefficients, propeller removed, corresponded to the Mach number and inlet-velocity ratios for the cowling with the propeller operating. The difference in cowling pressure drag was then subtracted from the measured apparent propeller thrust, and the apparent efficiency of the propeller was recomputed as $\eta_{(T_a-\Delta D)_{max}}$. Results of these calculations, for a range of inlet-velocity ratios at approximately design Mach number and blade angle, are shown in figure 27. For this particular Mach number and blade angle, the difference in the two efficiencies was about 0.05.

CONCLUSIONS

An investigation of an NACA 4-(5)(05)-041 four-blade single-rotation propeller in combination with an NACA 1-46.5-047 spinner and an NACA 1-62.8-070 D-type cowling at Mach numbers up to 0.83 indicated the following results:

1. Variation of cowling inlet-velocity ratio and change in propeller-spinner junctures had no significant effects on the characteristics of the propeller operating in the presence of the cowling.

2. The maximum apparent efficiency of the propeller with the spinner-cowling combination was higher, at all test Mach numbers, than the efficiency of the propeller with the spinner. At Mach numbers of 0.20 and 0.83, the maximum apparent efficiency of the propeller with the spinner-cowling combination was about 0.91 and 0.75, respectively, as compared to maximum efficiencies of about 0.86 and 0.55, respectively, for the propeller with the spinner.

3. For the range of inlet-velocity ratios, at a Mach number of 0.79, there was a difference of about 0.05 between the maximum apparent efficiency of the propeller based on the apparent propeller thrust and the efficiency based on the apparent thrust less the increase in pressure drag of the cowling due to operation of the propeller.

4. With the propeller removed, the static-pressure distributions on the surfaces of the cowling were affected by compressibility and variation of inlet-velocity ratio in a manner typical for the 1-series profile. At the design inlet-velocity ratio of 0.42, the measured critical Mach number 0.79 was somewhat higher than the predicted critical Mach number 0.75.

5. Operation of the propeller resulted in more positive pressure coefficients on the external surfaces of the cowling, as compared with the distributions obtained with the propeller removed, at all inlet-velocity ratios and Mach numbers.

6. The pressure distributions were unaffected, at least for the inlet-velocity ratios of these tests, by the change from ideal to platform propeller-spinner junctures.

Ames Aeronautical Laboratory
National Advisory Committee for Aeronautics
Moffett Field, Calif.

REFERENCES

1. Reynolds, Robert M., Buell, Donald A., and Walker, John H.: Investigation of an NACA 4-(5)(05)-041 Four-Blade Propeller With Several Spinners at Mach Numbers Up to 0.90. NACA RM A52I19a, 1952.

2. Sammonds, Robert I., and Molk, Ashley J.: Effects of Propeller-Spinner Juncture on the Pressure-Recovery Characteristics of an NACA 1-Series D-Type Cowl in Combination With a Four-Blade Single-Rotation Propeller at Mach Numbers Up to 0.83 and at an Angle of Attack of 0°. NACA RM A52D01a, 1952.

3. Herriot, John G.: Blockage Corrections for Three-Dimensional-Flow Closed-Throat Wind Tunnels, With Consideration of the Effect of Compressibility. NACA Rep. 995, 1950. (Supersedes NACA RM A7B28)

4. Young, A. D.: Note on the Application of the Linear Perturbation Theory to Determine the Effect of Compressibility on the Wind Tunnel Constraint On a Propeller. RAE TN No. Aero 1539, British, 1944.

5. Glauert, H.: Airplane Propellers. Body and Wing Interference. Vol. IV, div. L, ch. VIII of Aerodynamic Theory, W. F. Durand, ed., Julius Springer (Berlin), 1935. (CIT reprint 1943)

6. Weick, Fred E.: Aircraft Propeller Design. McGraw-Hill Book Co., Inc., 1930.

7. Nichols, Mark R., and Keith, Arvid L., Jr.: Investigation of a Systematic Group of NACA 1-Series Cowlings With and Without Spinners. NACA Rep. 950, 1949. (Supersedes NACA RM L8A15)

8. Boswinkle, Robert W., Jr., and Keith, Arvid L., Jr.: Surface-Pressure Distributions on a Systematic Group of NACA 1-Series Cowlings With and Without Spinners. NACA RM L8I24, 1948.

9. Reynolds, Robert M., and Sammonds, Robert I.: Subsonic Mach and Reynolds Number Effects on the Surface Pressures, Gap Flow, Pressure Recovery, and Drag of a Nonrotating NACA 1-Series E-Type Cowling at an Angle of Attack of 0°. NACA RM A51E03, 1951.

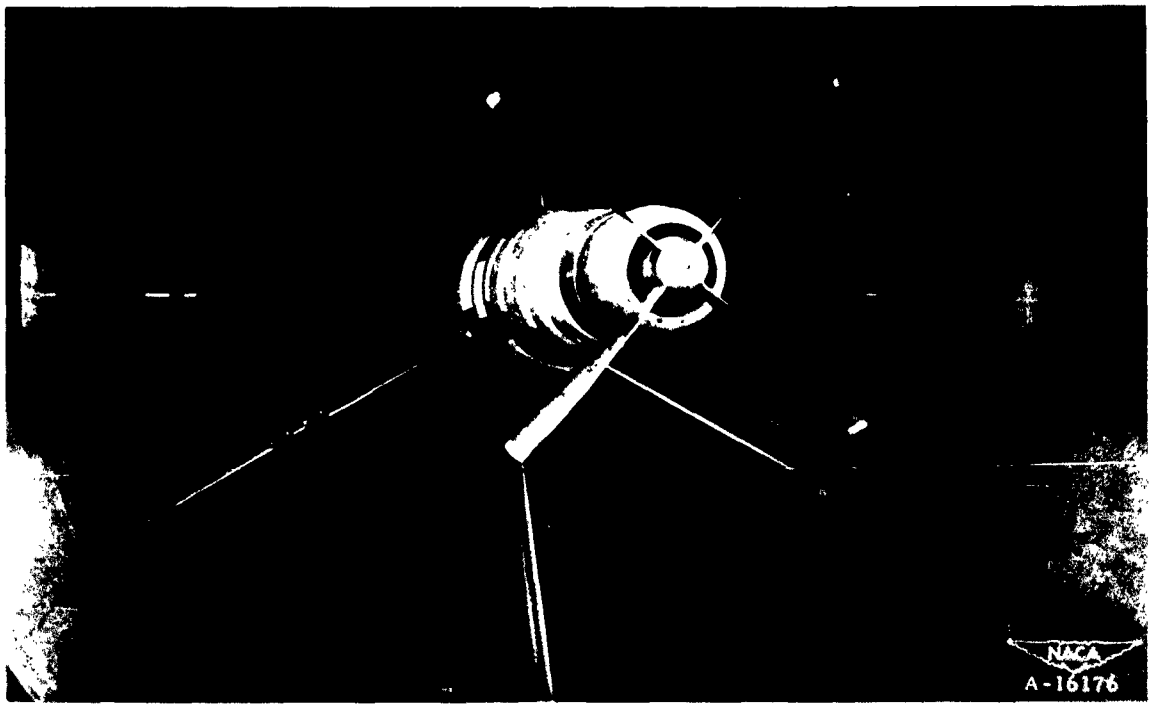

Figure 1.- The model mounted on the 1000-horsepower propeller dynamometer in the 12-foot pressure wind tunnel.

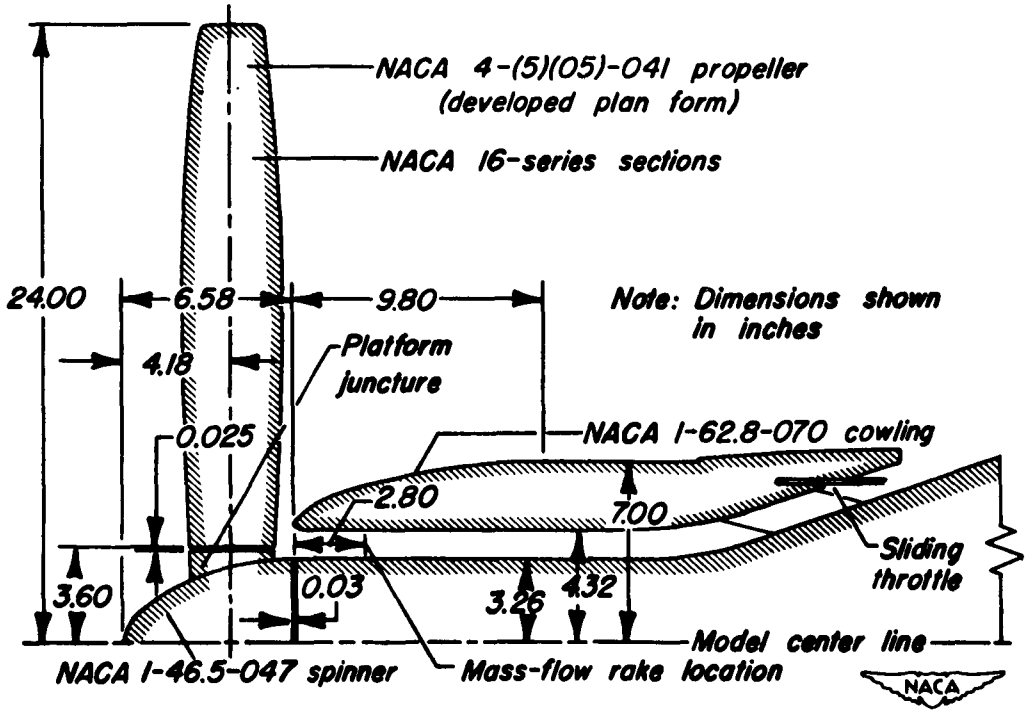

Figure 2.- Model arrangement.

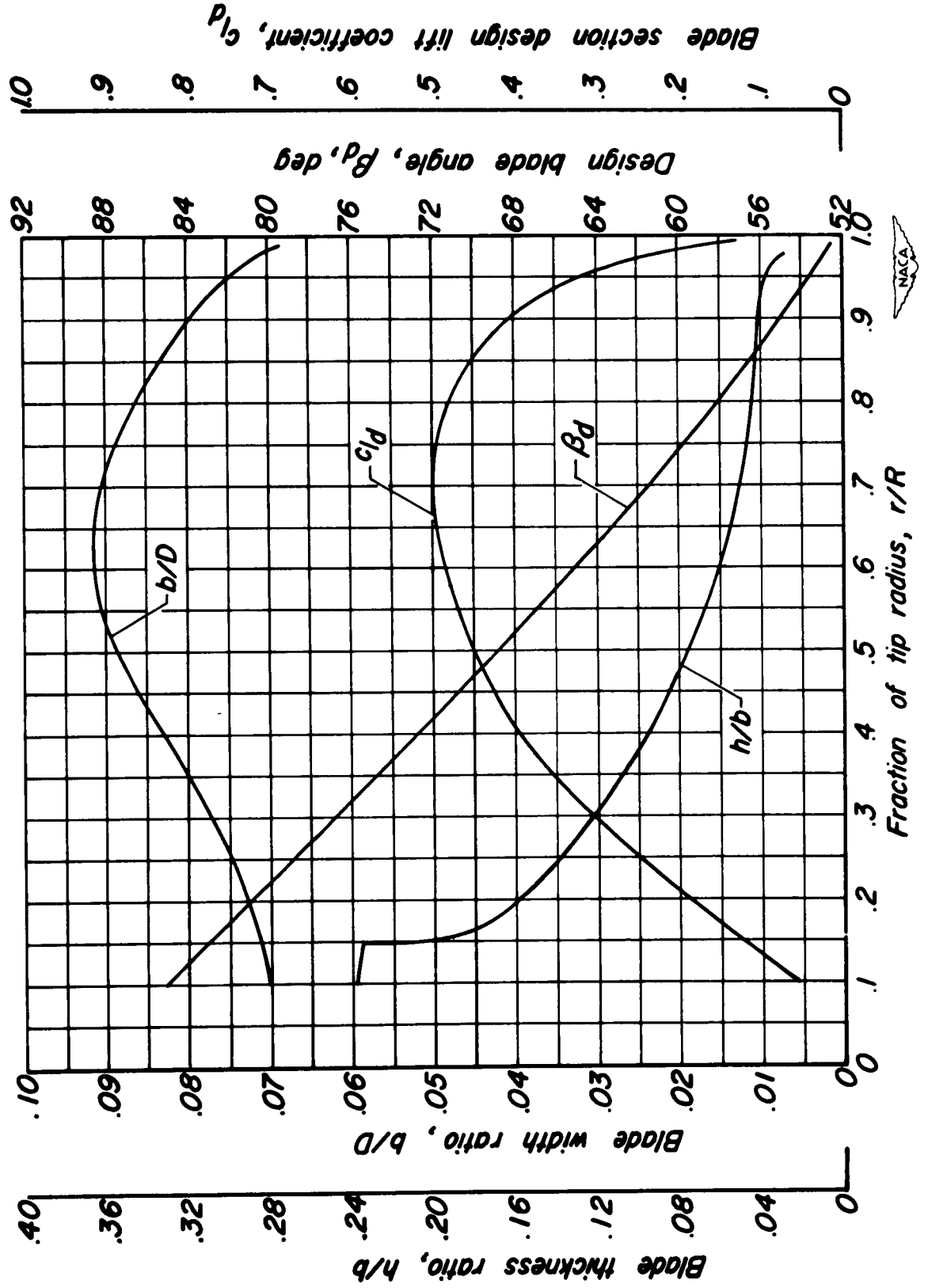

Figure 3.- Plan-form and blade-form curves for the NACA 4-(5)(05)-041 propeller.

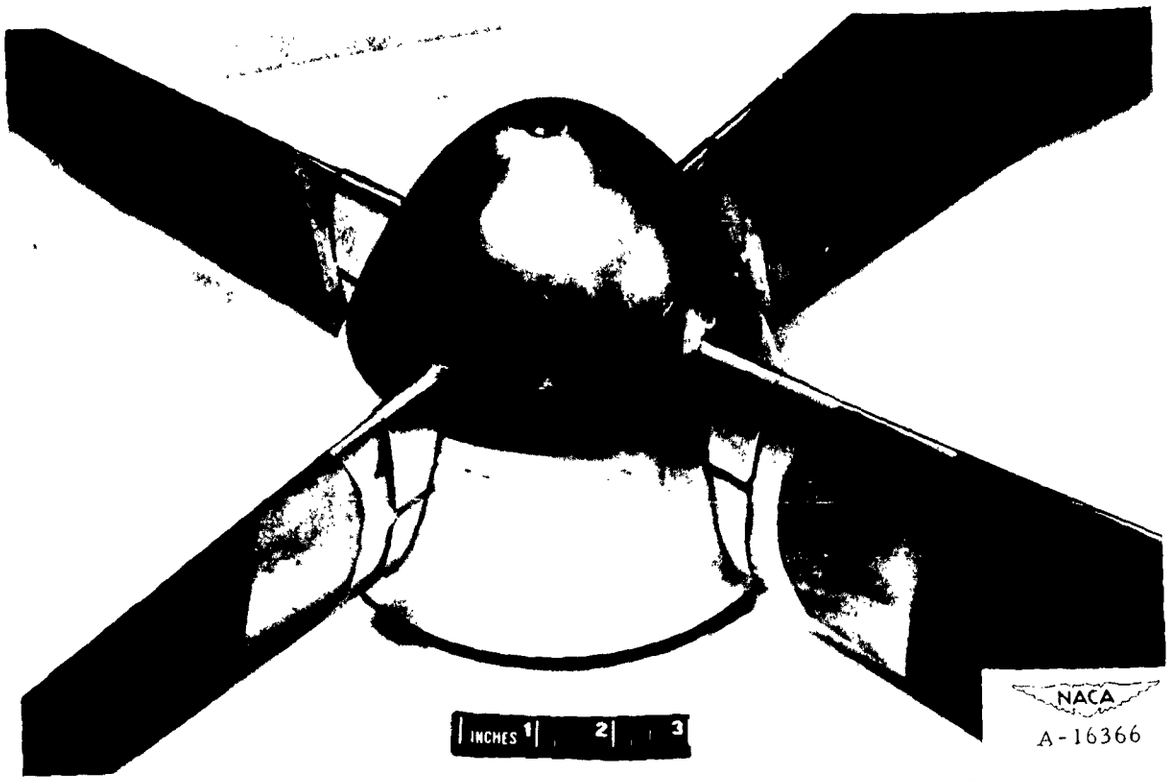

Figure 4.- Ideal propeller-spinner juncture; β, 60°.

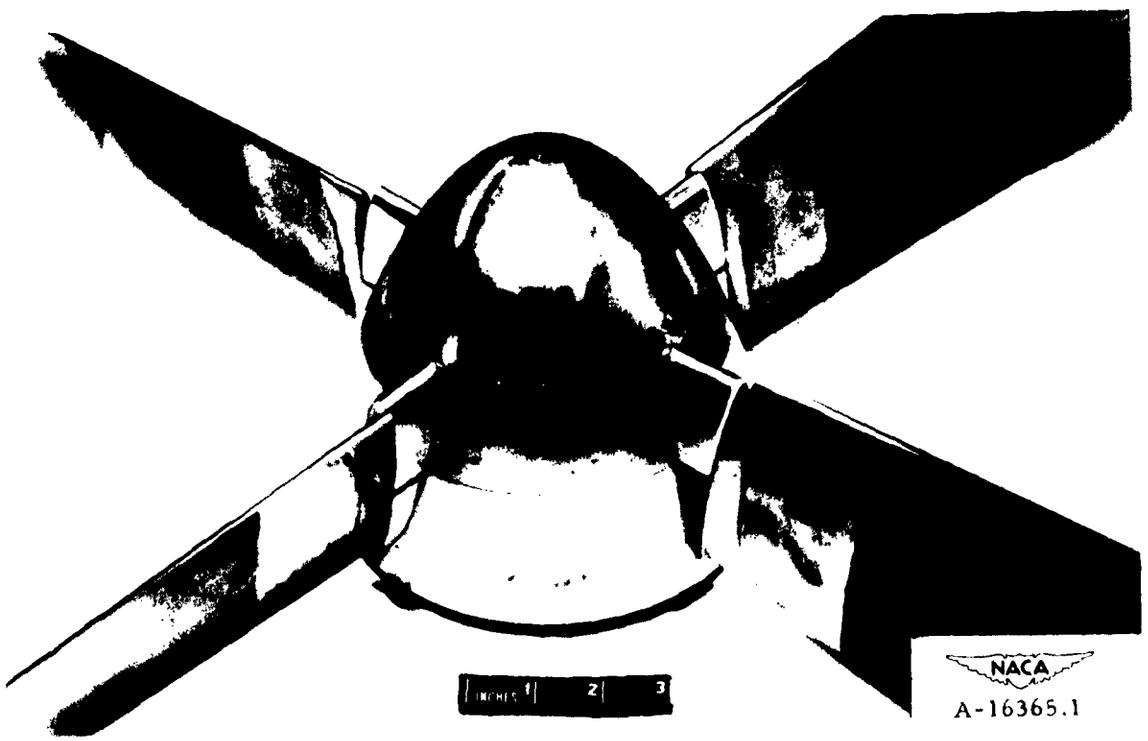

Figure 5.- Platform propeller-spinner juncture; β, 50°.

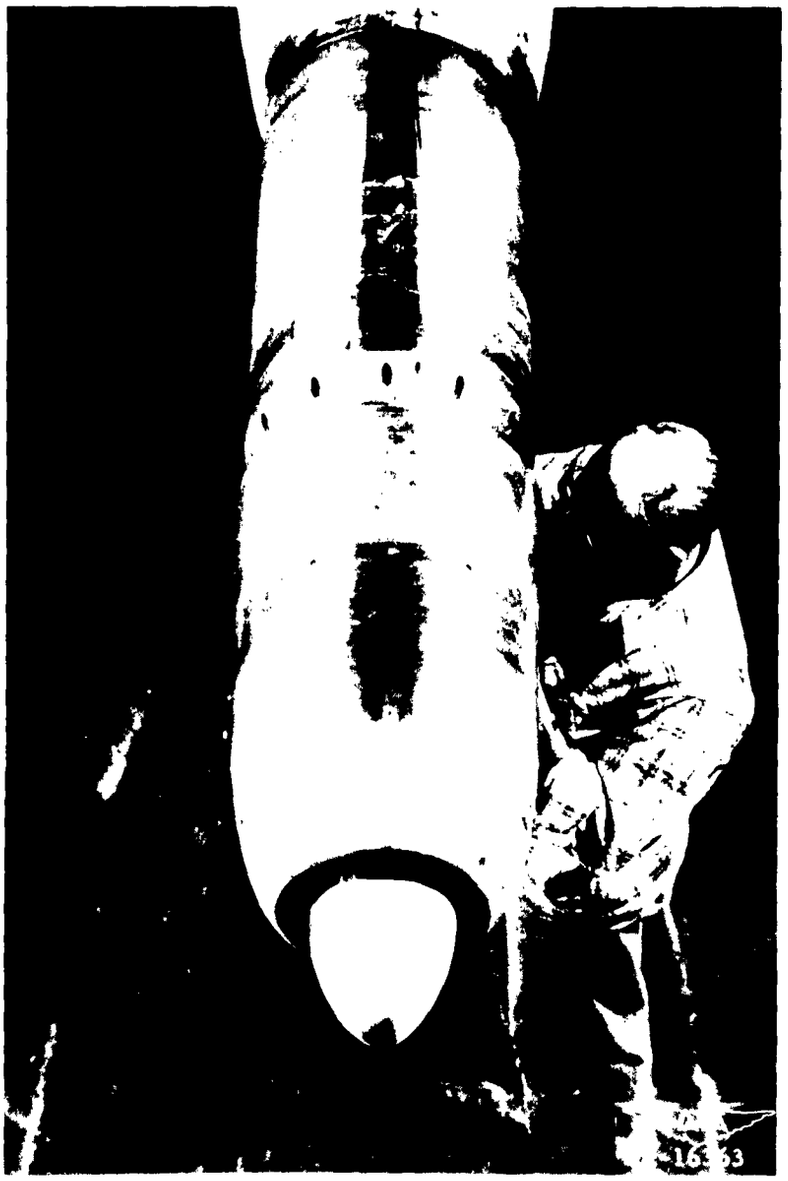

Figure 6.- The spinner-cowling combination mounted on a 14-inch-diameter, 2-foot-long extension of the dynamometer.

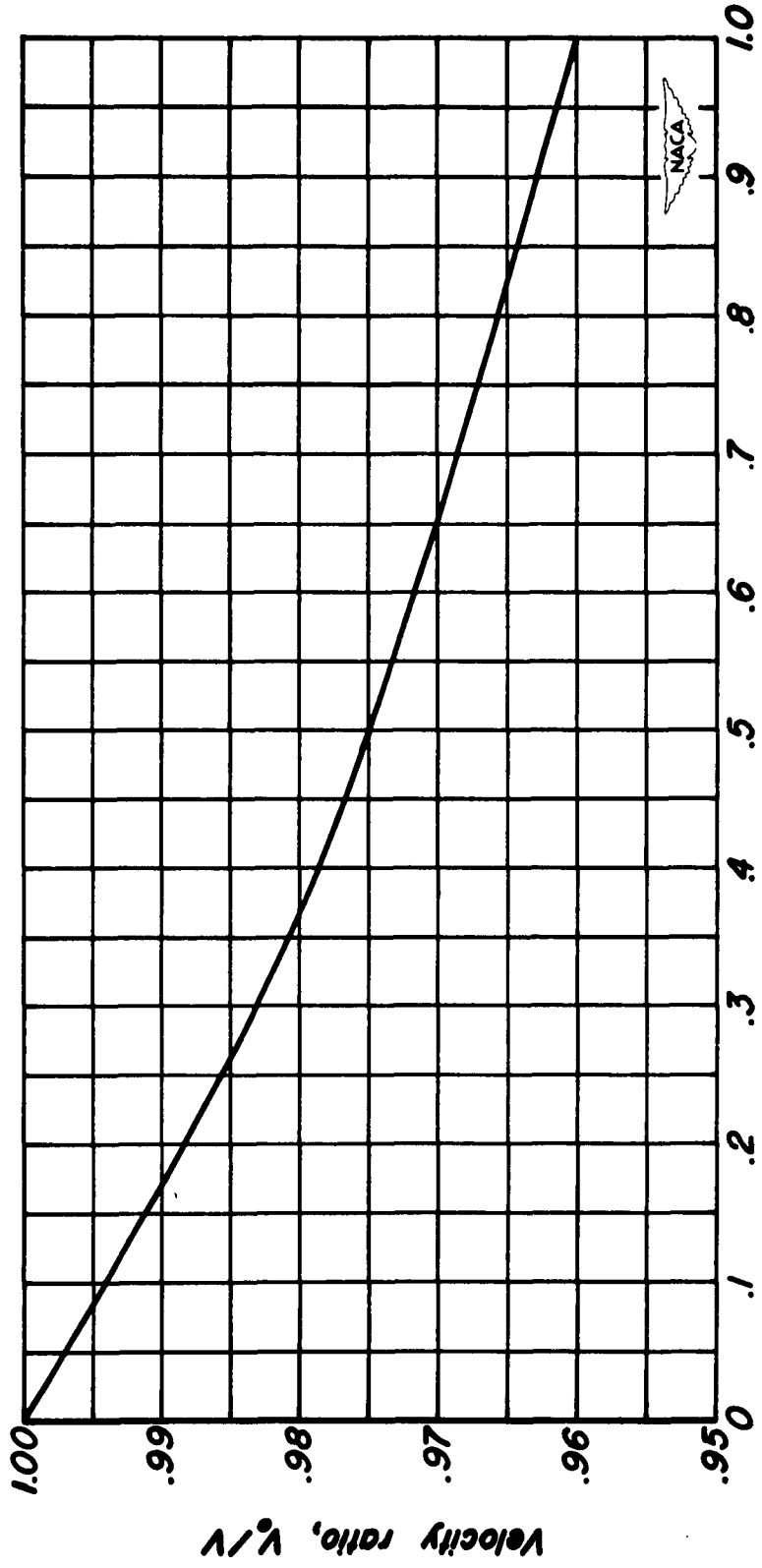

Figure 7.- Tunnel-wall-interference correction for a 4-foot-diameter propeller in the Ames 12-foot pressure wind tunnel.

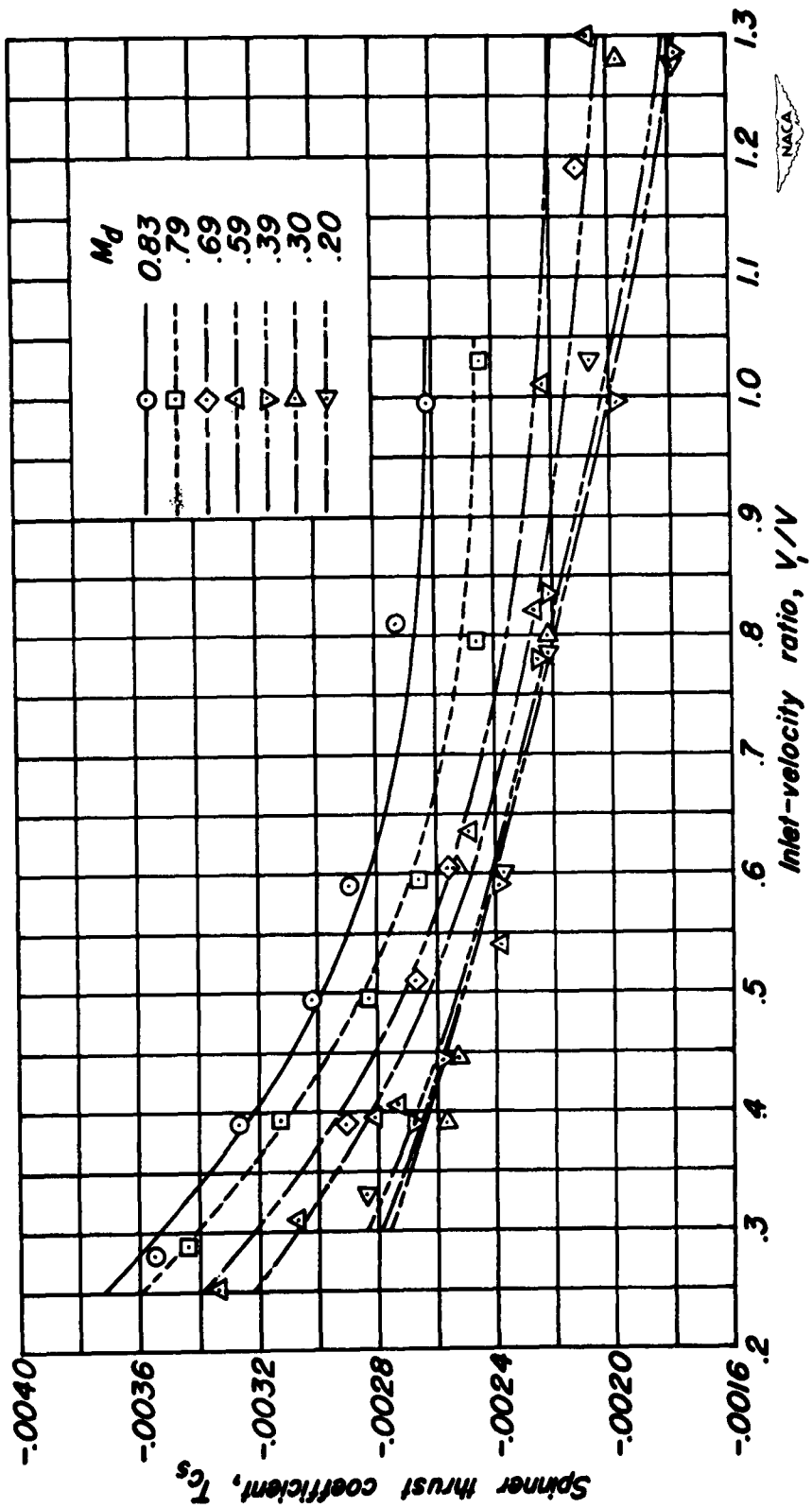

Figure 8.- The variation, with inlet-velocity ratio, of the spinner thrust coefficient applied in correcting the propeller thrust coefficient.

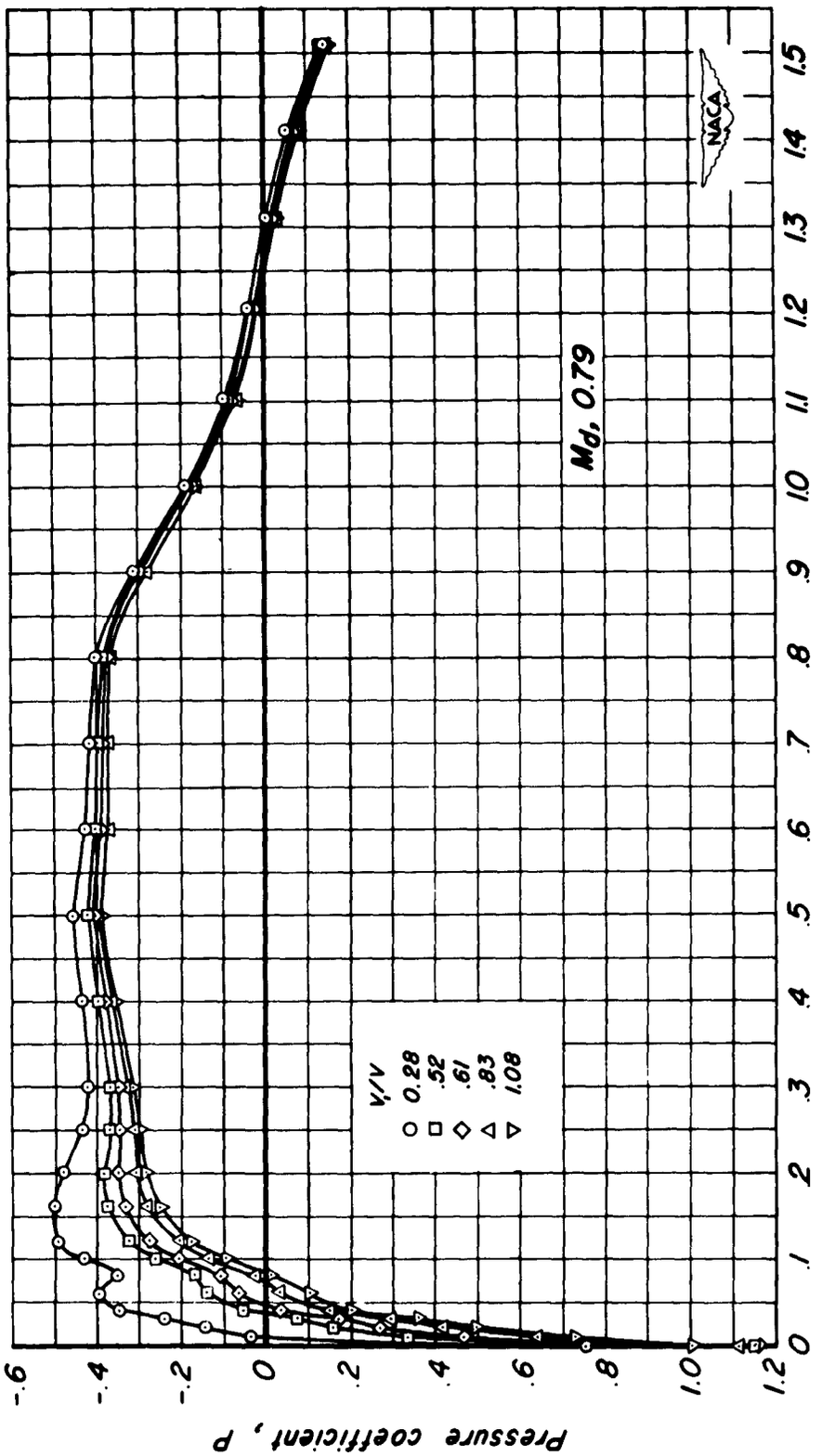

(a) Pressure coefficients for the cowl in normal position.

Figure 9.-Typical effect of cowling location on the static-pressure distribution over the external surface of the NACA 1-62.8-070 cowling, propeller removed.

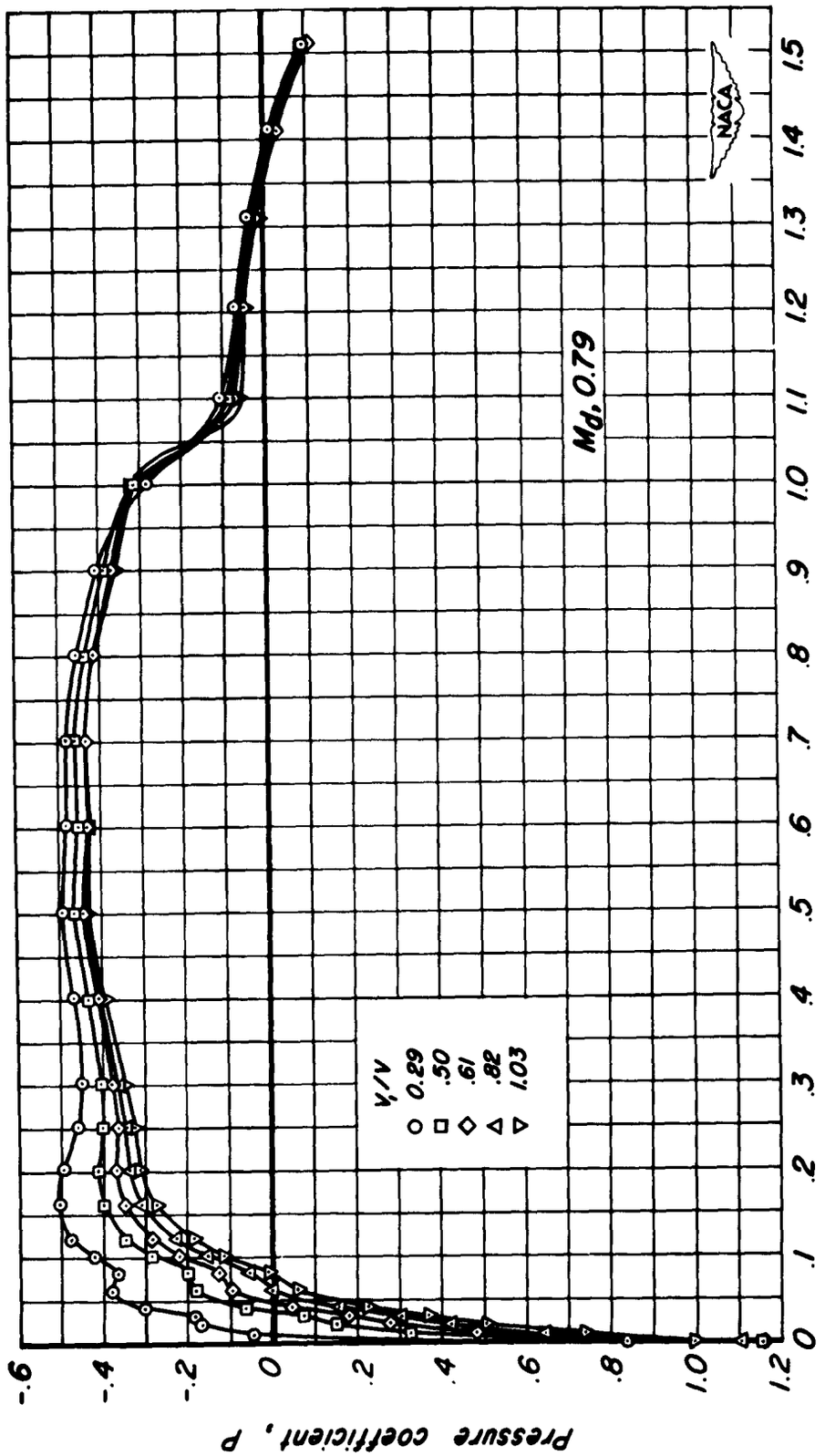

(b) Pressure coefficients for the cowl in extended position.

Figure 9.— Continued.

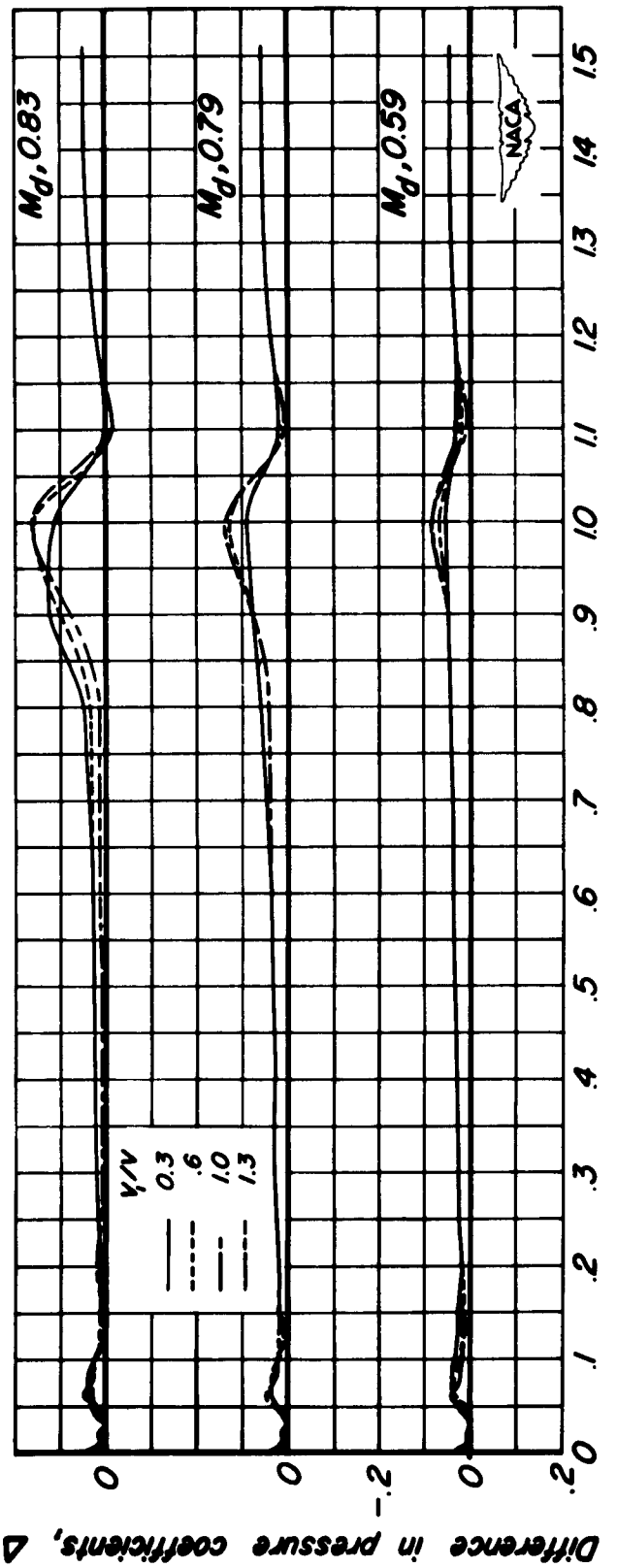

(c) Difference in pressure coefficients.

Figure 9.— Concluded.

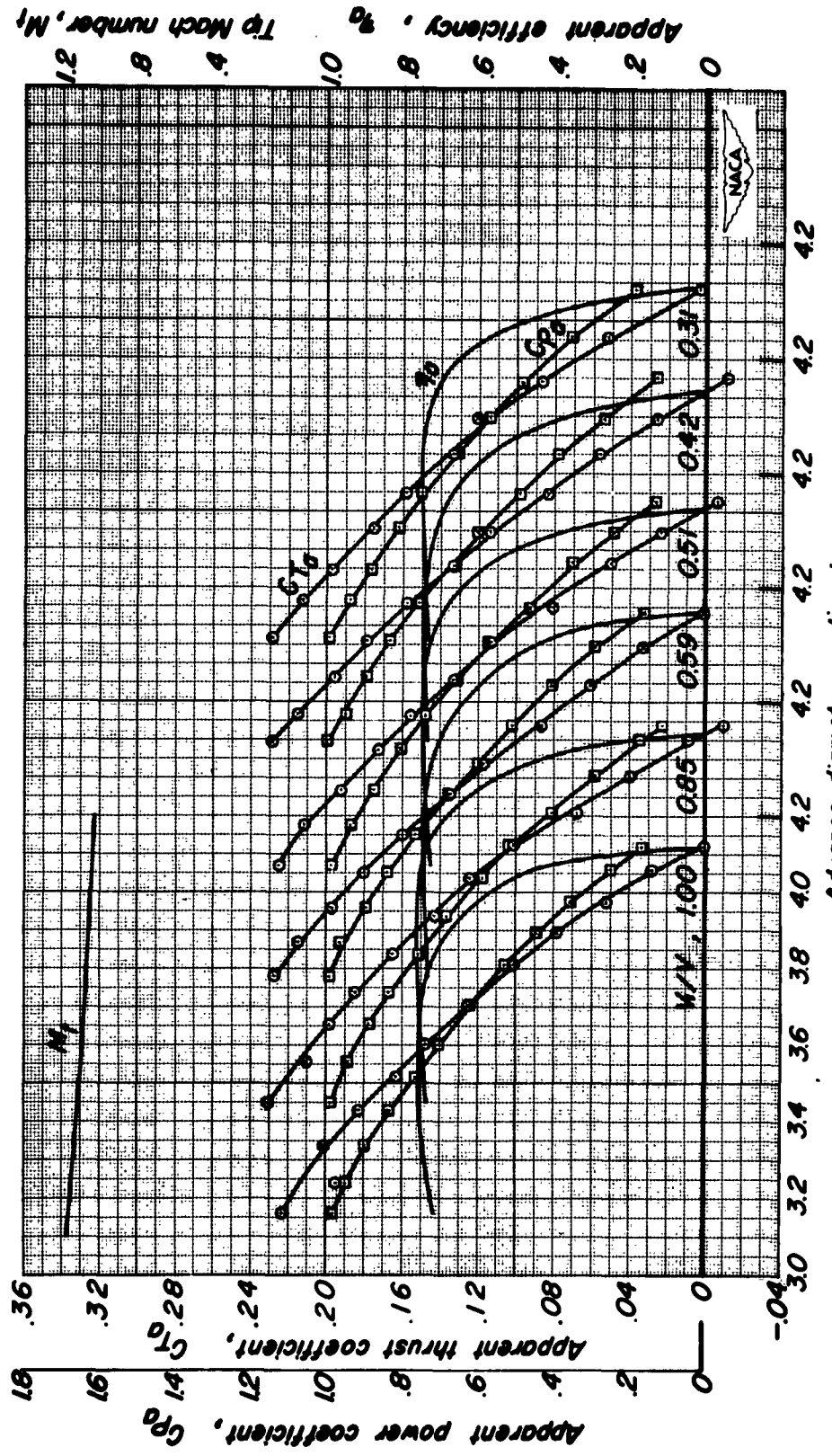

Figure 10.- Characteristics of the NACA 4-(5)(05)-041 propeller in combination with the NACA 1-46.5-047 spinner and the NACA 1-62.8-070 D-type cowling, ideal propeller- spinner juncture.
(a) M_d, 0.83; β, 60°

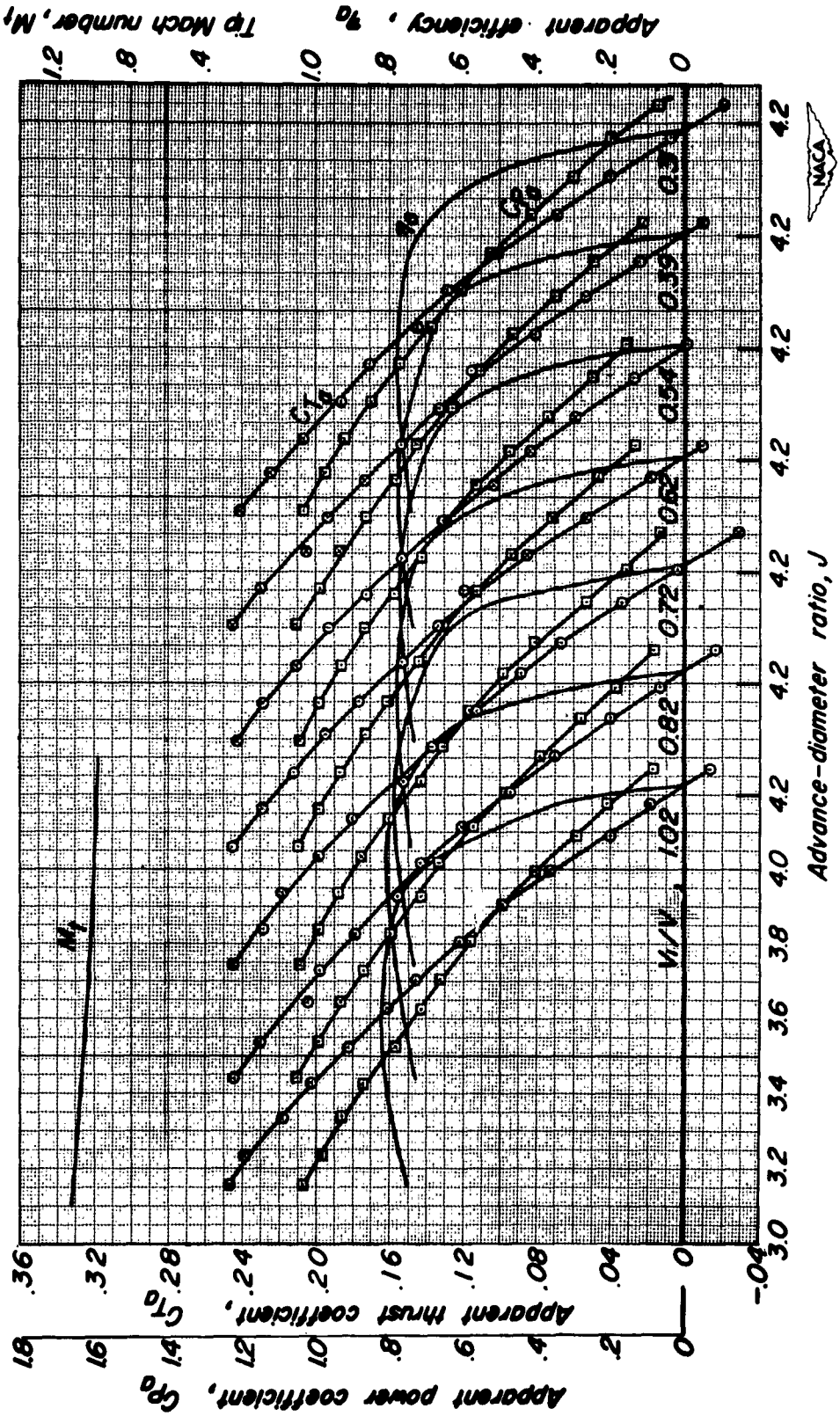

(b) M_d,0.79; β,60°

Figure 10.-Continued.

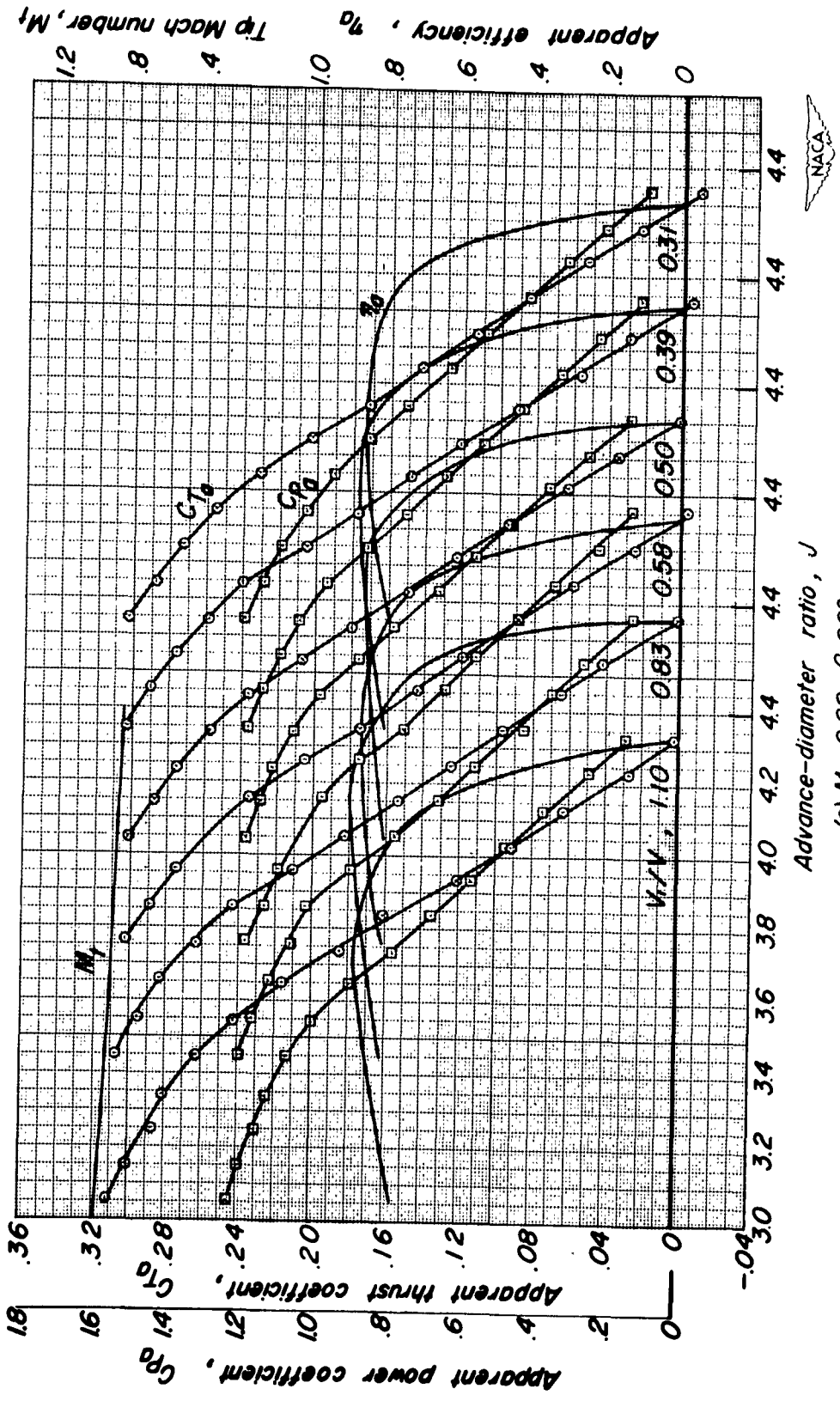

(c) M_d, 0.69; β, 60°

Figure 10.- Continued.

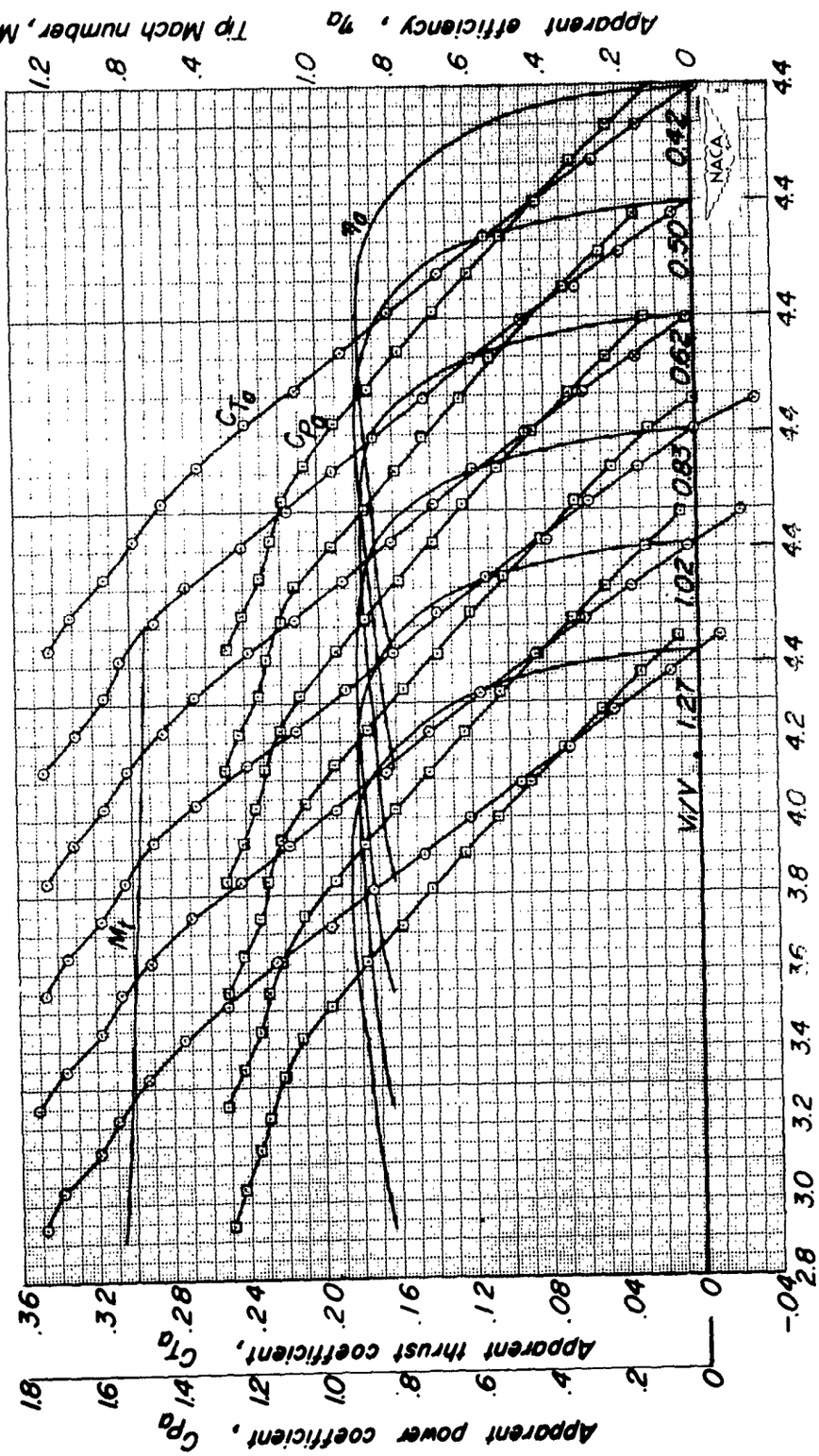

(d) M_a, 0.59; β, 60°

Figure 10.- Continued.

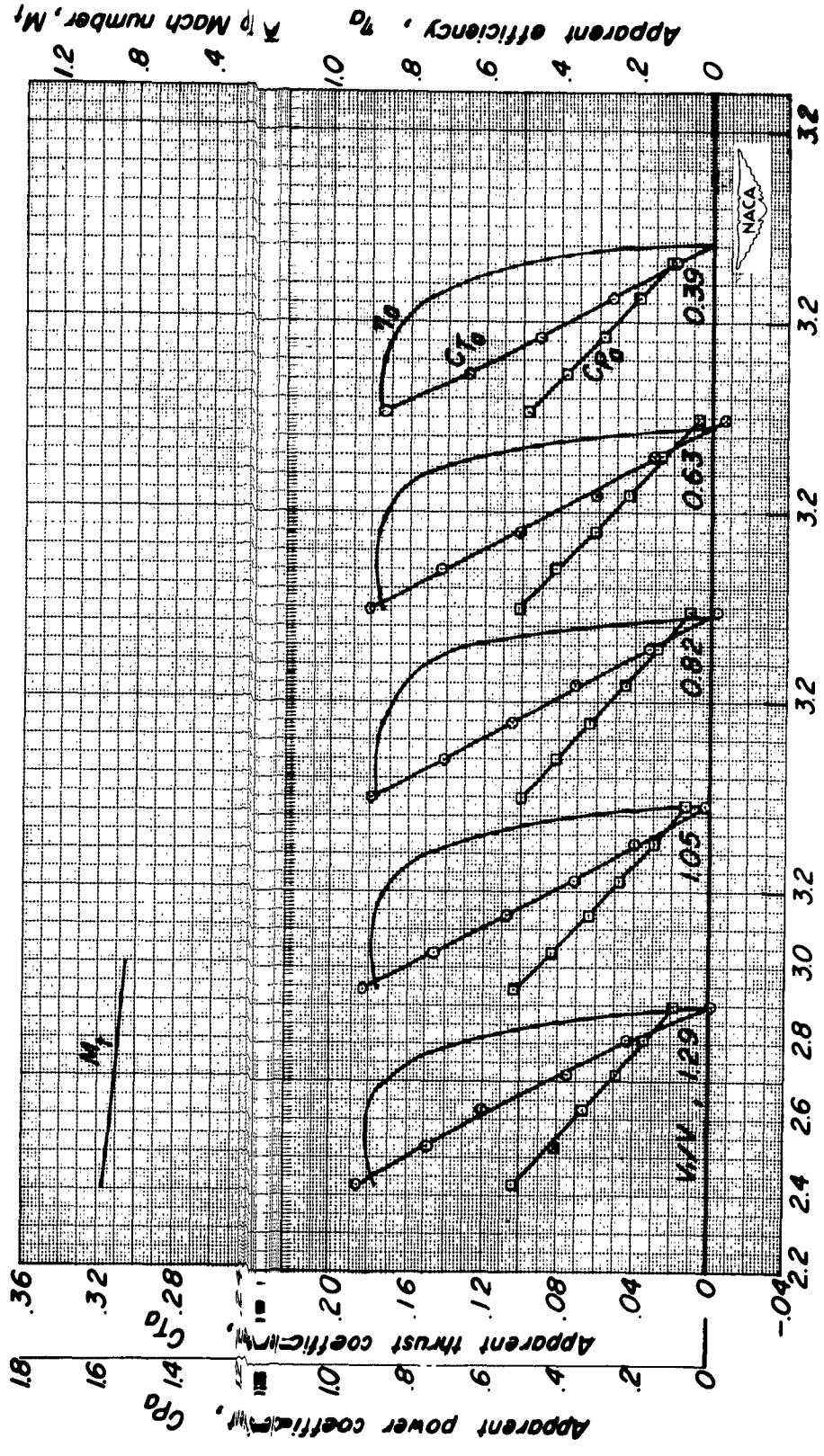

(e) M_d, 0.59; β, 50°

Figure 10.- Continued.

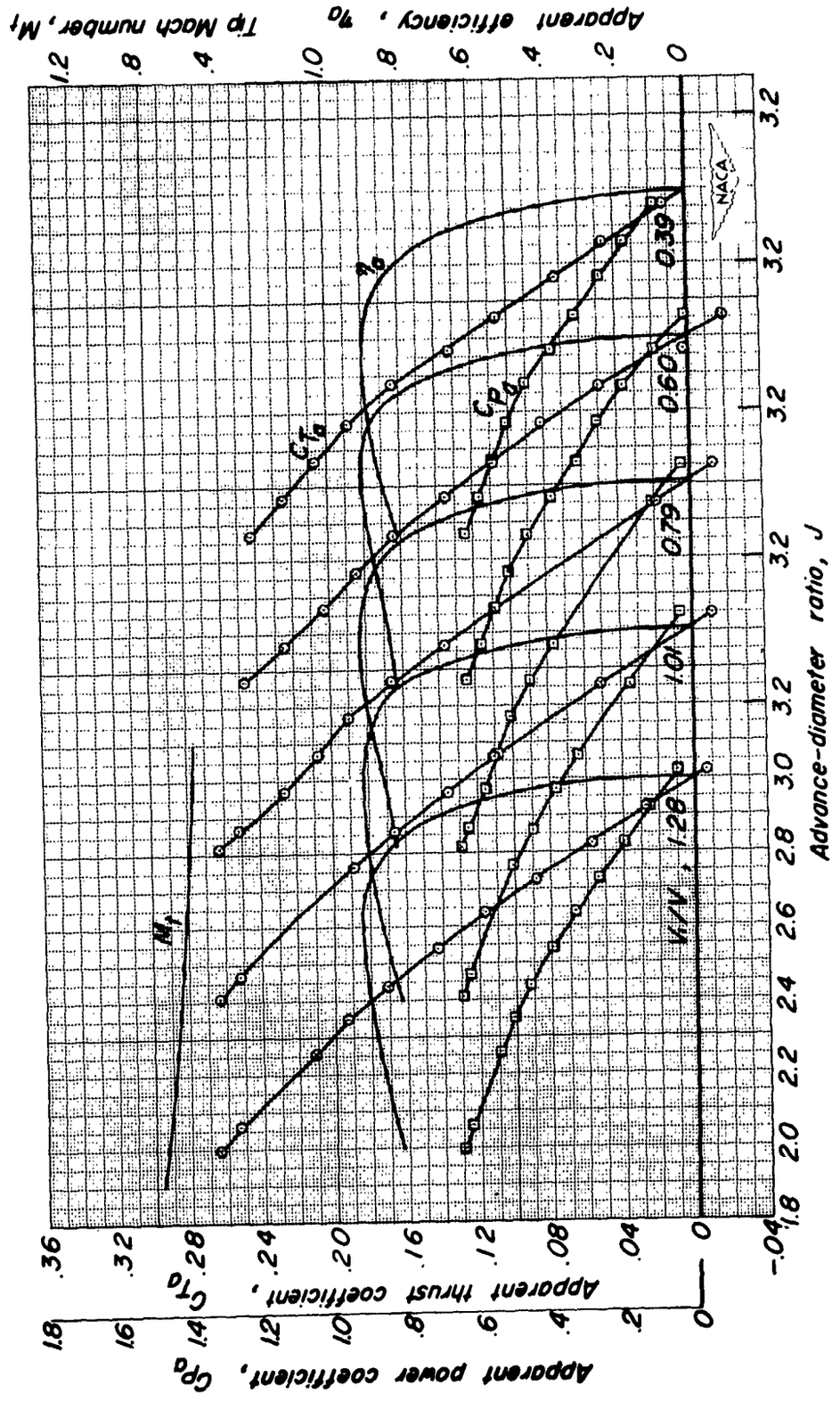

(f) M_d,0.39;β,50°

Figure 10.-Continued.

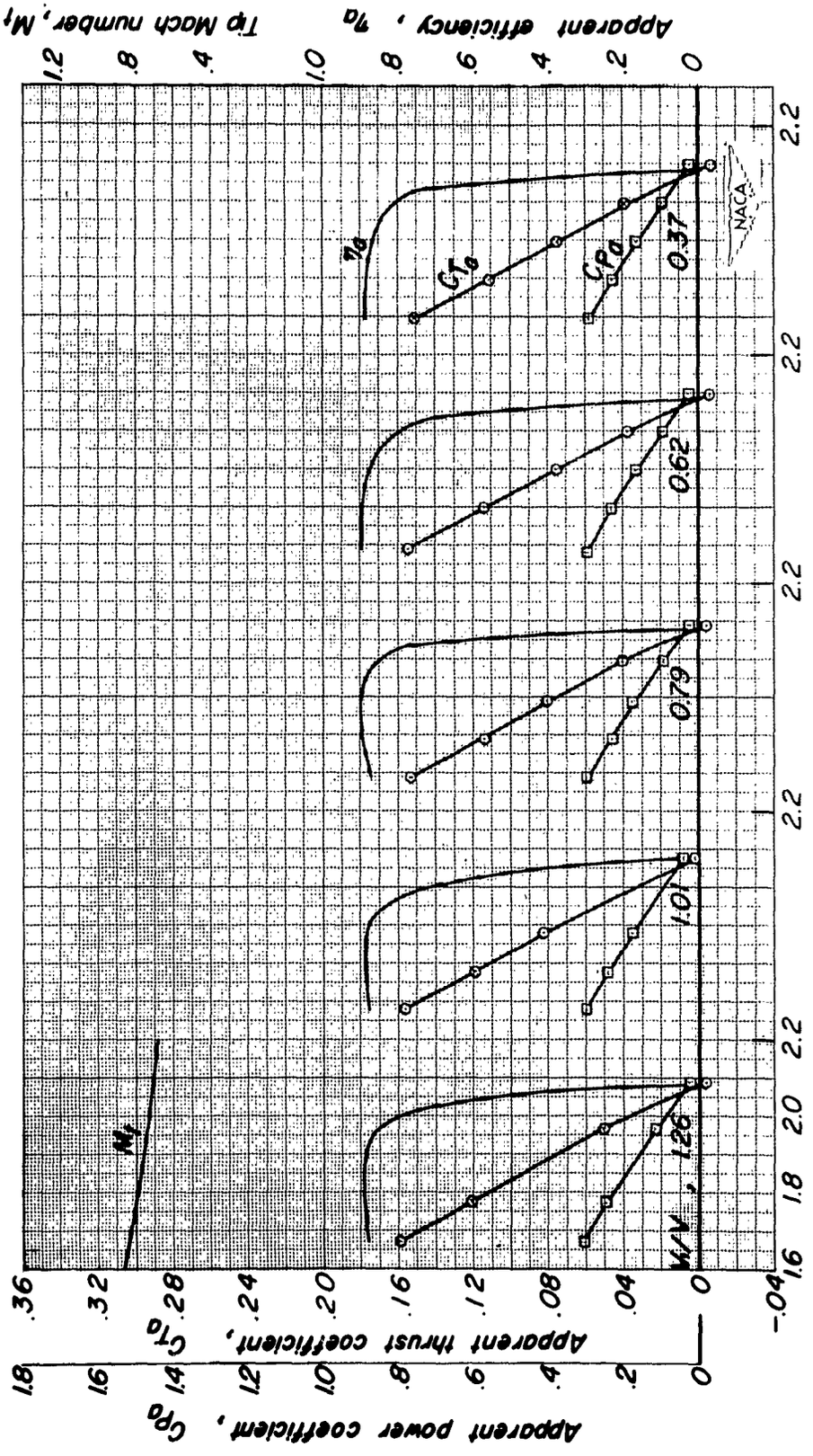

(g) M_d, 0.39; β, 40°

Figure 10.- Continued.

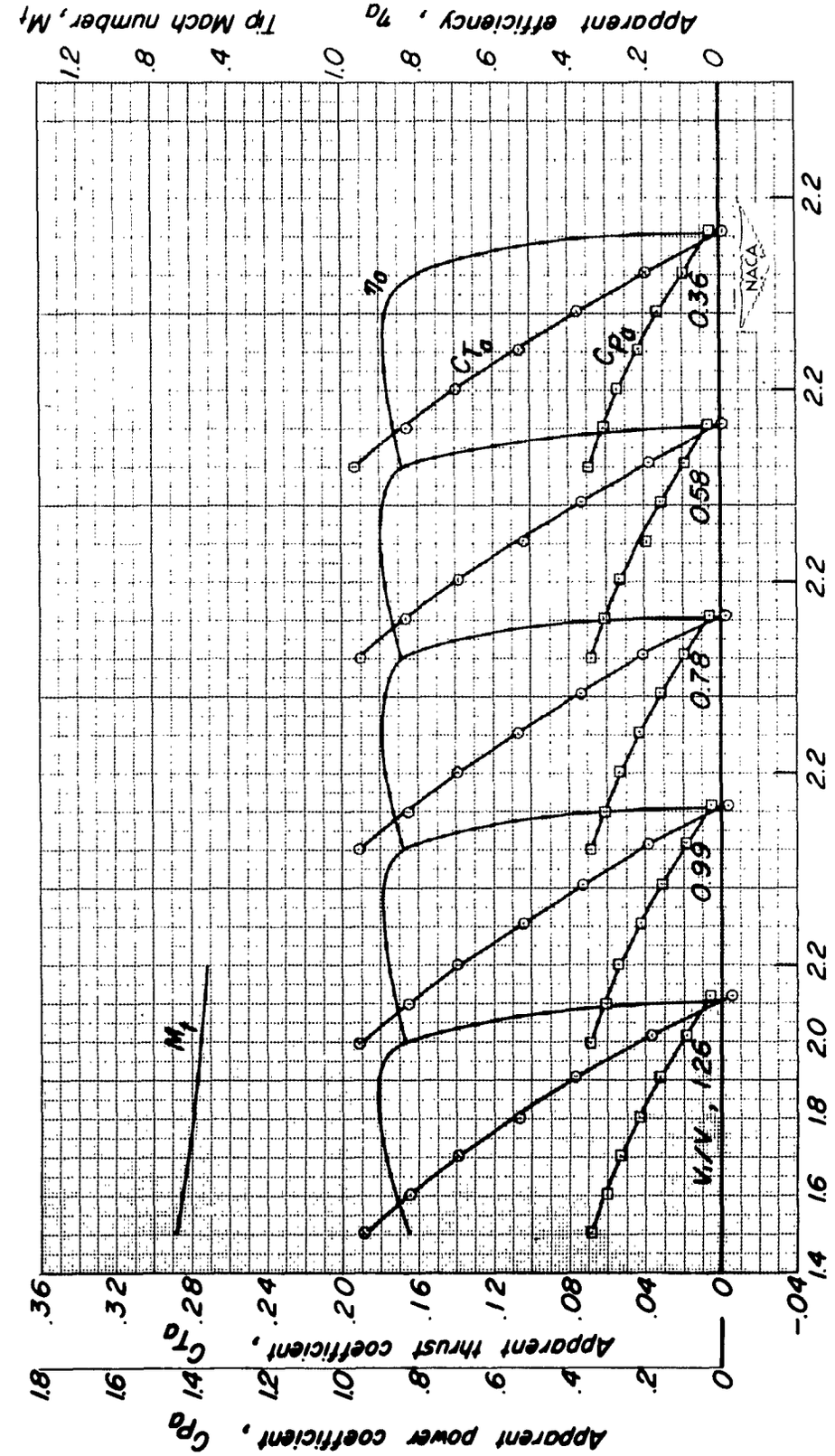

(h) M_d,0.30;β,40°

Figure 10.-Continued.

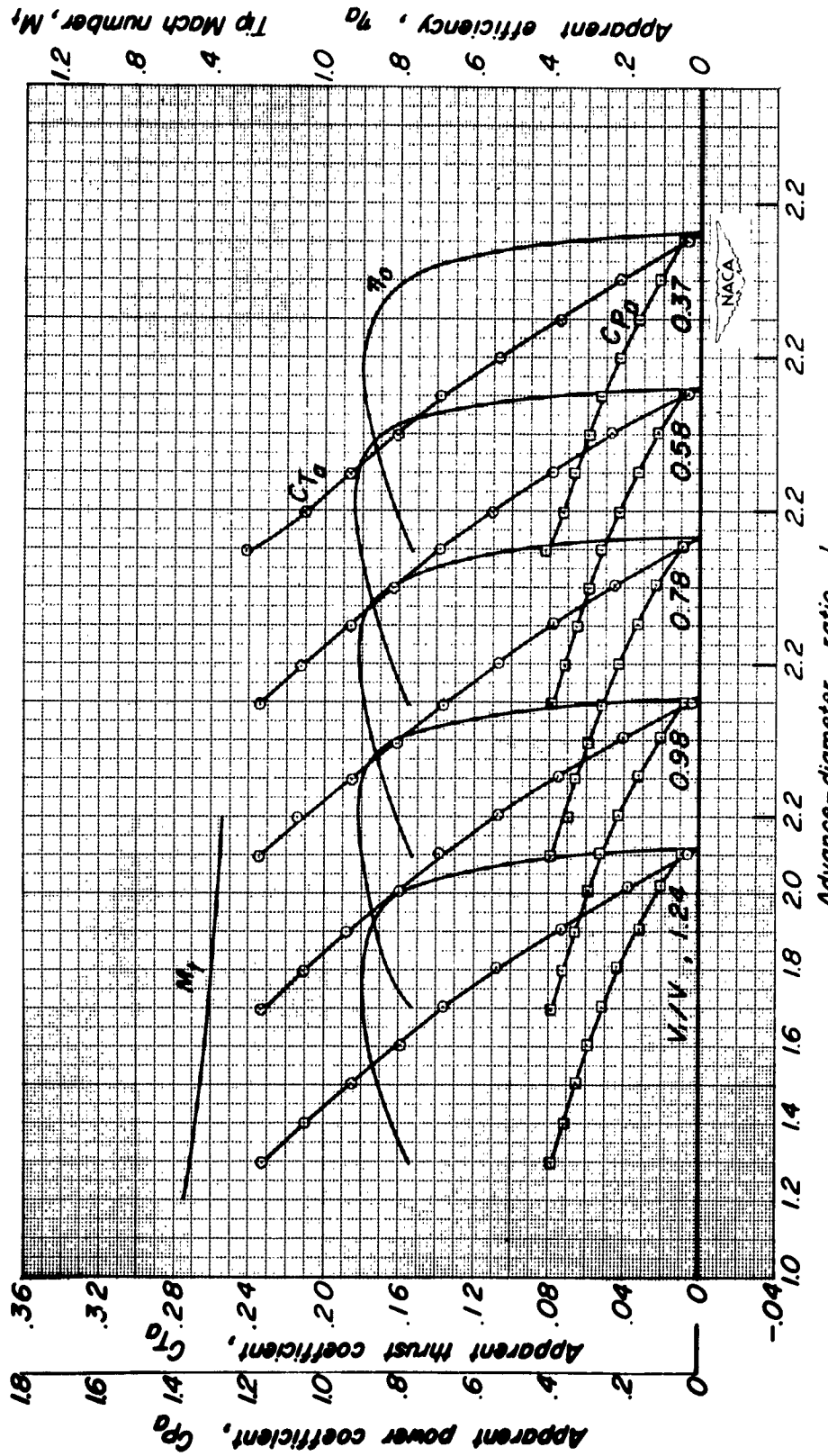

(l) M_d, 0.20; β, 40°

Figure 10.-Concluded.

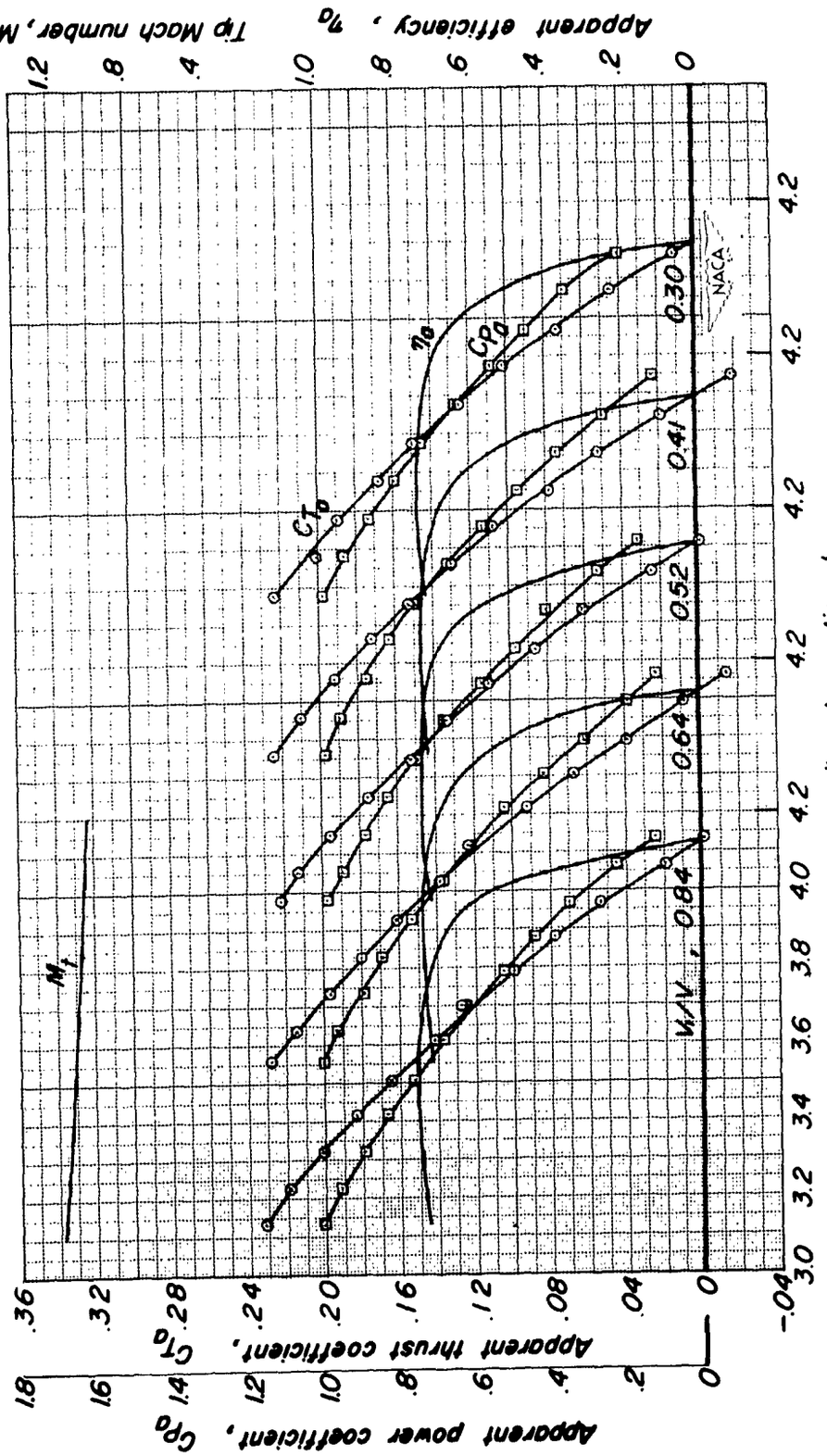

Figure 11.- Characteristics of the NACA 4-(5)(05)-041 propeller in combination with the NACA 1-46.5-047 spinner and the NACA 1-62.8-070 D-type cowling, platform propeller-spinner juncture.
(a) M_d,0.83; β,60°

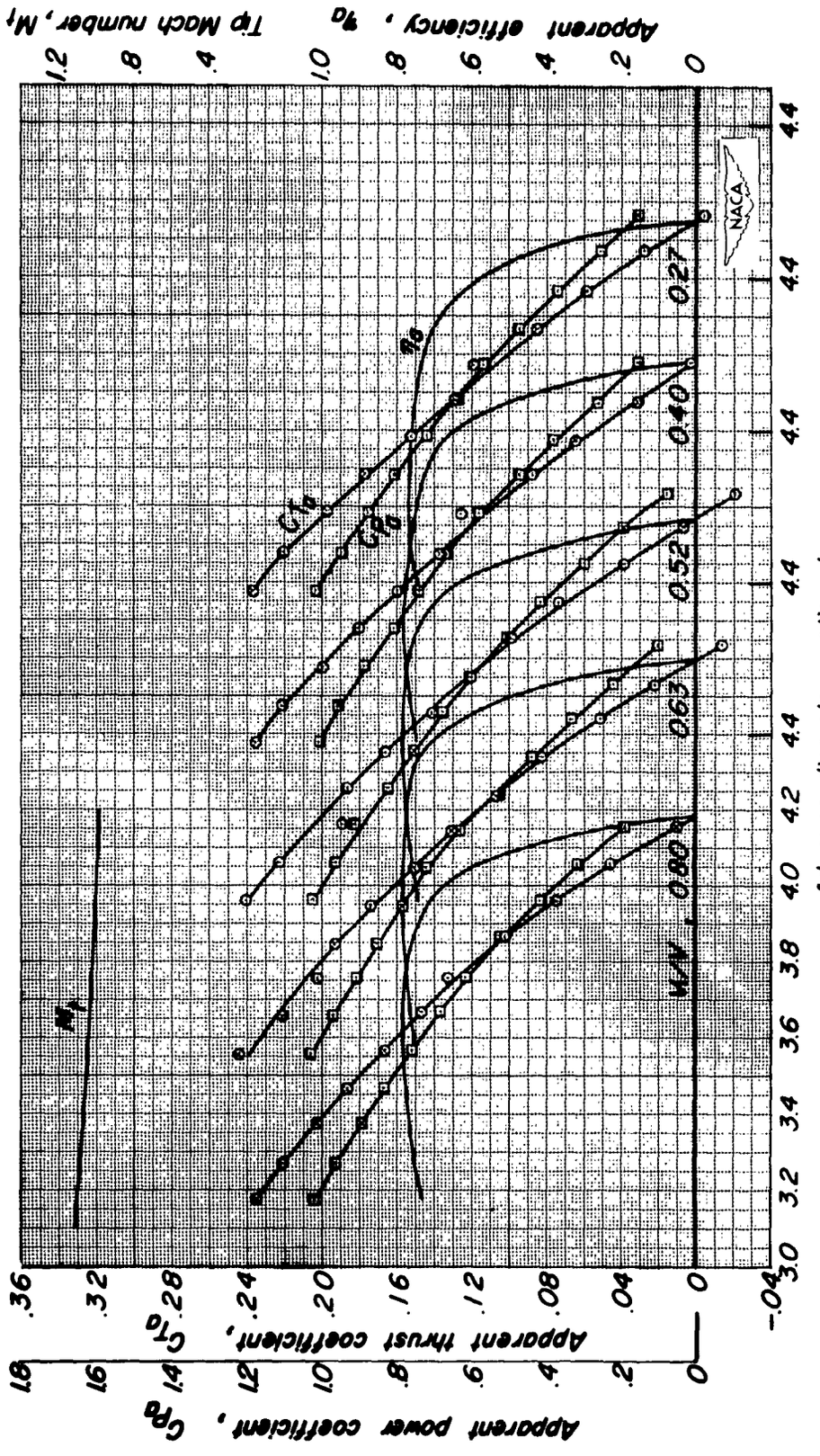

(b) M_d, 0.79; β, 60°

Figure 11.- Continued.

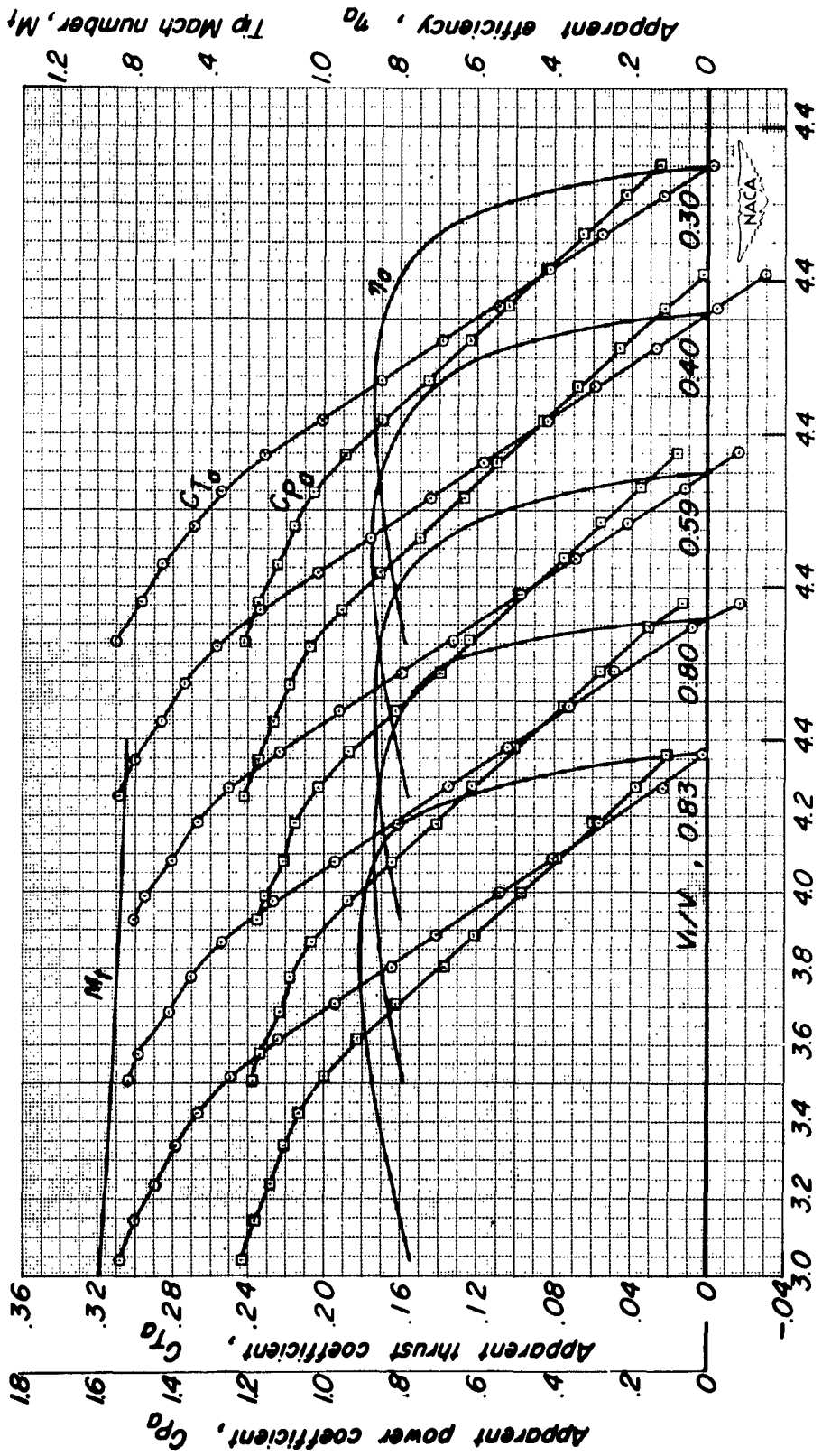

(c) M_d, 0.69; β, 60°

Figure 11.- Continued.

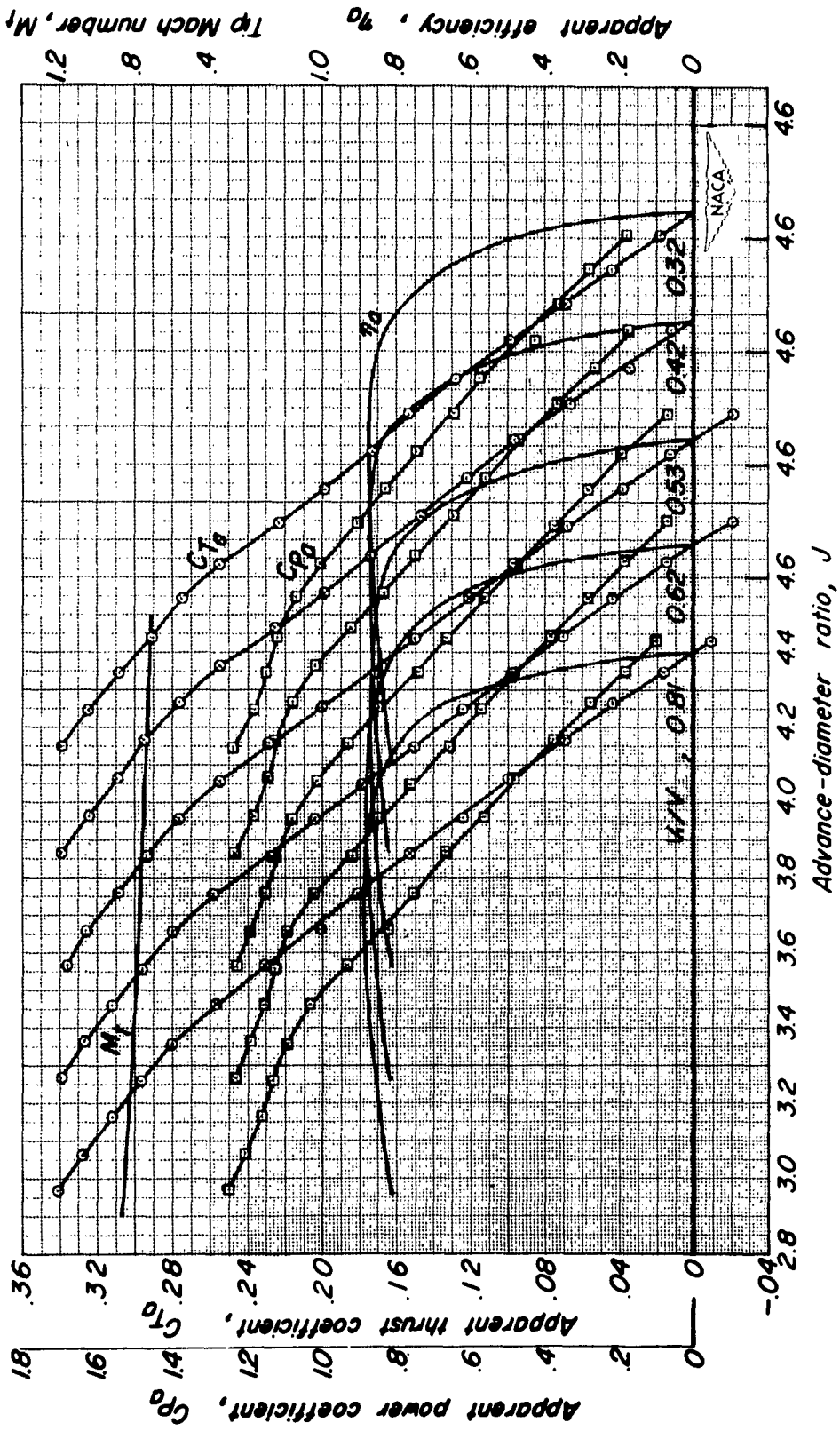

(d) M_d, 0.59; β, 60°

Figure 11.- Continued.

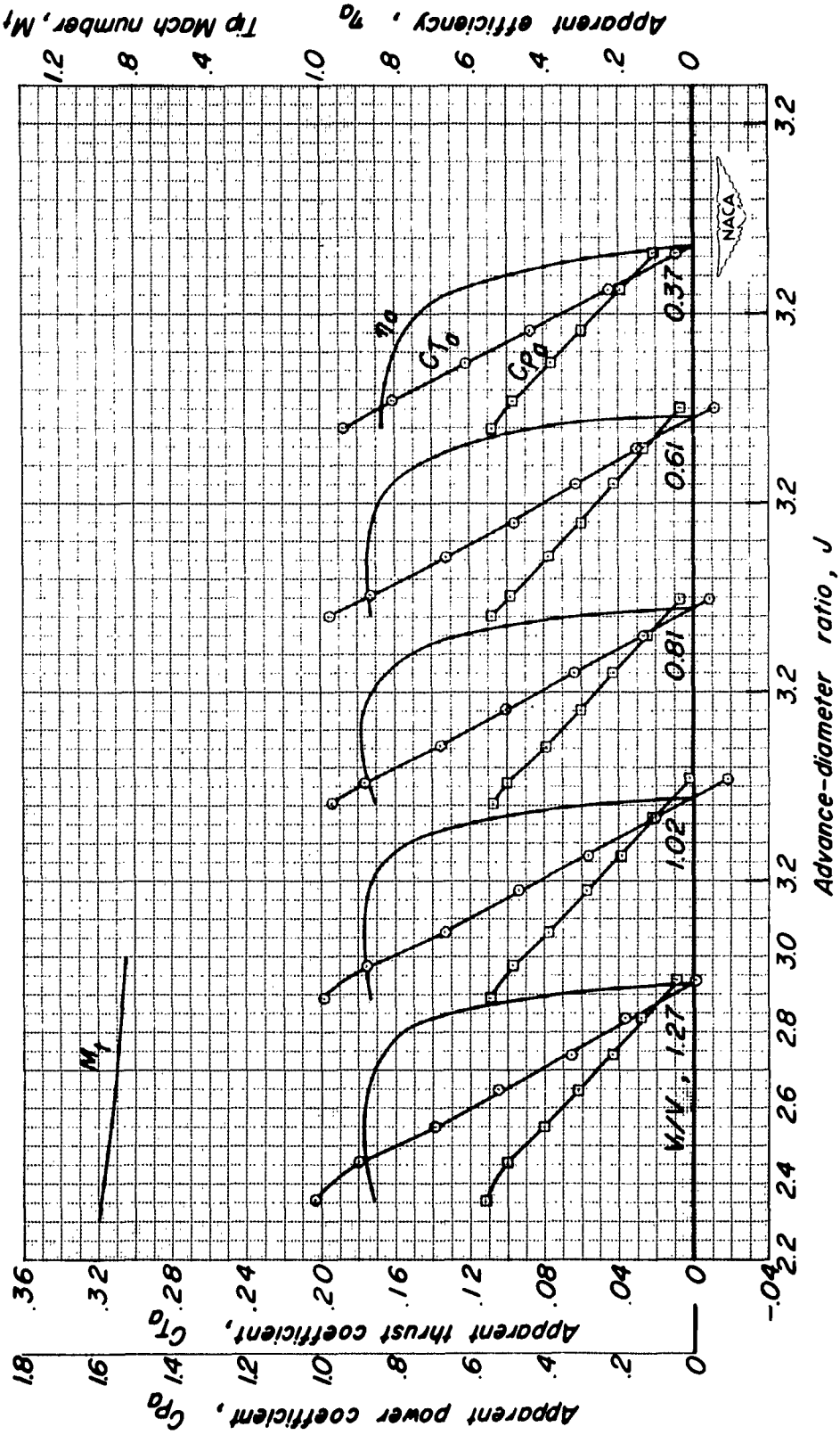

(e) M_d,0.59; β,50°

Figure 11.-Continued.

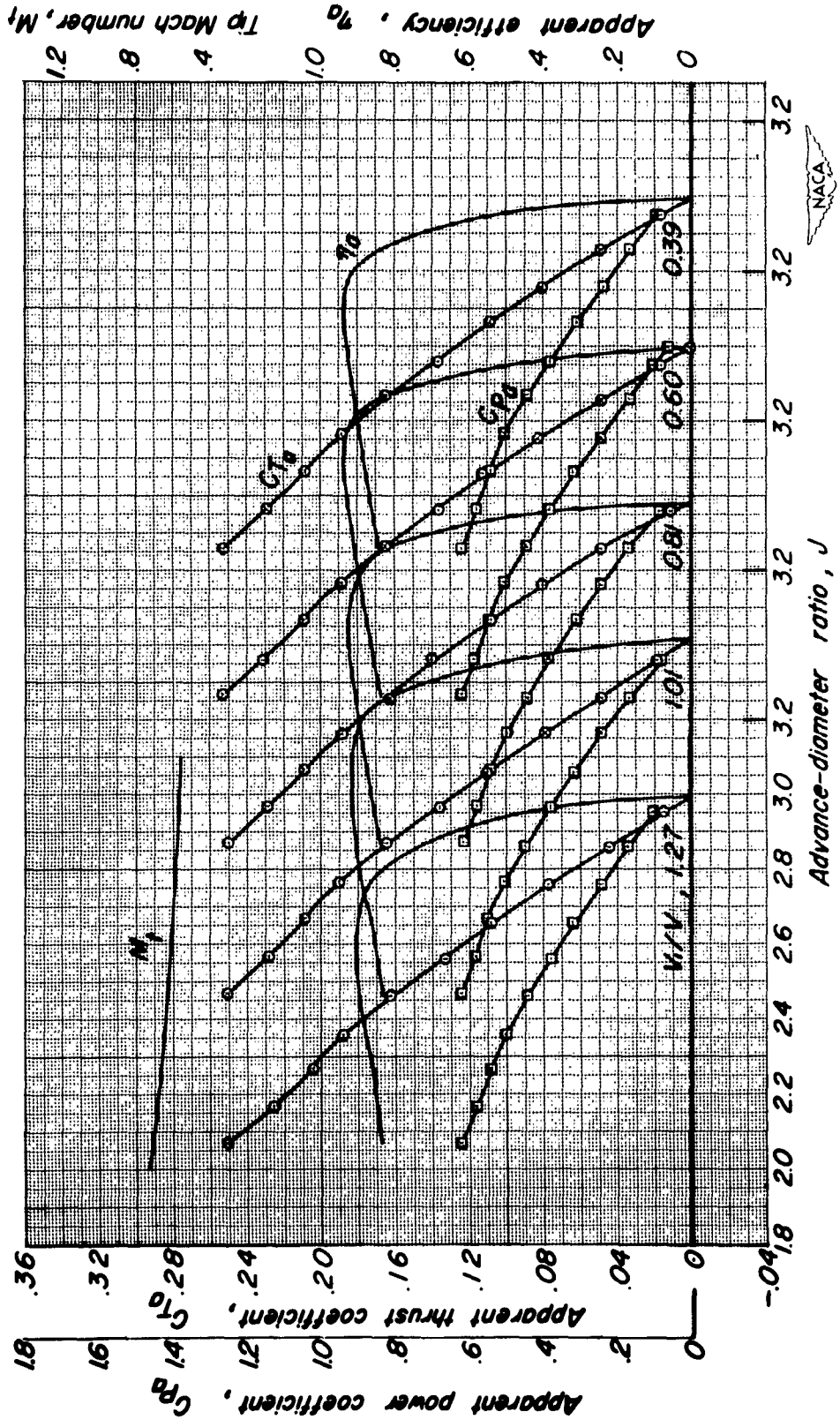

(f) M_d, 0.39; β, 50°

Figure 11.- Continued.

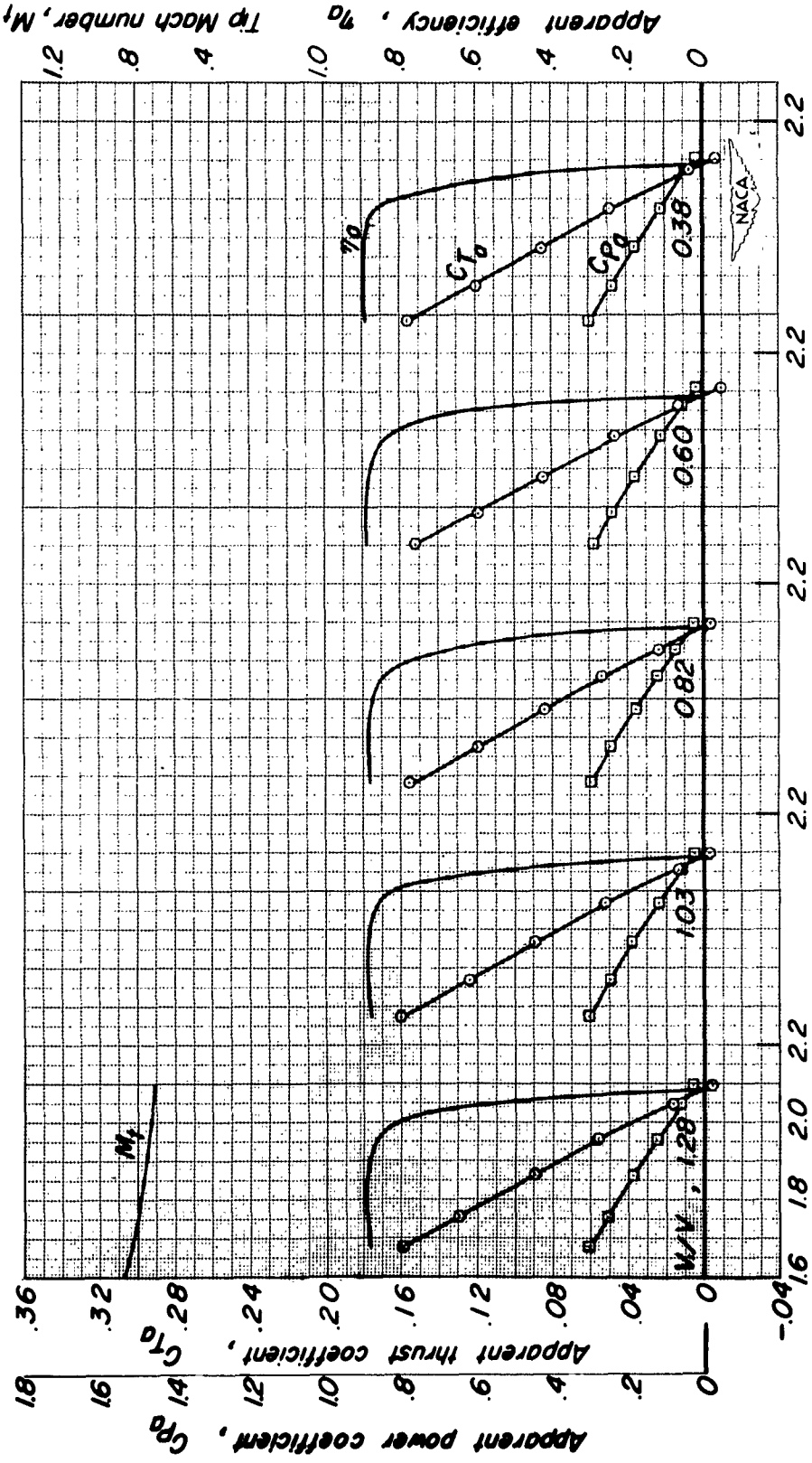

(g) M_d, 0.39; β, 40°

Figure 11.-Continued.

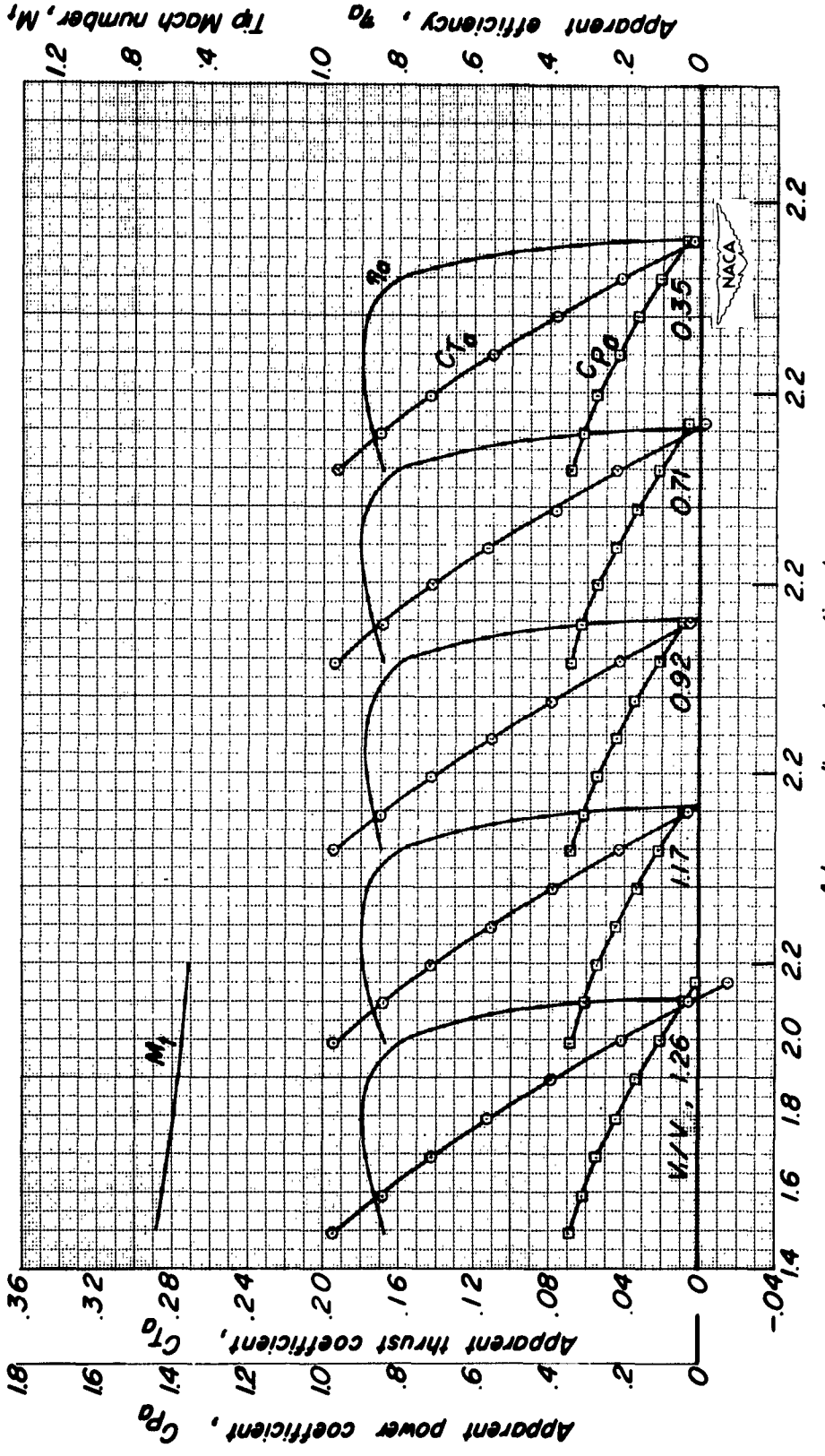

(h) M_d, 0.30; β, 40°

Figure 11.- Continued.

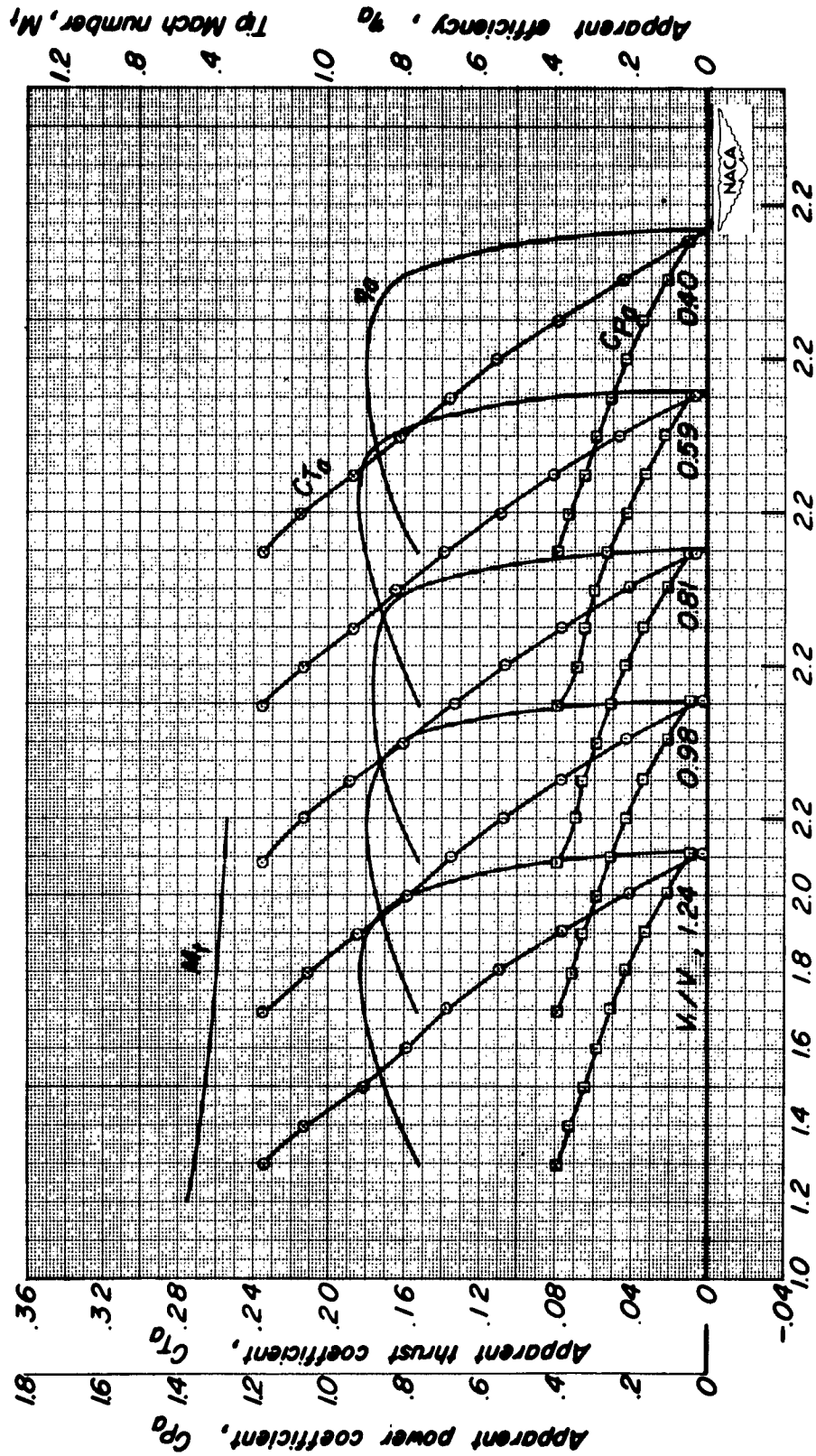

(i) M_d, 0.20; β, 40°

Figure 11.- Concluded.

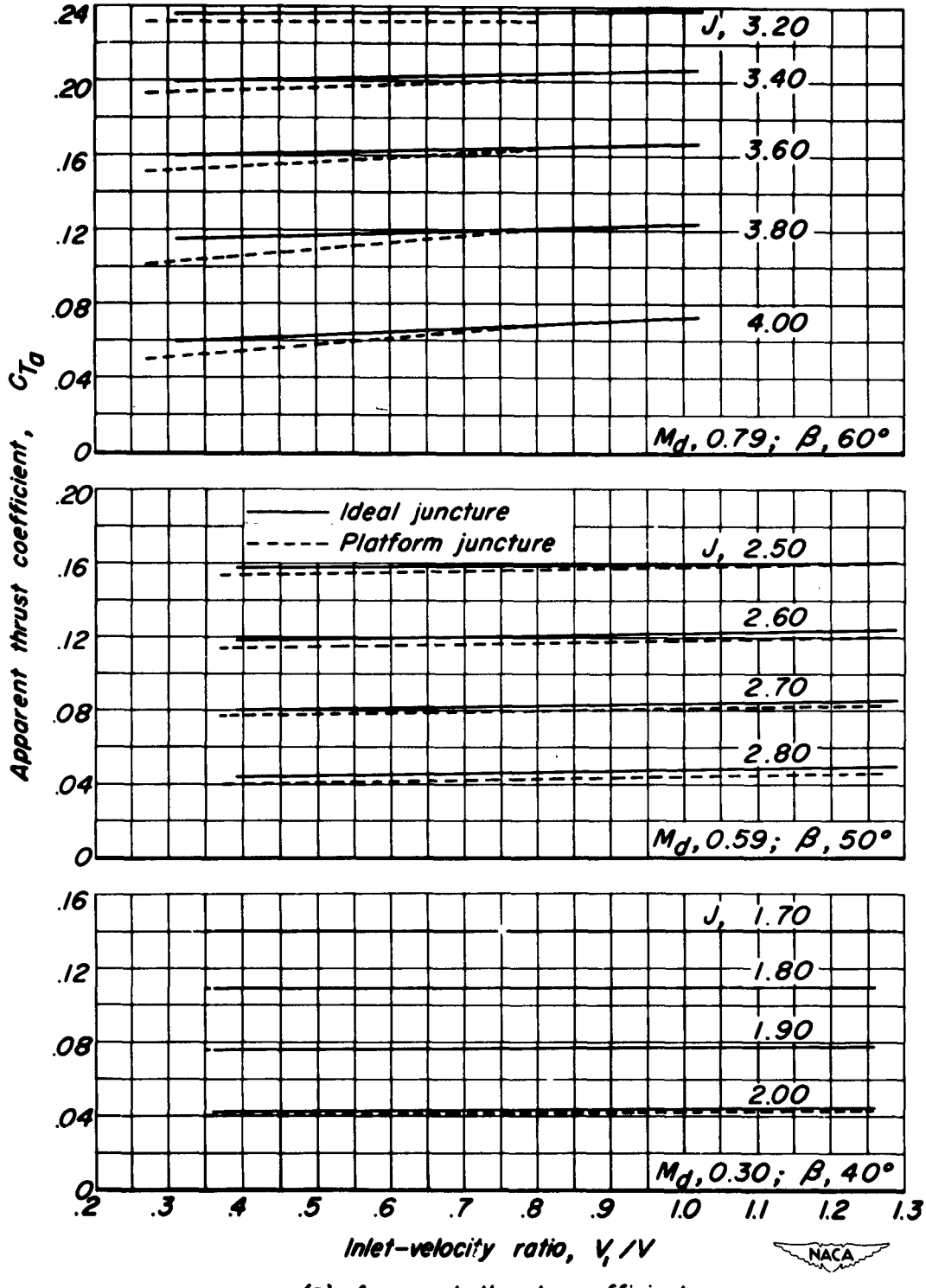

(a) Apparent thrust coefficient.

Figure 12.-Typical effect of inlet-velocity ratio on the apparent thrust and power coefficients of the propeller.

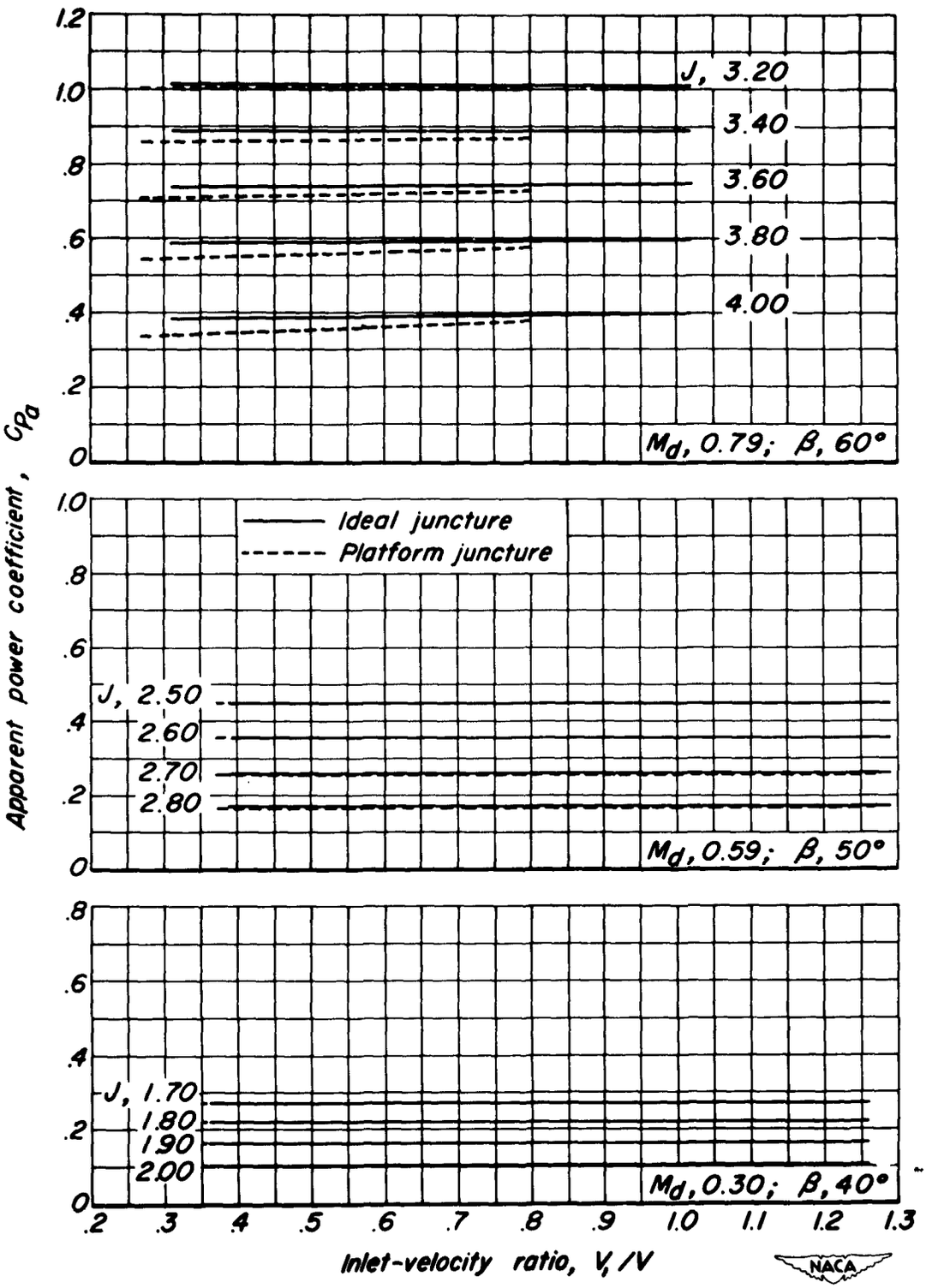

(b) Apparent power coefficient.

Figure 12.- Concluded.

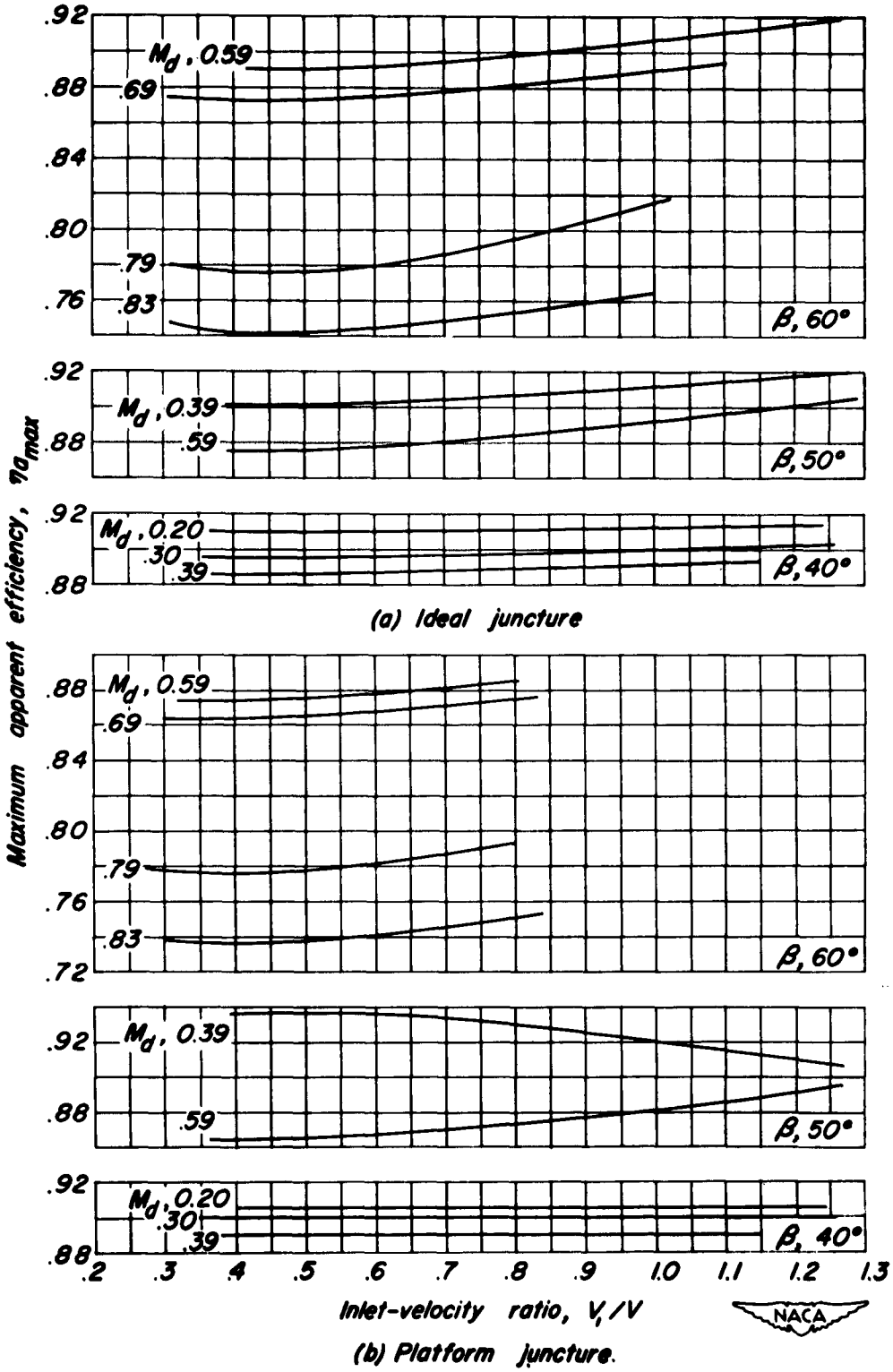

(a) Ideal juncture

(b) Platform juncture.

Figure 13.-Effect of inlet-velocity ratio on the maximum apparent efficiency of the propeller.

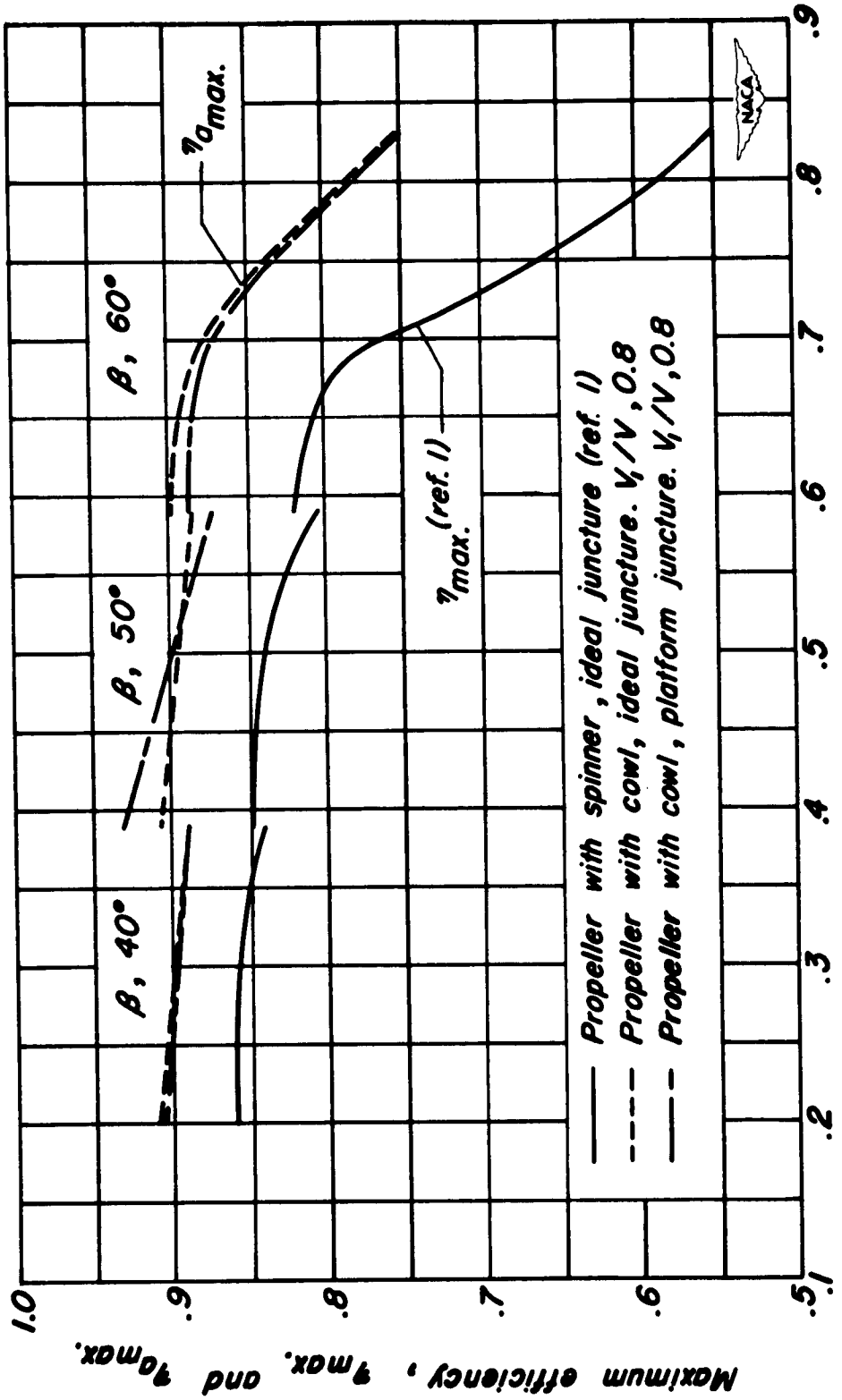

Figure 14.- Effect of Mach number on the maximum efficiency of the propeller.

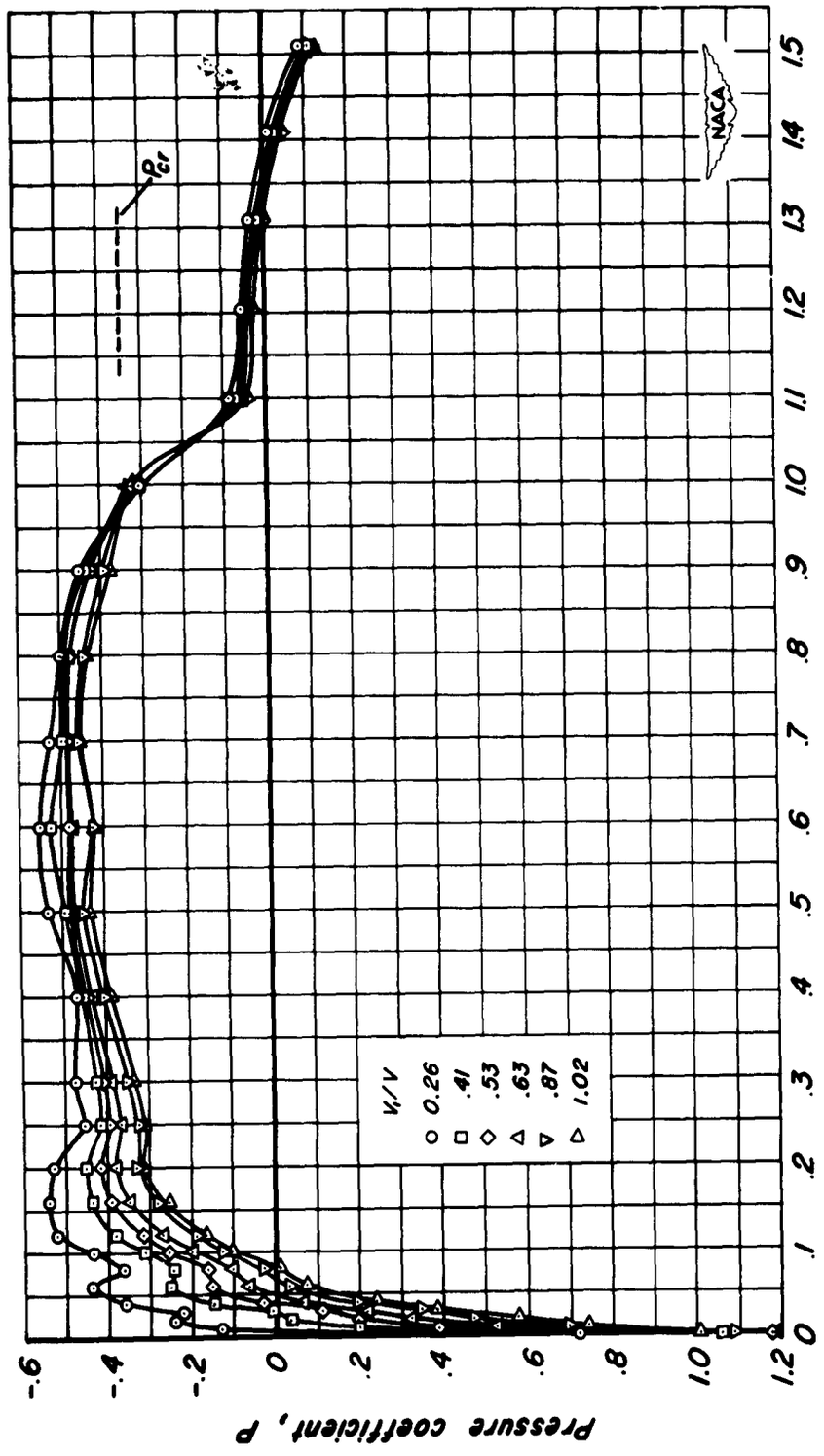

(a) M_d, 0.83

Figure 15.—Typical static-pressure distribution over the external surface of the NACA 1-62.8-070 cowling, propeller removed.

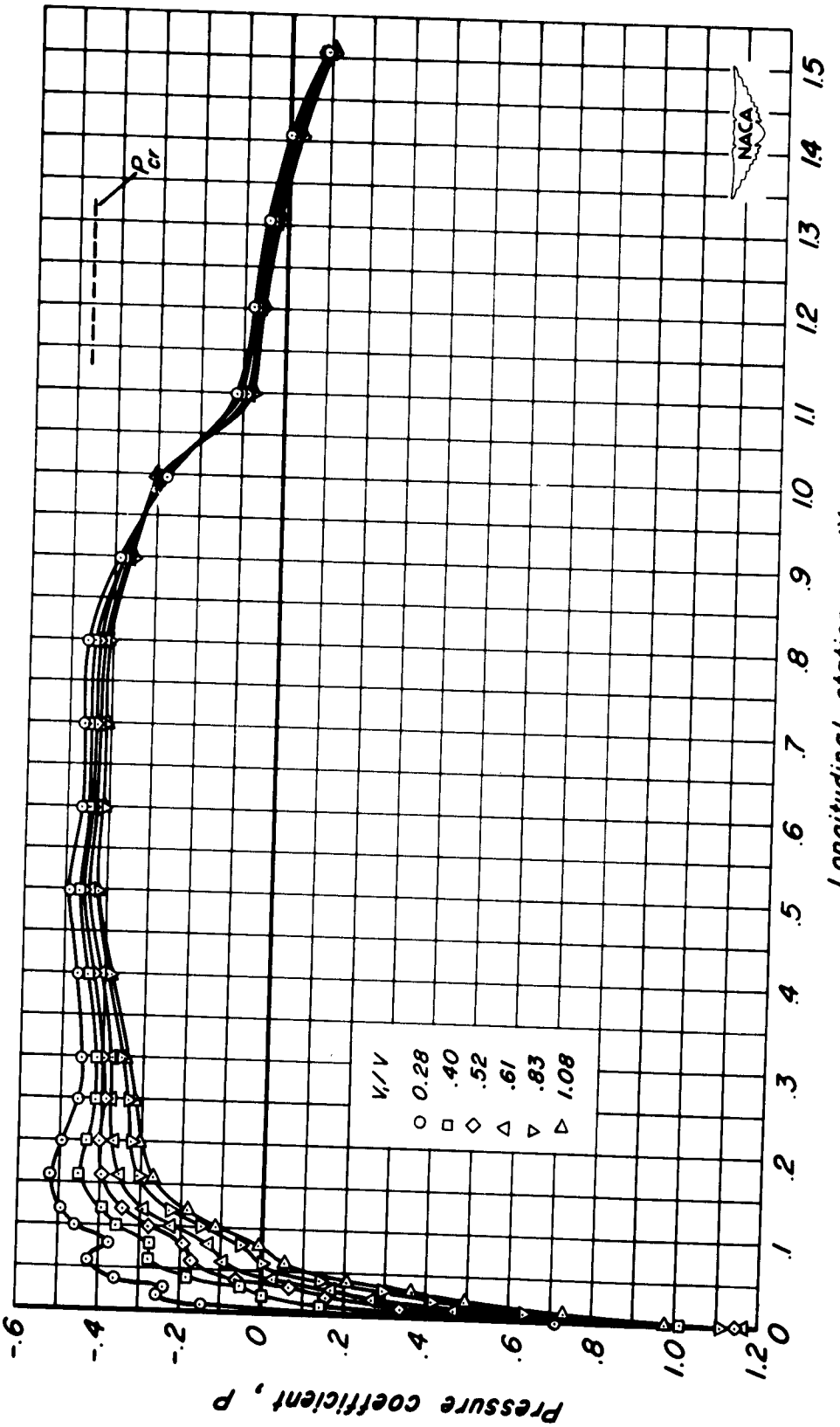

(b) M_d, 0.79

Figure 15.— Continued.

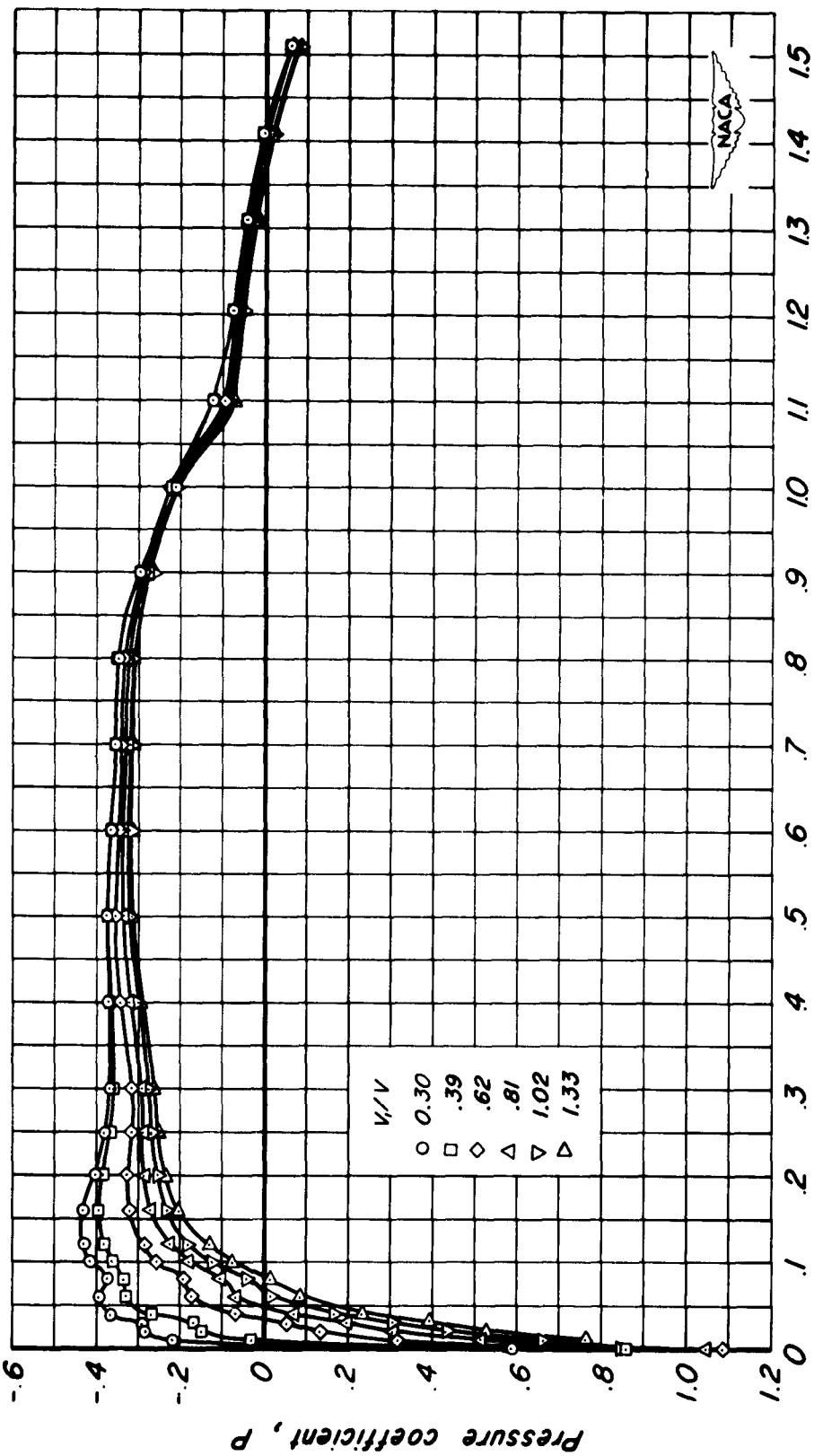

(c) M_d, 0.59

Figure 15.— Continued.

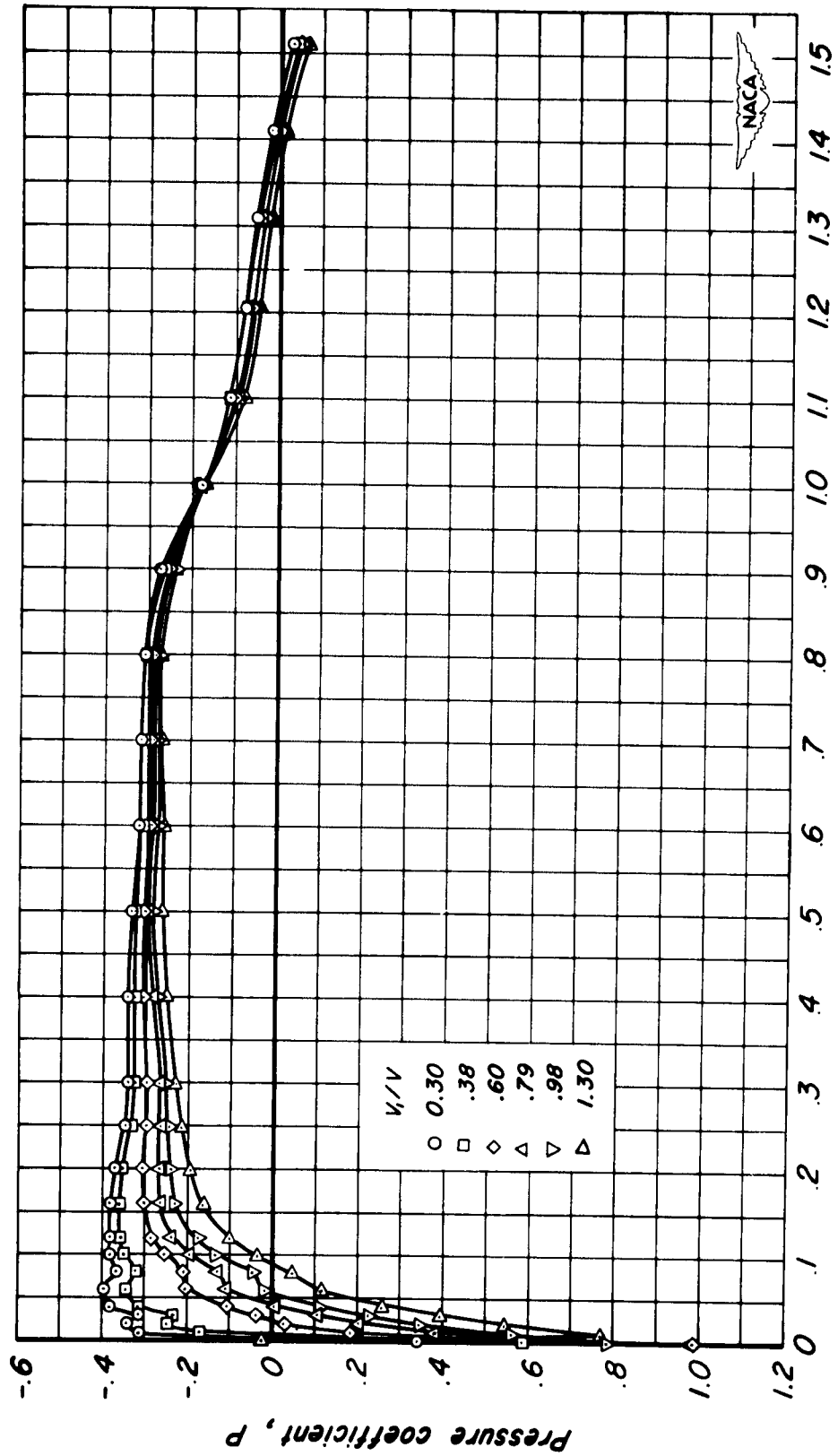

(d) M_d, 0.20

Figure 15.— Concluded.

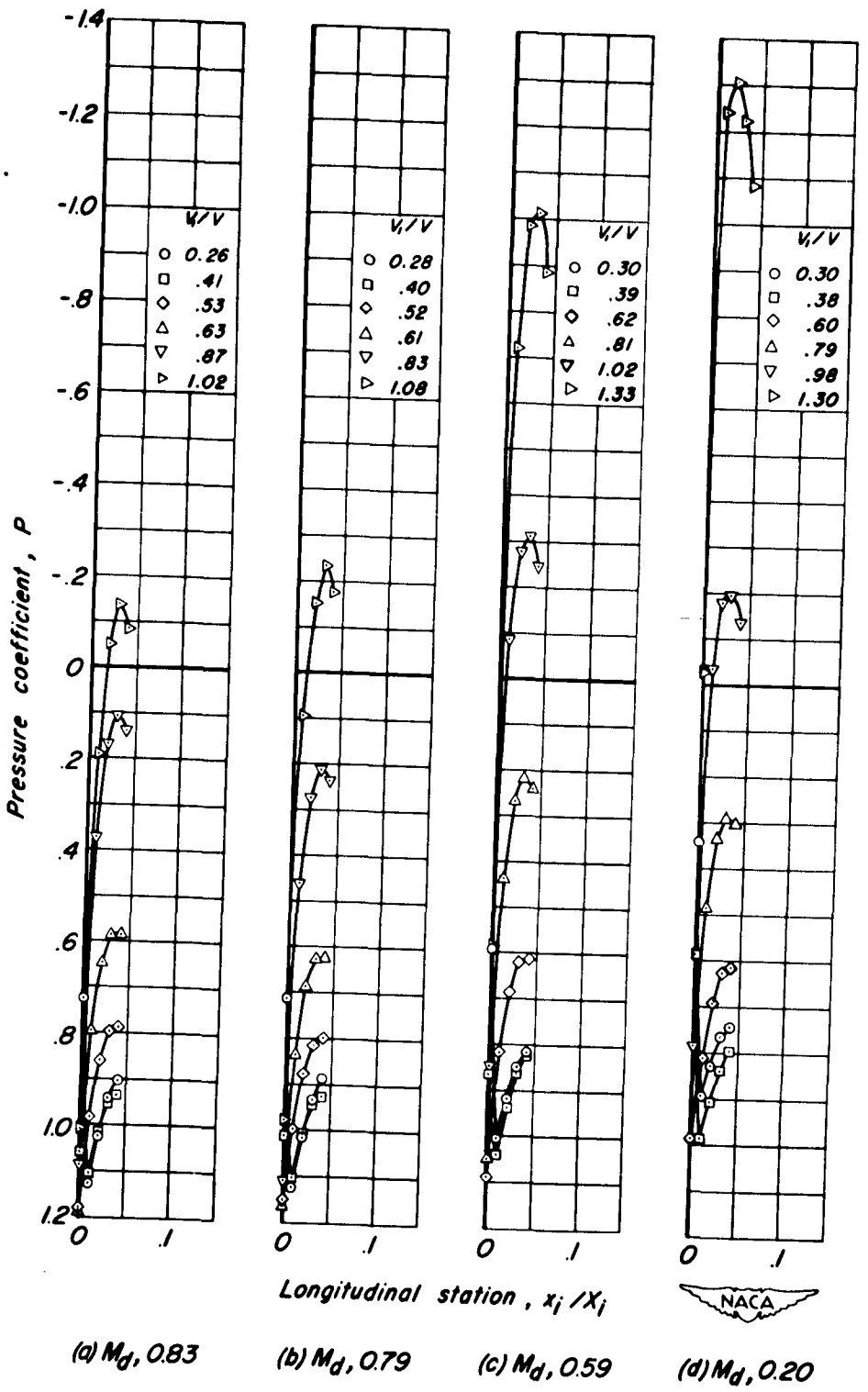

Figure 16.—Typical static-pressure distribution over the inner lip of the NACA 1-62.8-070 cowling, propeller removed.

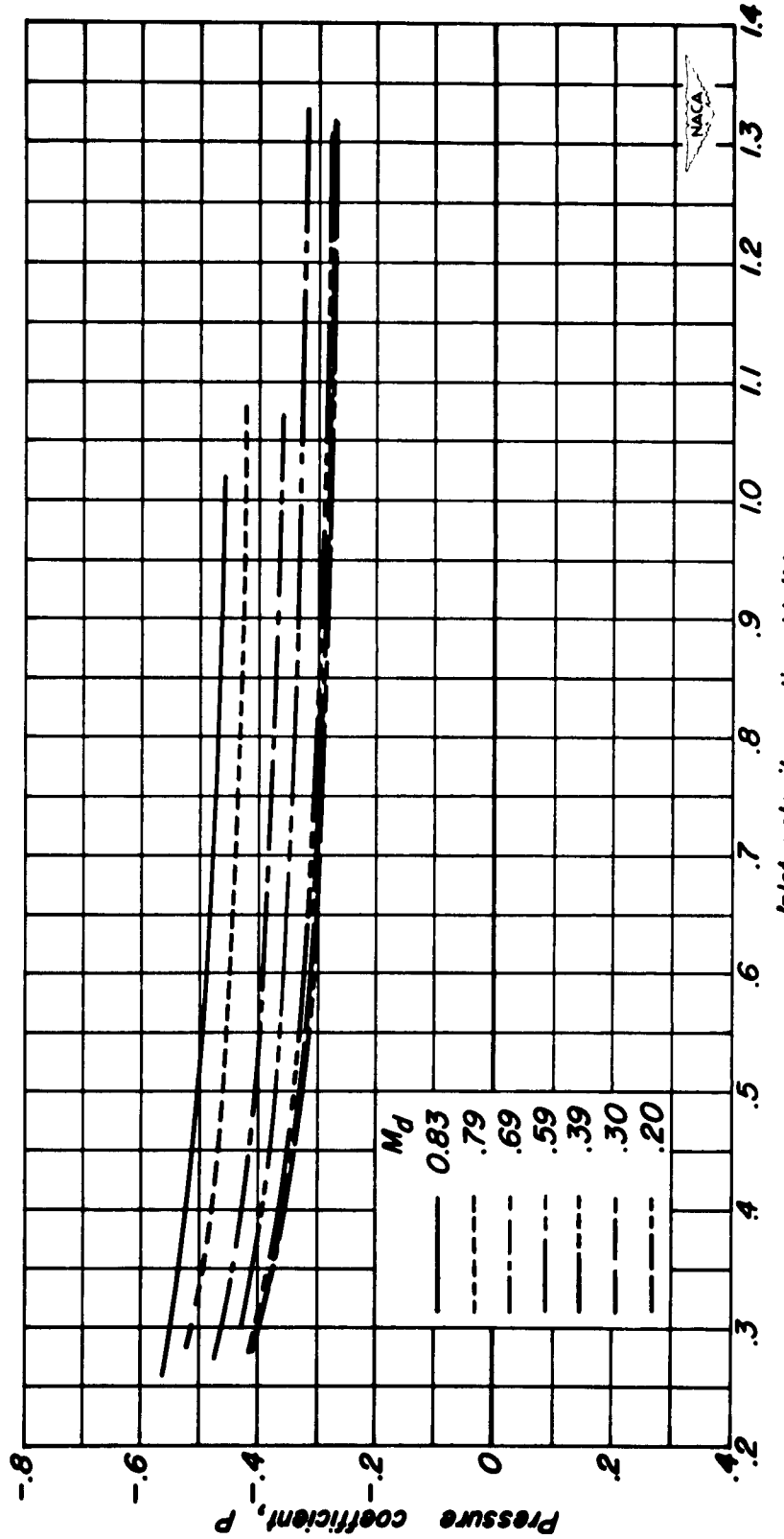

Figure 17.- The effect of inlet-velocity ratio on the minimum pressure coefficient on the external surface of the NACA 1-62.8-070 cowling, propeller removed.

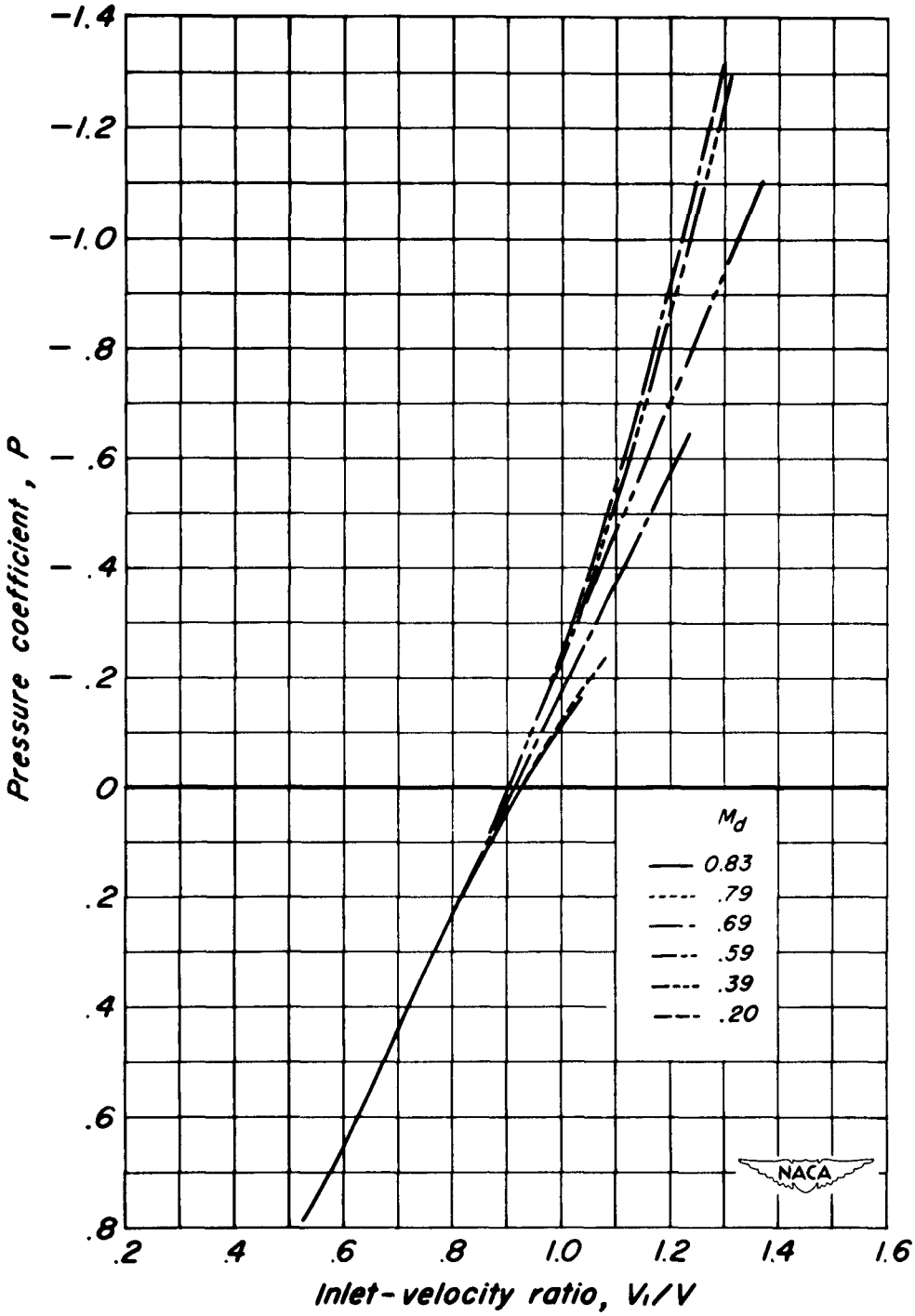

Figure 18.— The effect of inlet-velocity ratio on the minimum pressure coefficient on the inner lip of the NACA 1-62.8-070 cowling, propeller removed.

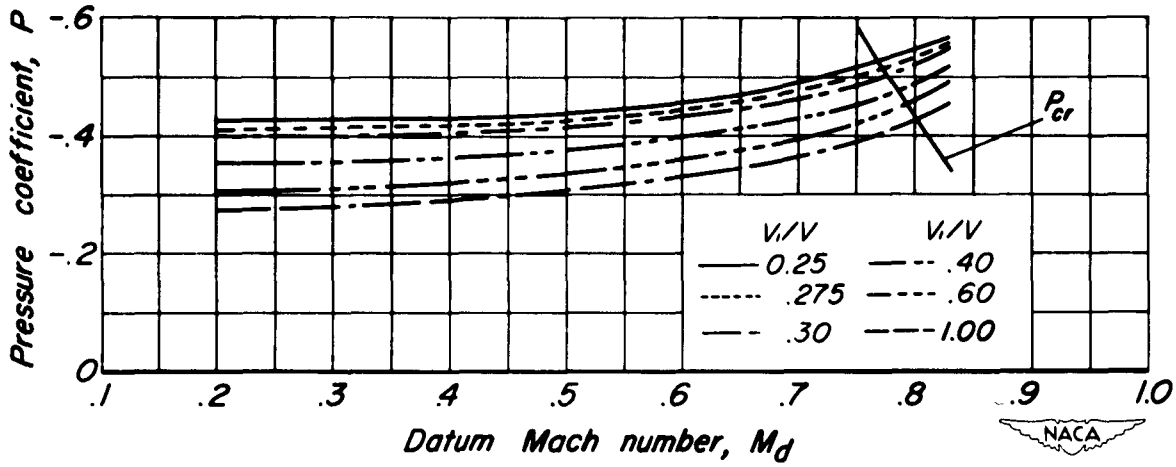

Figure 19.— The effect of Mach number on the minimum pressure coefficient on the external surface of the NACA 1-62.8-070 cowling, propeller removed.

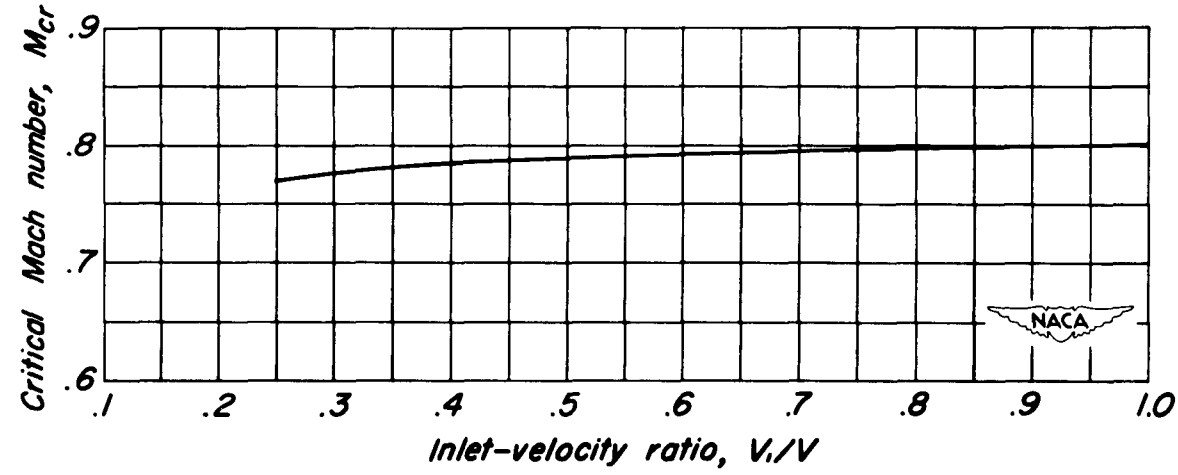

Figure 20.— The effect of inlet-velocity ratio on the critical Mach number for the NACA 1-62.8-070 cowling with the NACA 1-46.5-047 spinner, propeller removed.

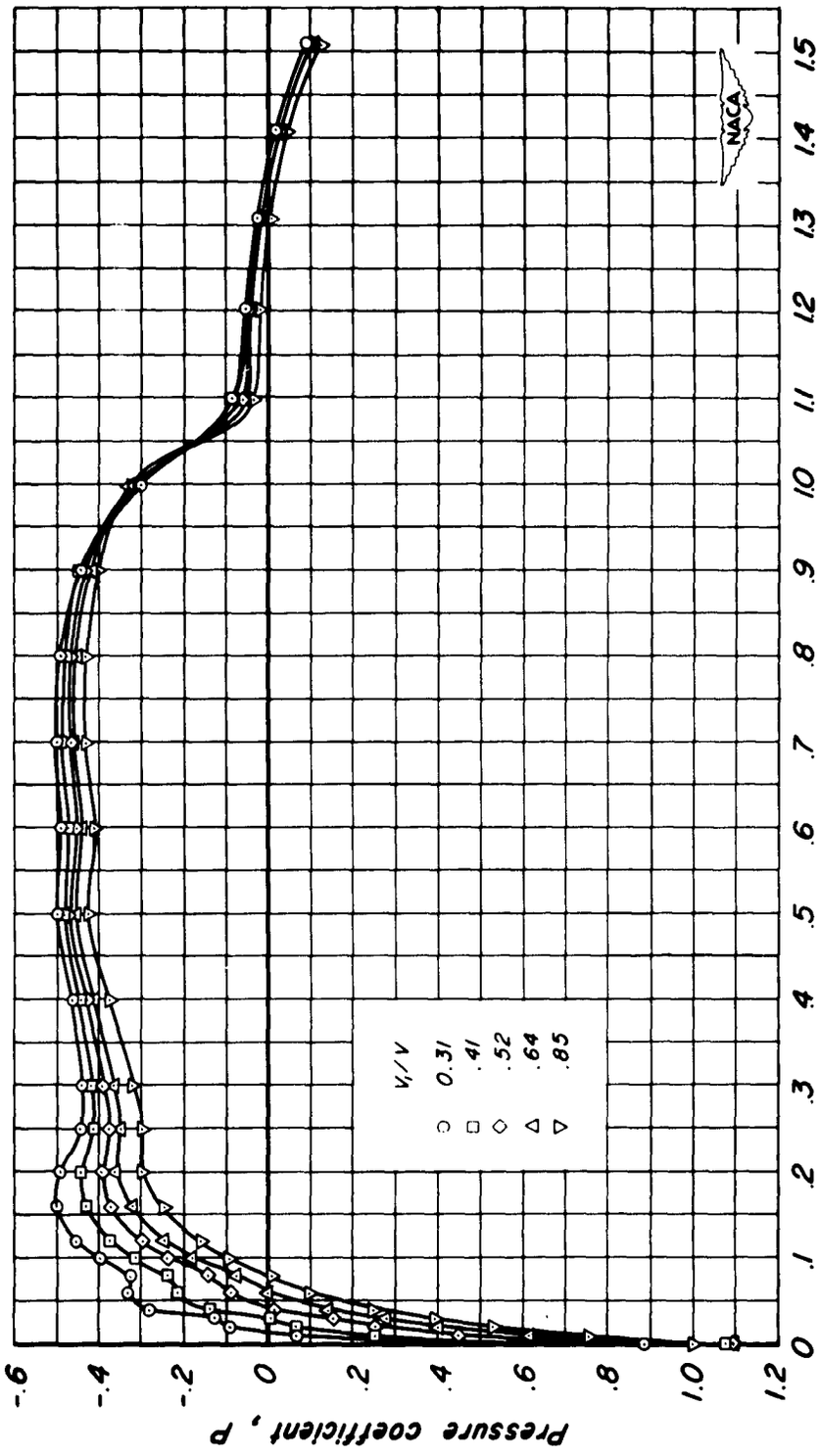

(a) M_d, 0.83; β, 60°; J, 4.10

Figure 21.—Typical static-pressure distribution over the external surface of the NACA 1-62.8-070 cowling with the propeller operating, platform propeller-spinner juncture.

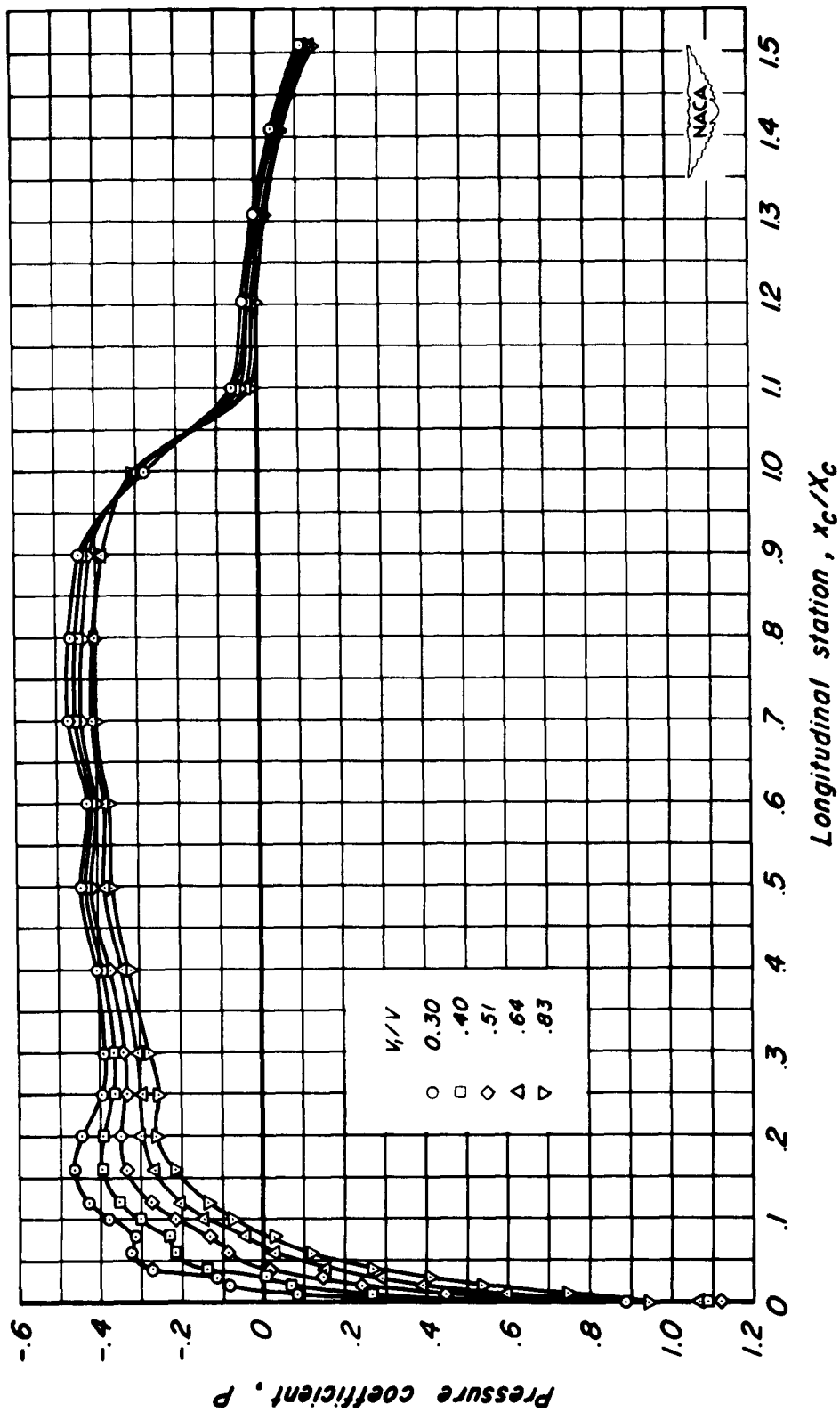

(b) M_d, 0.83; β, 60°; J, 3.20

Figure 21.— Continued.

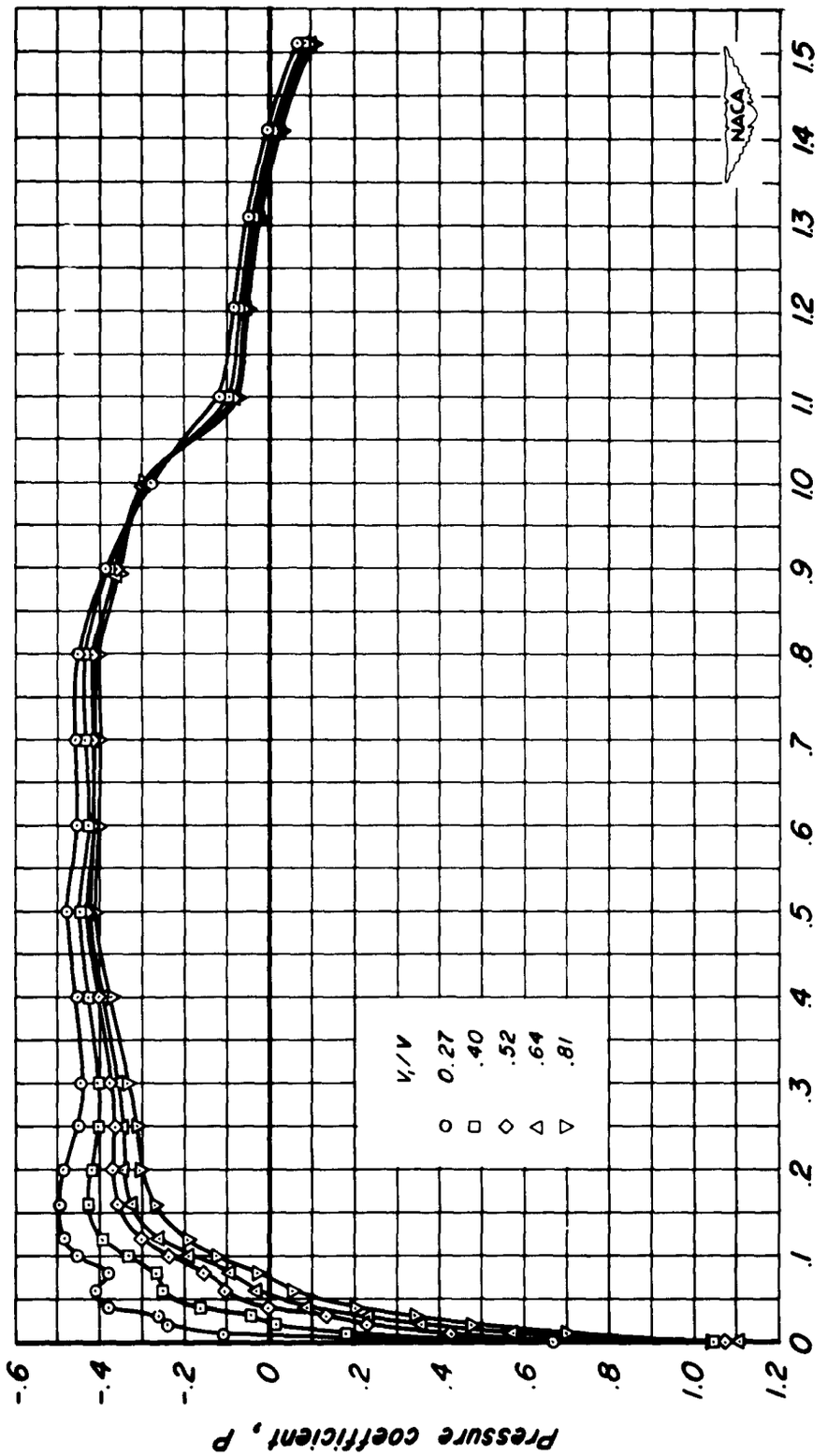

(d M_d, 0.79; β, 60°; J, 4.15

Figure 21.— Continued.

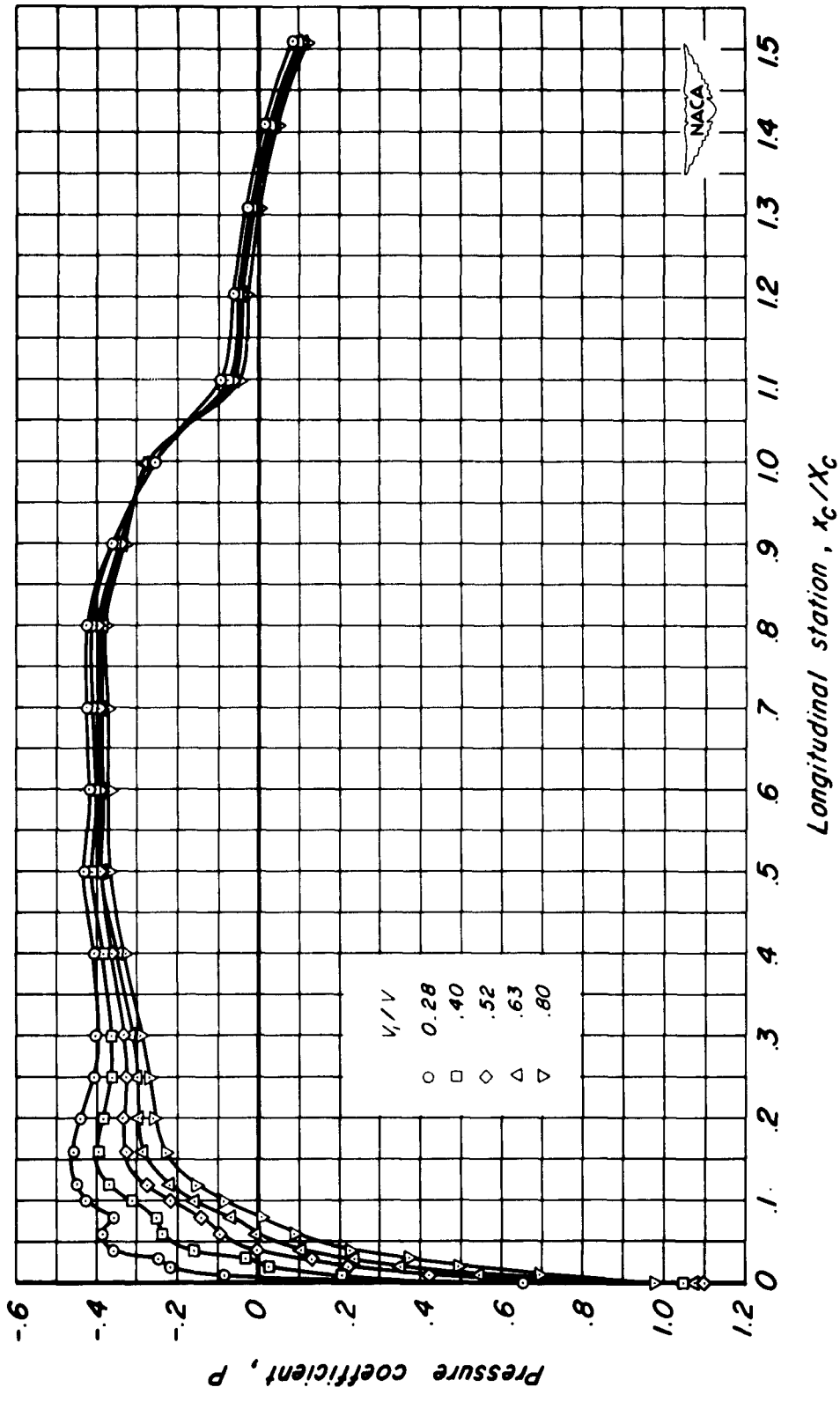

(d) M_d, 0.79; β, 60°; J, 3.20

Figure 21.— Continued.

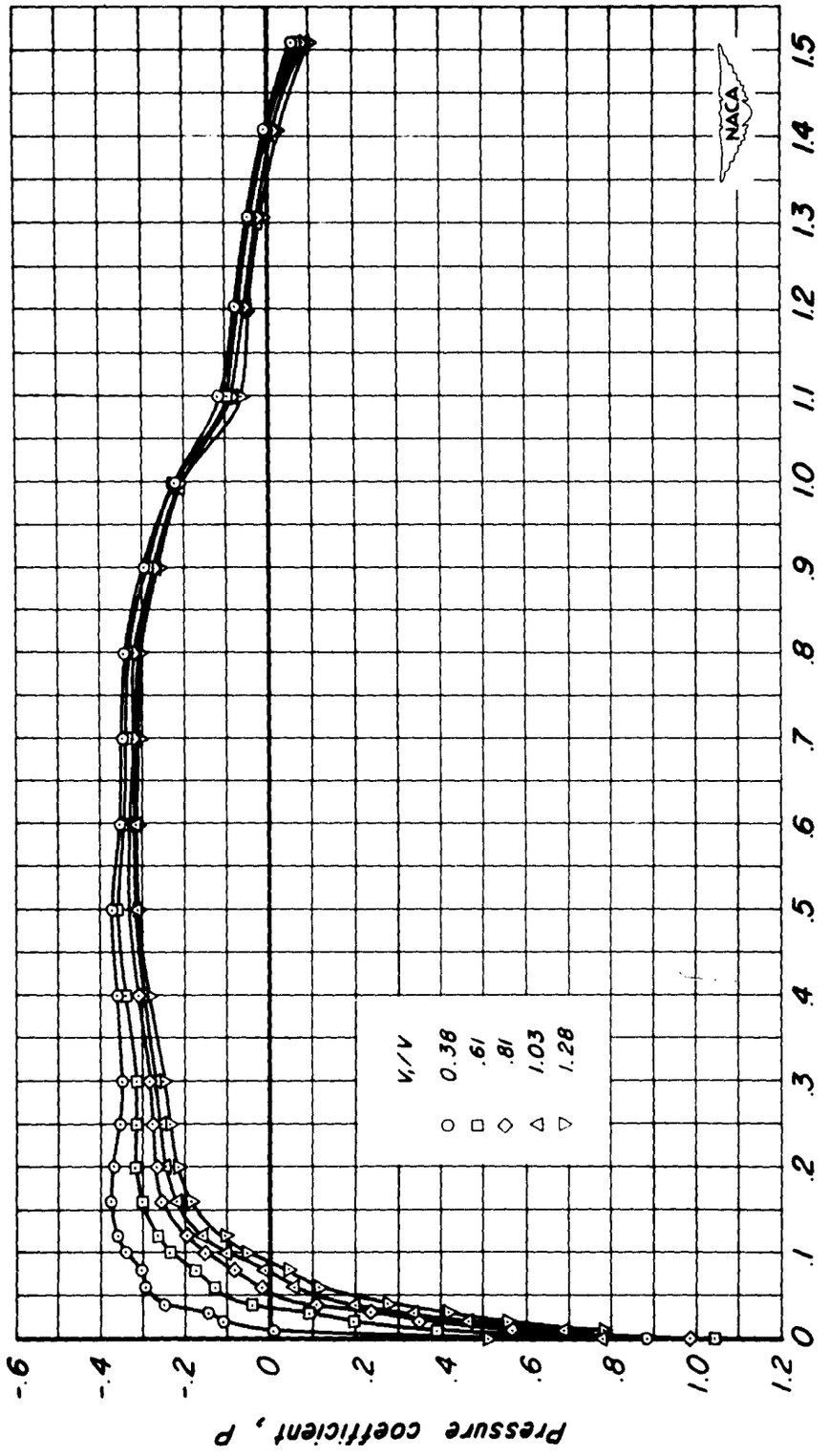

(e) M_d, 0.59; β, 50°; J, 2.90

Figure 21 — Continued.

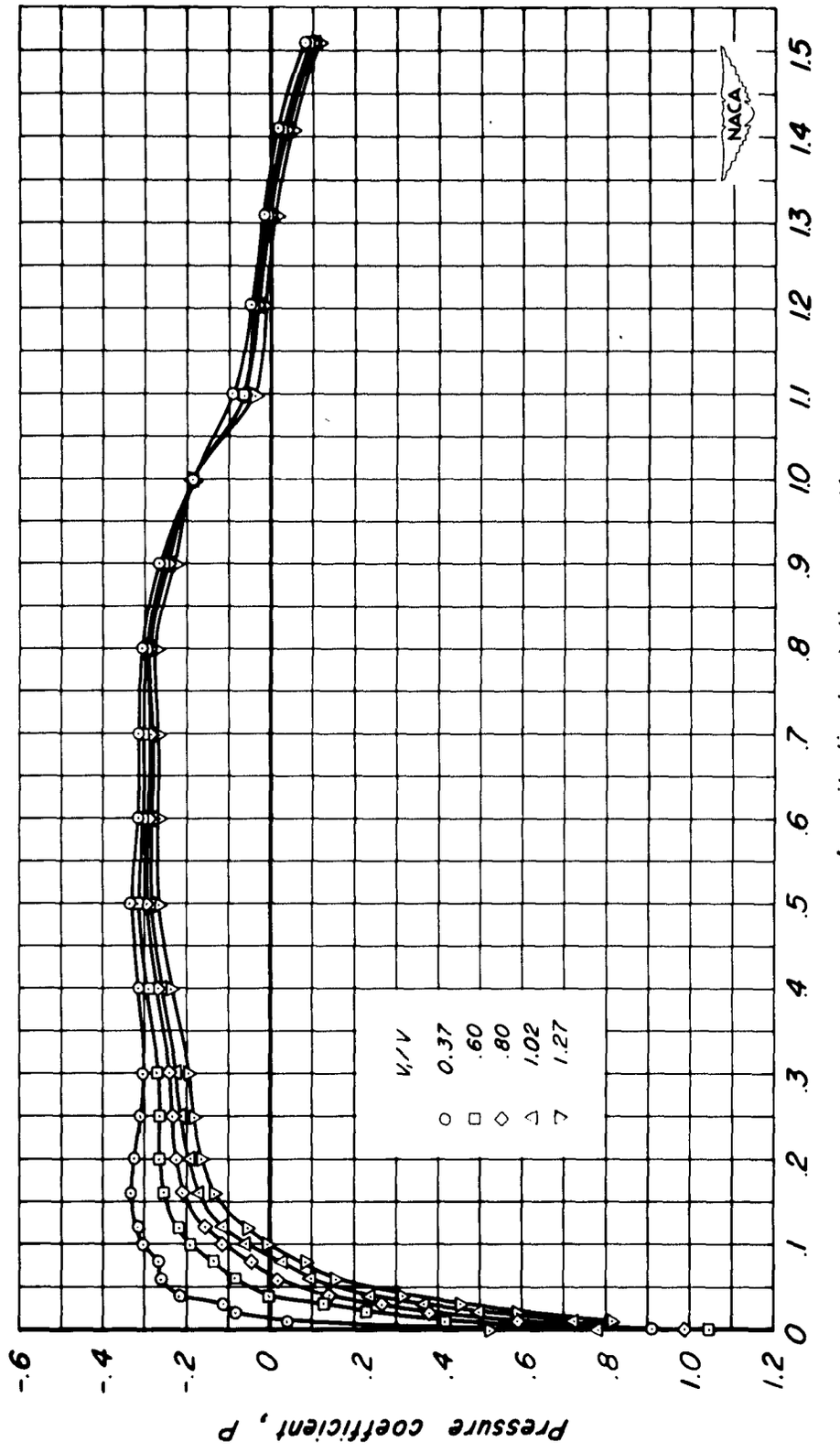

(f) M_d, 0.59; β, 50°; J, 2.45

Figure 21.— Continued.

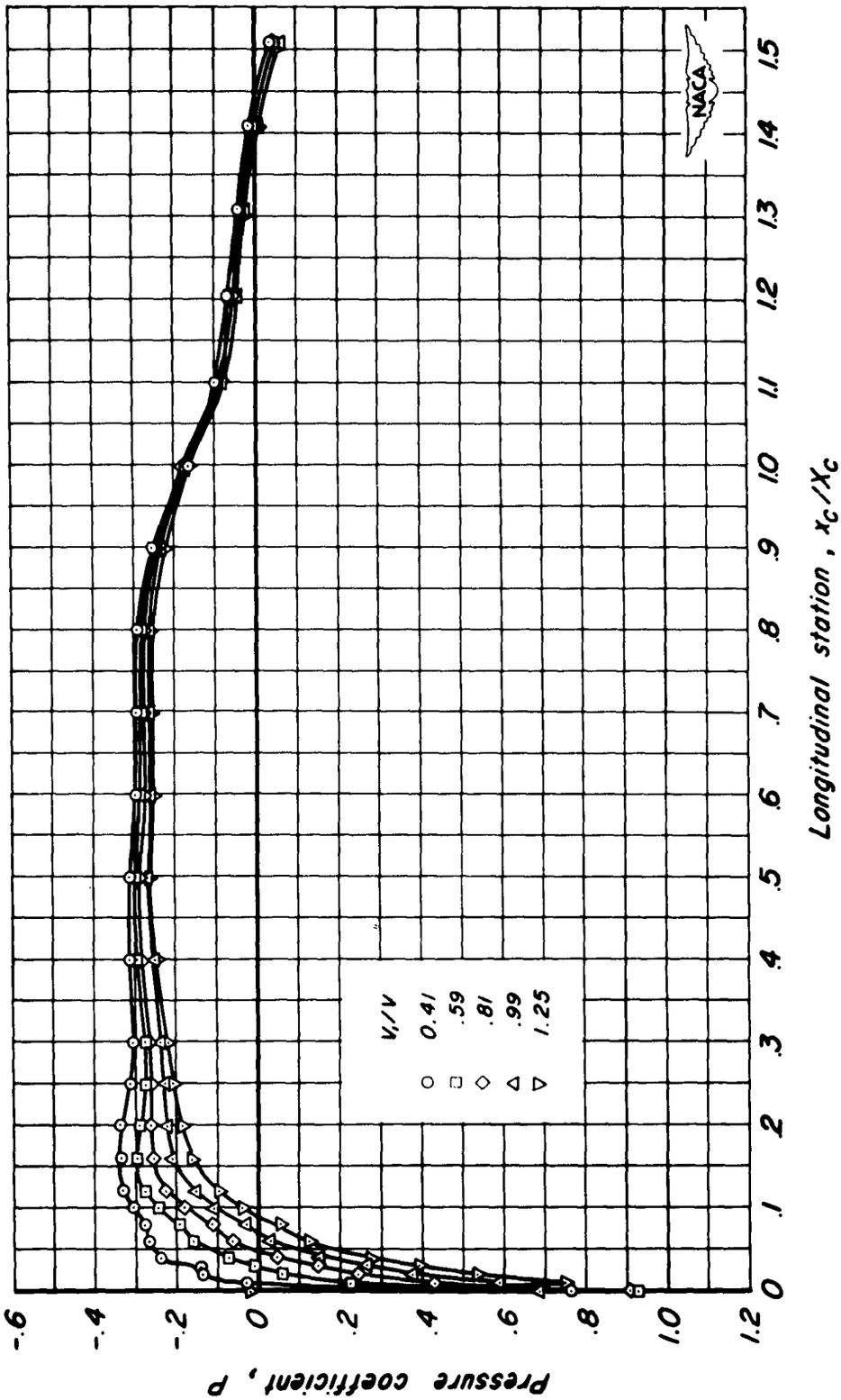

(g) M_d, 0.20; β 40°; J, 2.10

Figure 21.— Continued.

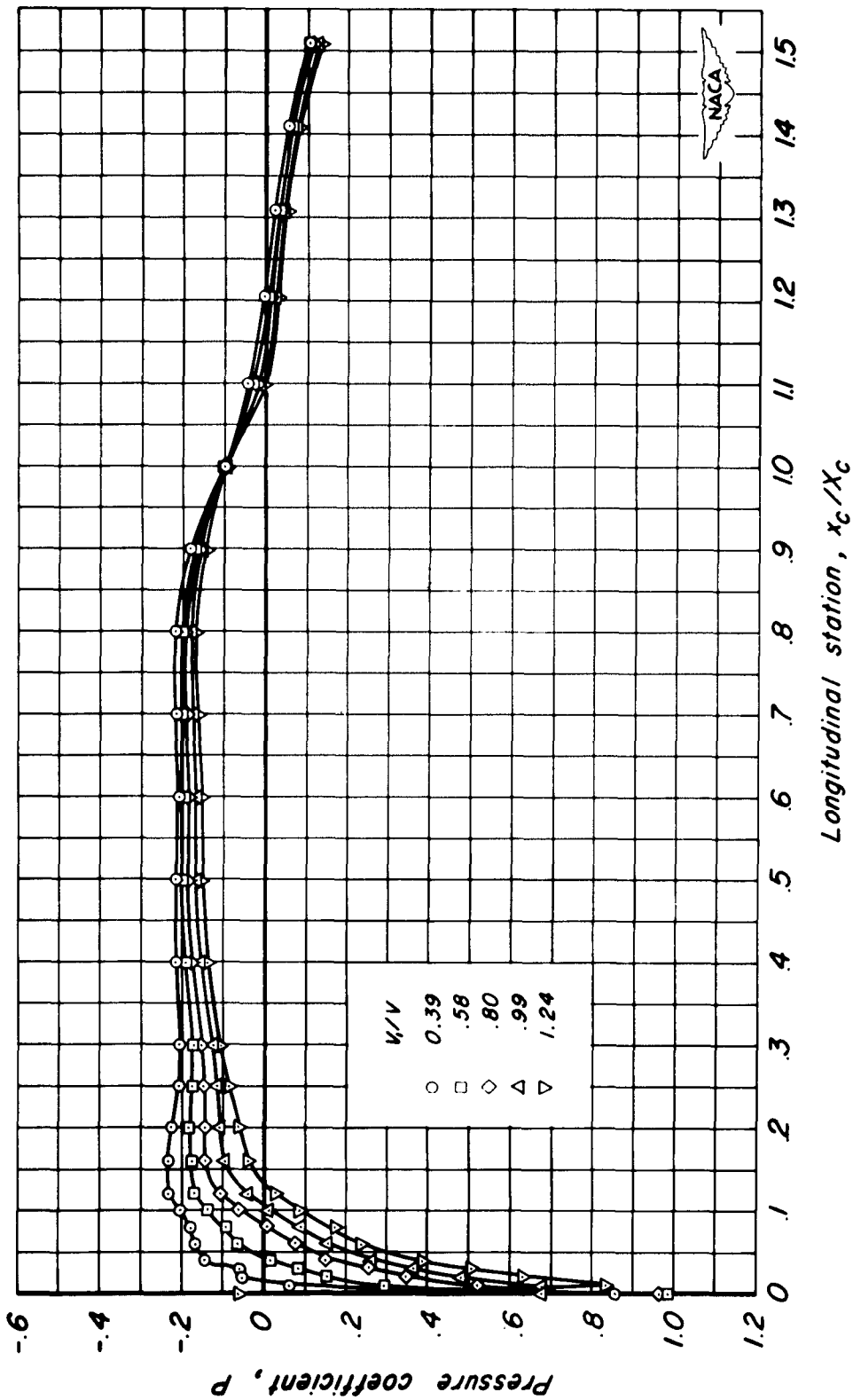

(h) M_d, 0.20; β 40°; J, 1.30

Figure 21.— Concluded.

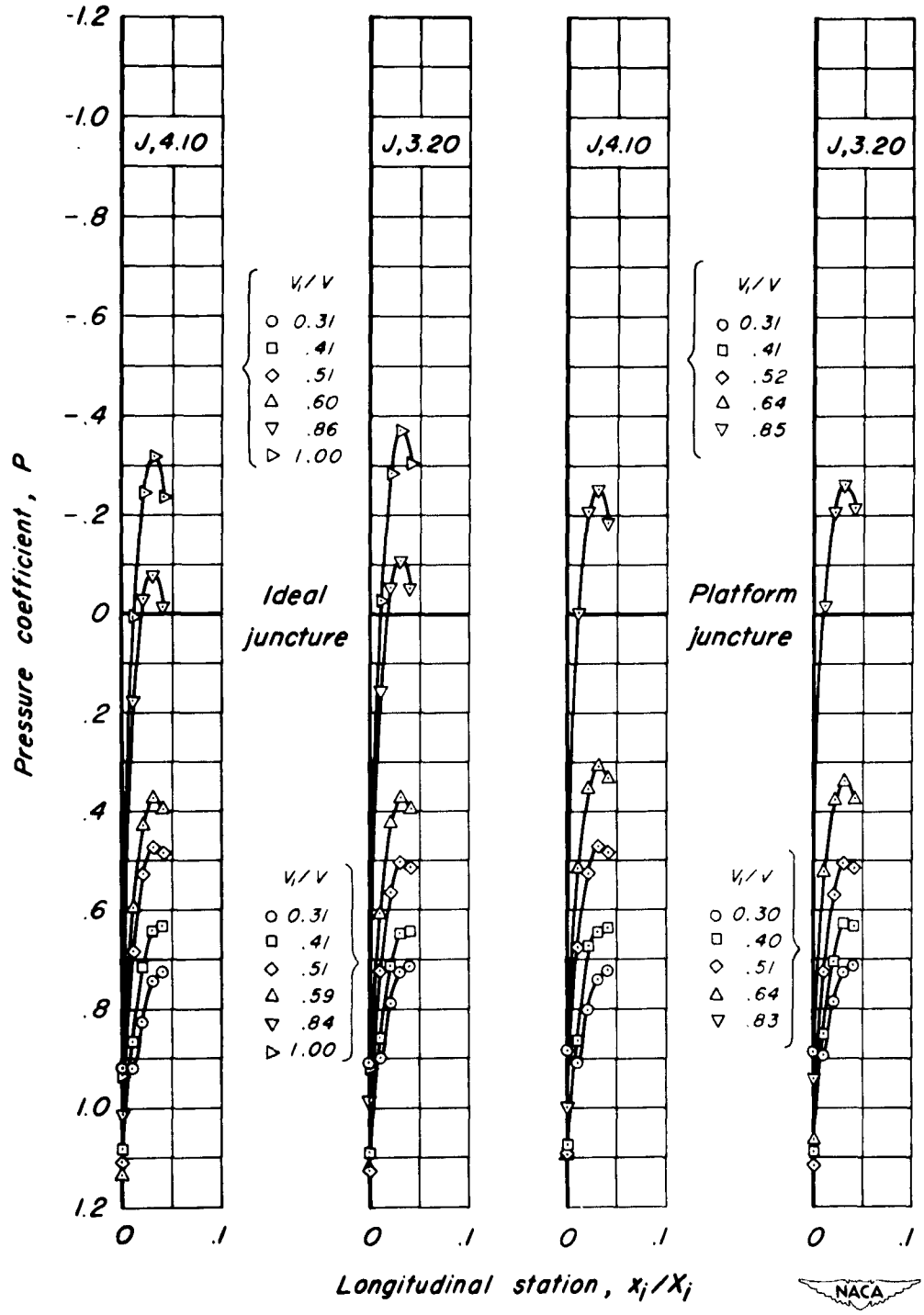

(a) M_d, 0.83; β, 60°

Figure 22 — Typical static-pressure distribution over the inner lip of the NACA 1-62.8-070 cowling with the propeller operating.

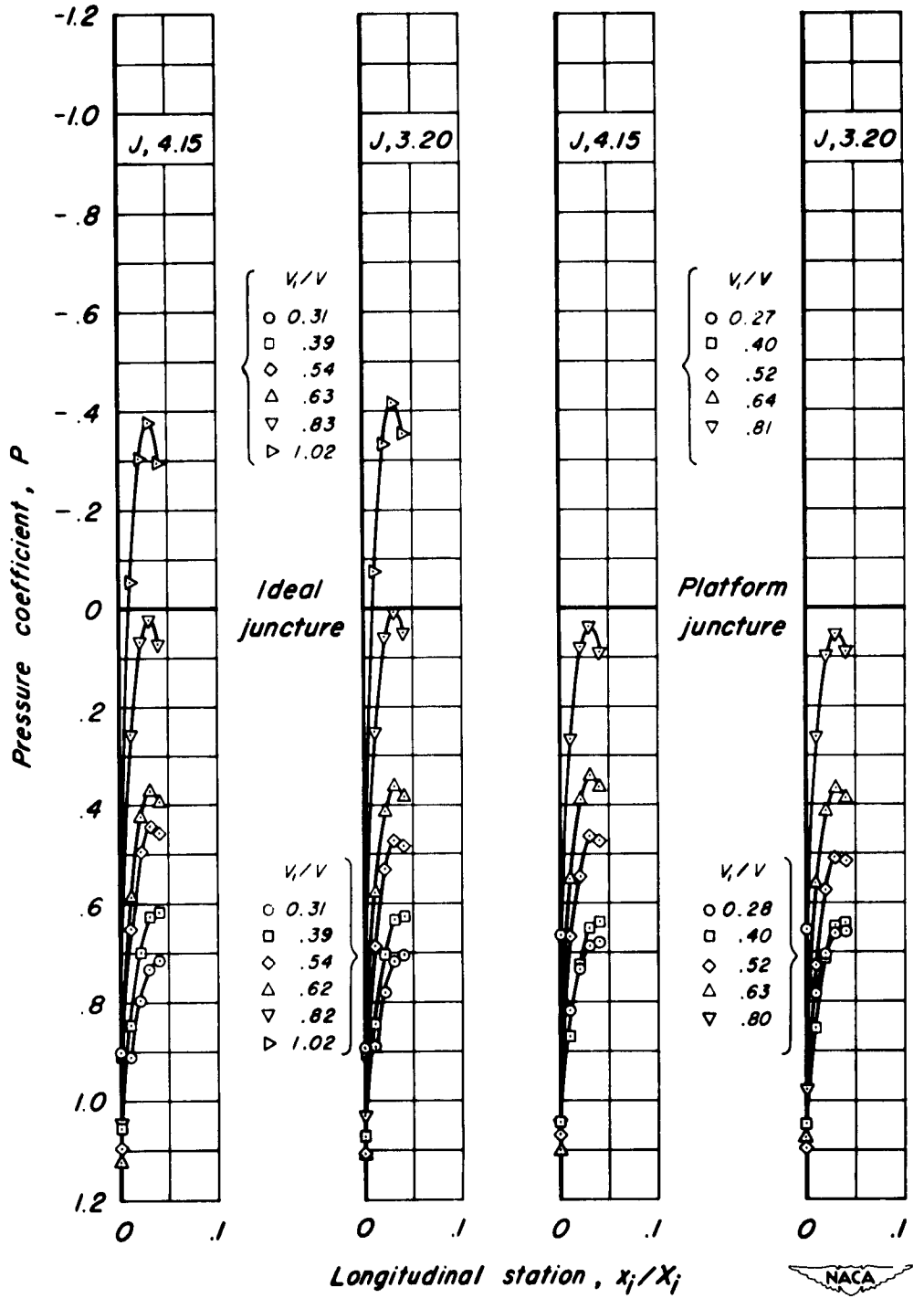

(b) M_d, 0.79; β, 60°

Figure 22.— Continued.

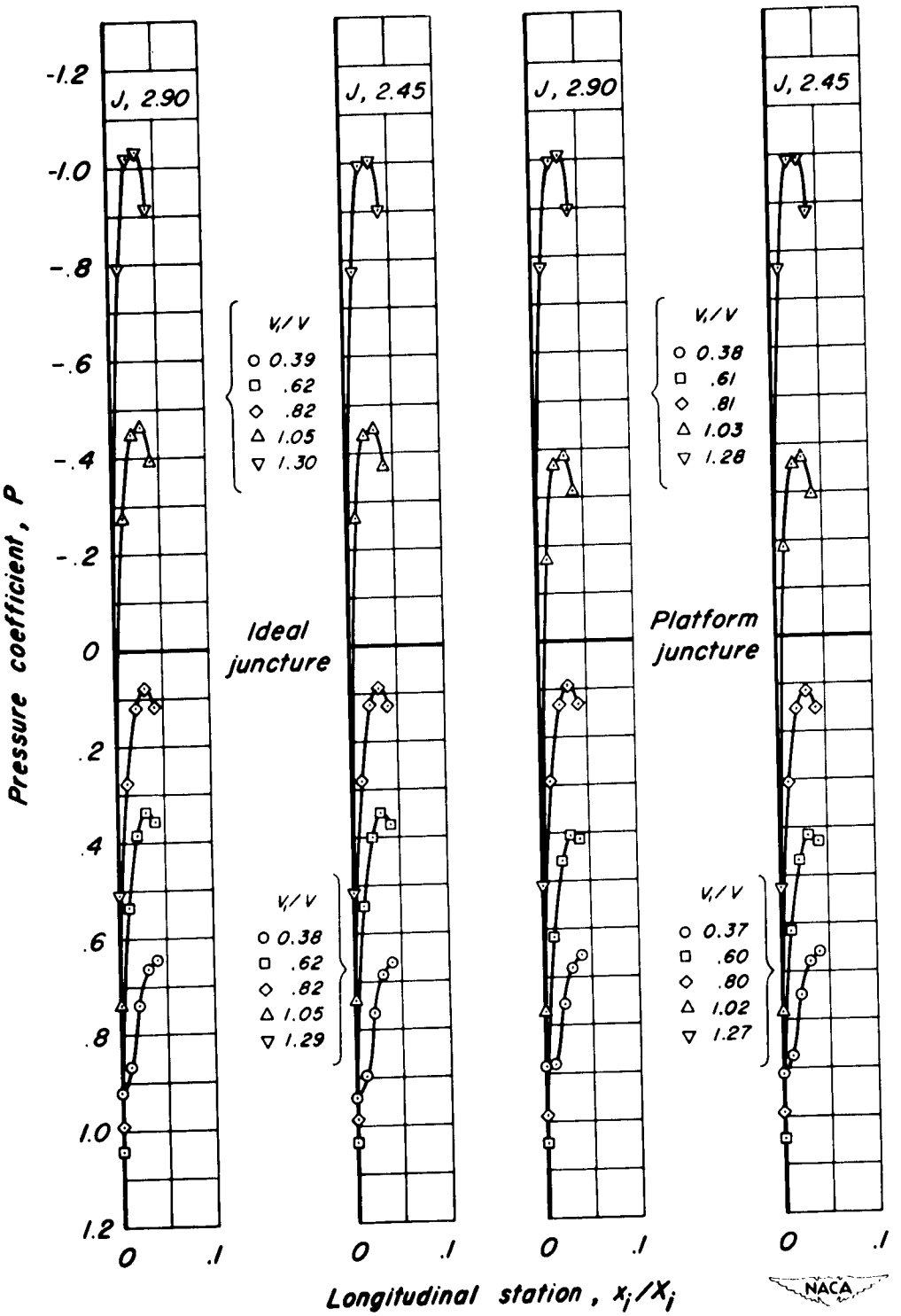

(c) M_d, 0.59; β, 50°

Figure 22.- Continued.

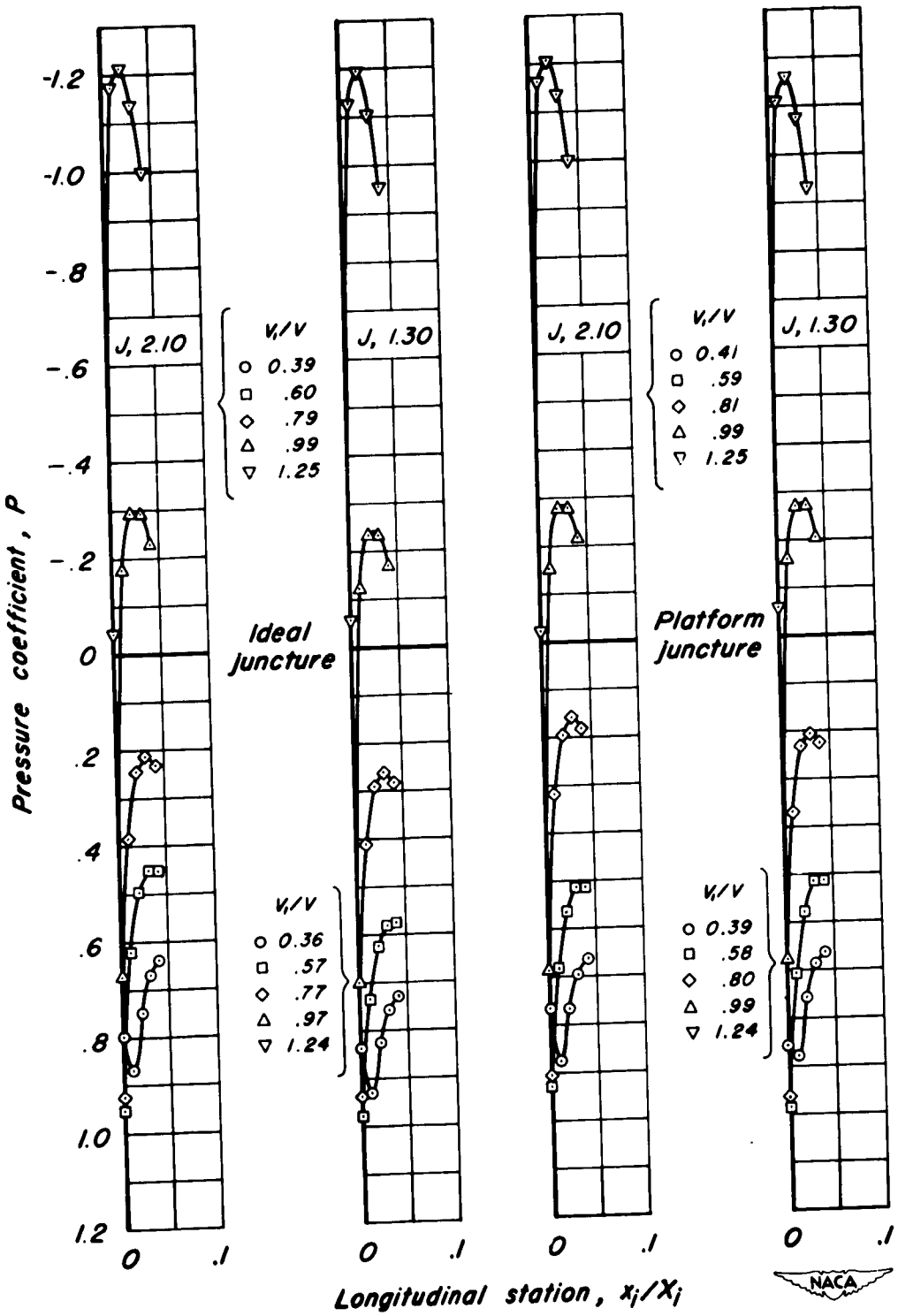

(d) M_d, 0.20; β 40°

Figure 22.— Concluded.

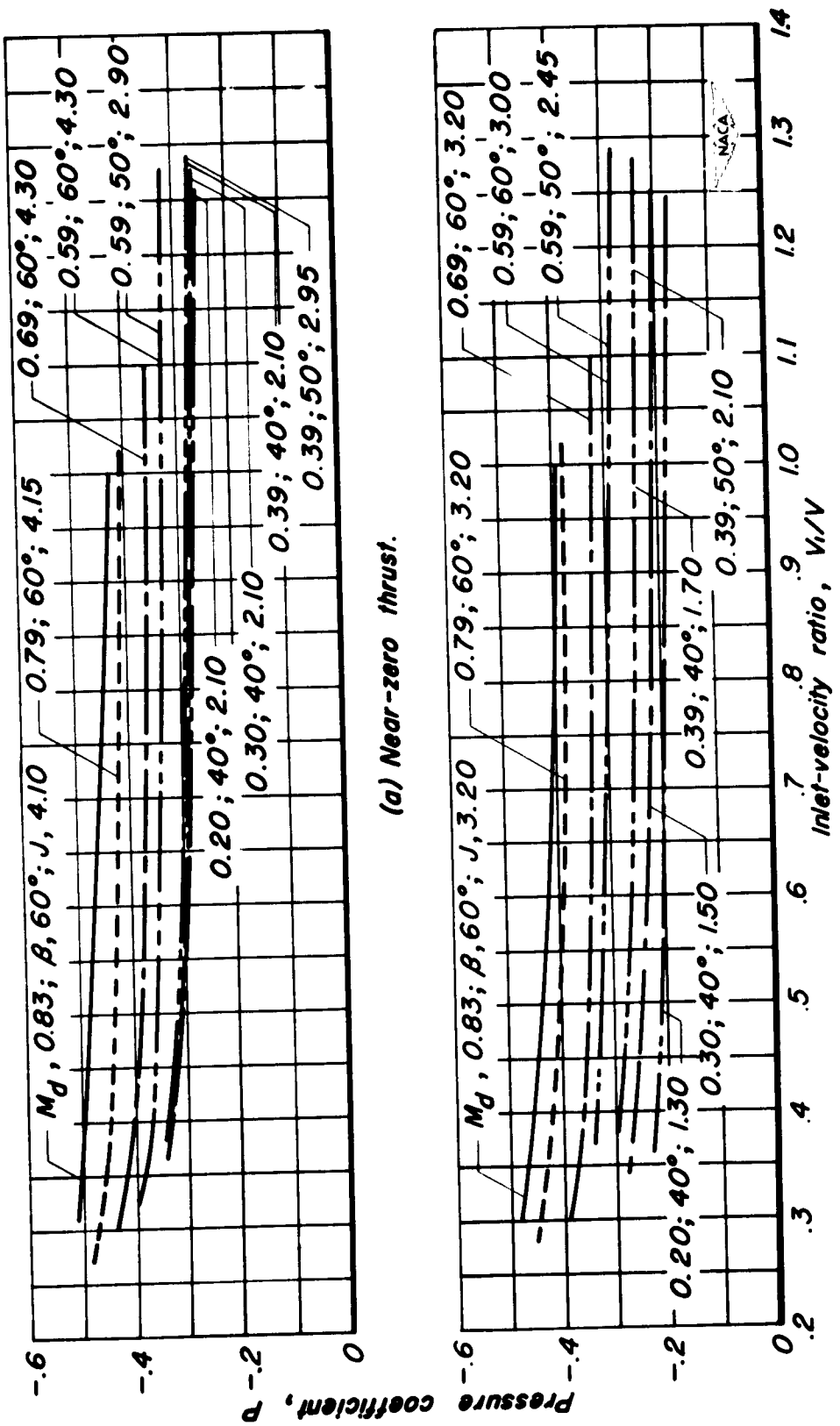

Figure 23.- The effect of inlet-velocity ratio on the minimum pressure coefficient on the external surface of the NACA 1-62.8-070 cowling with the propeller operating, ideal juncture.

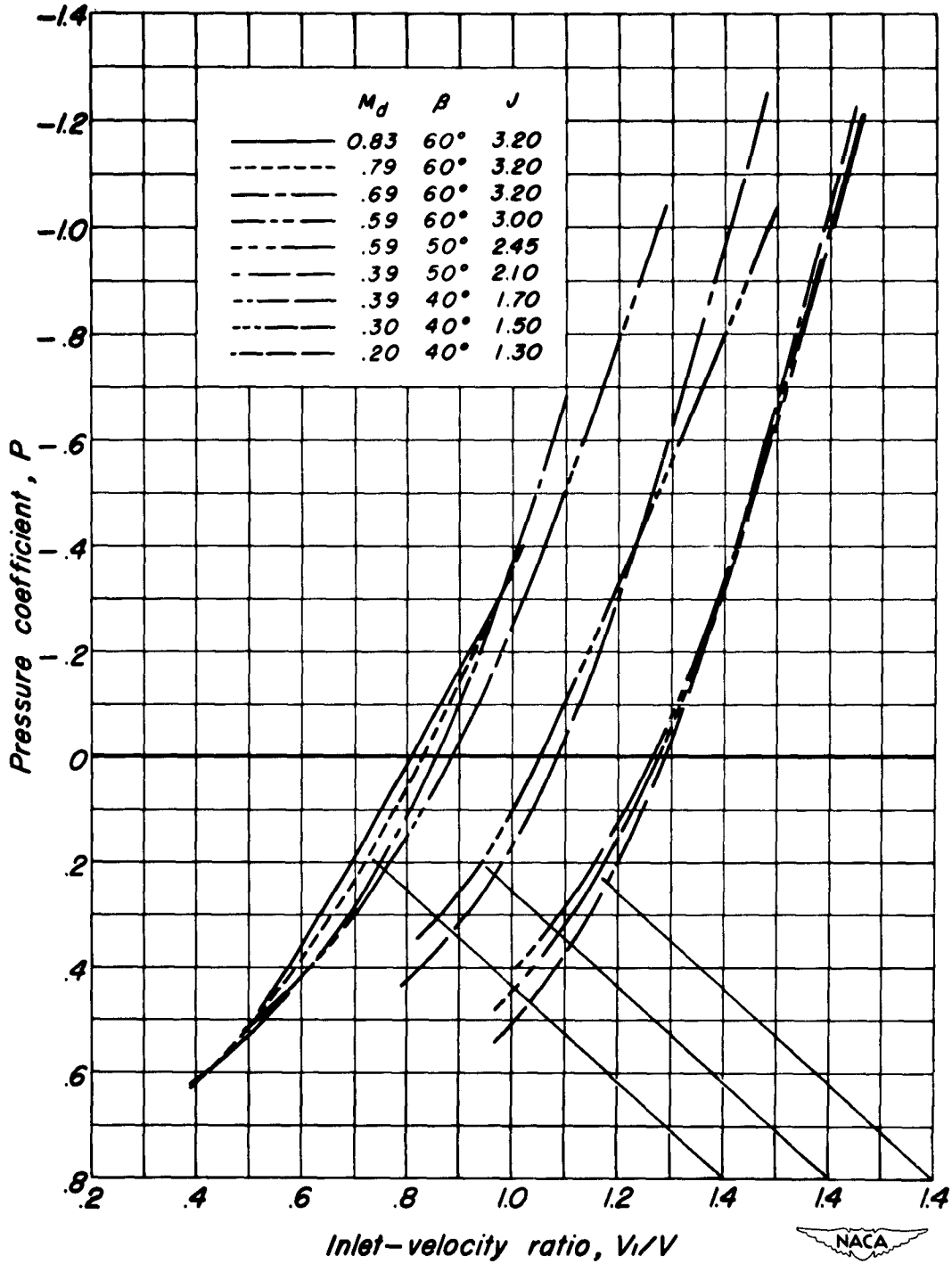

(a) Ideal juncture.

Figure 24.- The effect of inlet-velocity ratio on the minimum pressure coefficient on the inner lip of the NACA 1-62.8-070 cowling with the propeller operating.

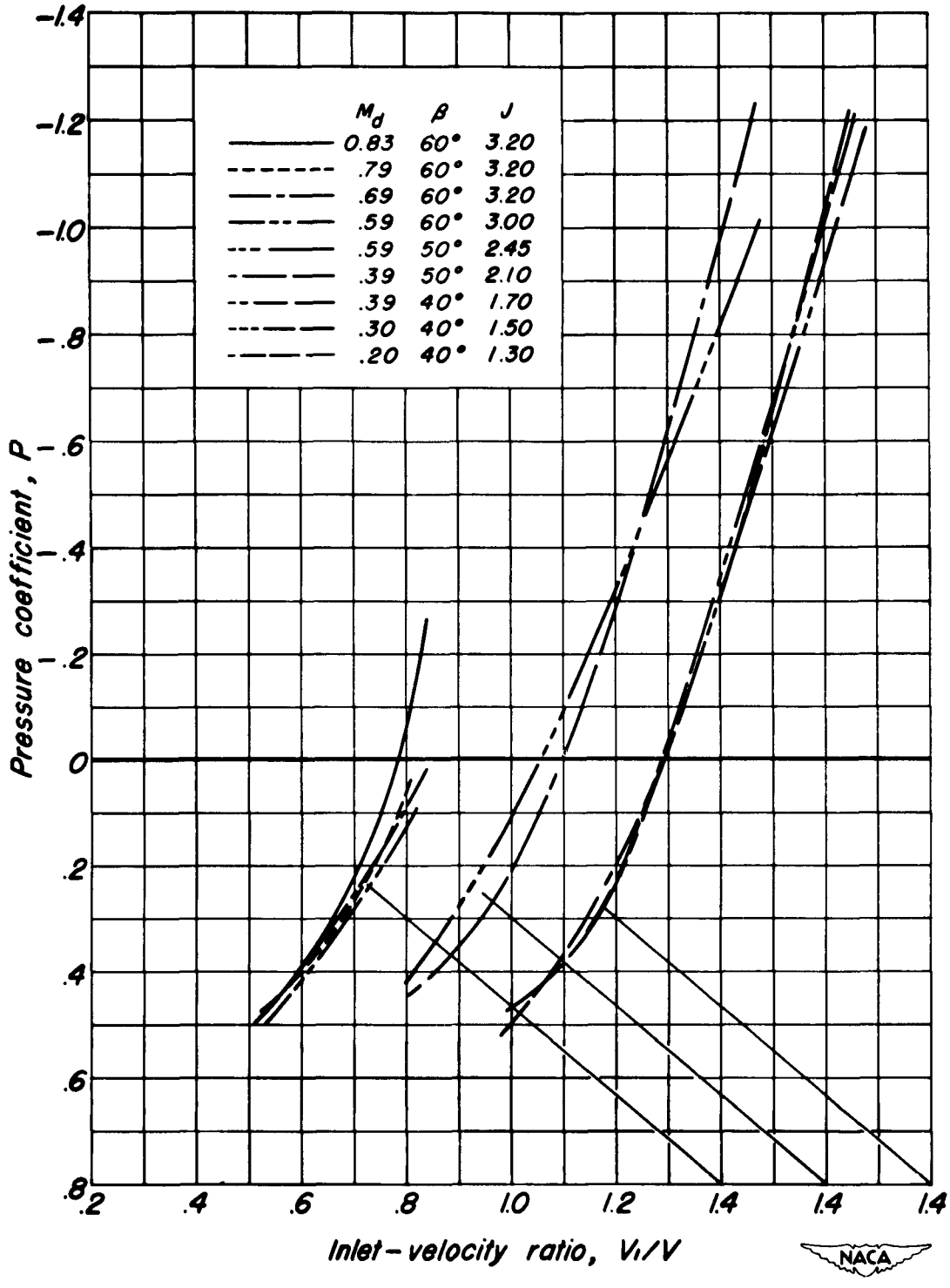

(b) Platform juncture.

Figure 24.- Concluded.

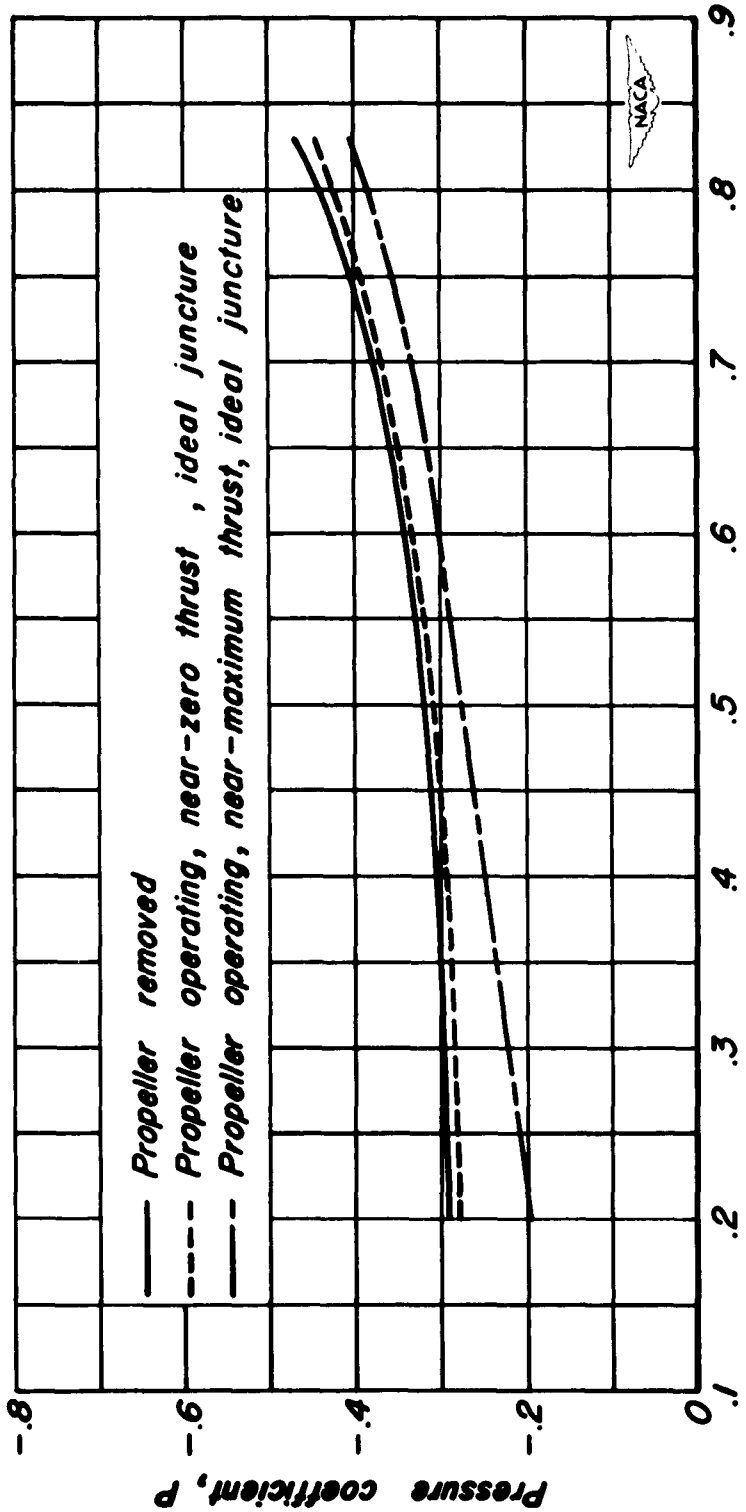

Figure 25.- The effect of Mach number on the minimum pressure coefficient on the external surface of the NACA 1-62.8-070 cowling. V_j/V, 0.8.

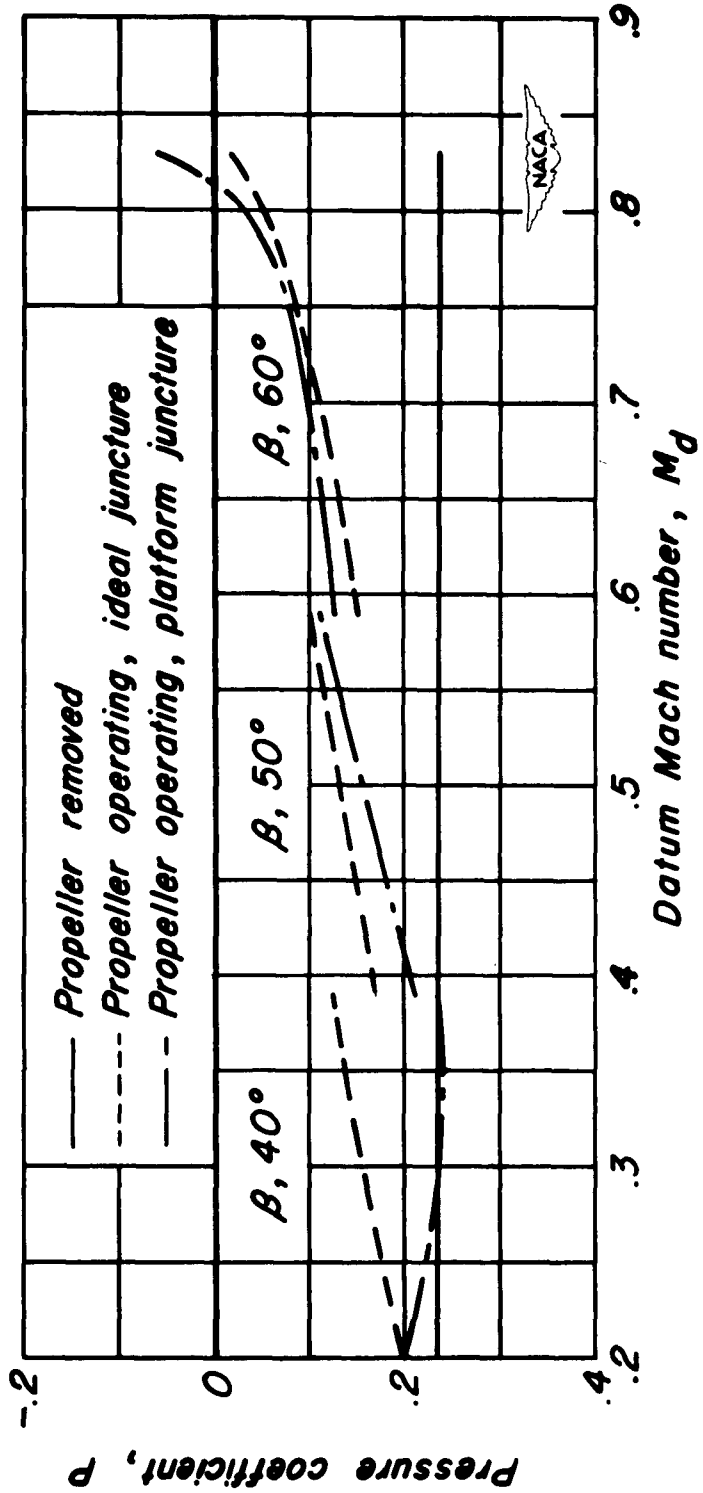

Figure 26.— Effect of Mach number on the minimum pressure coefficient on the inner lip of the NACA 1-62.8-070 cowling. V_i/V , 0.80.

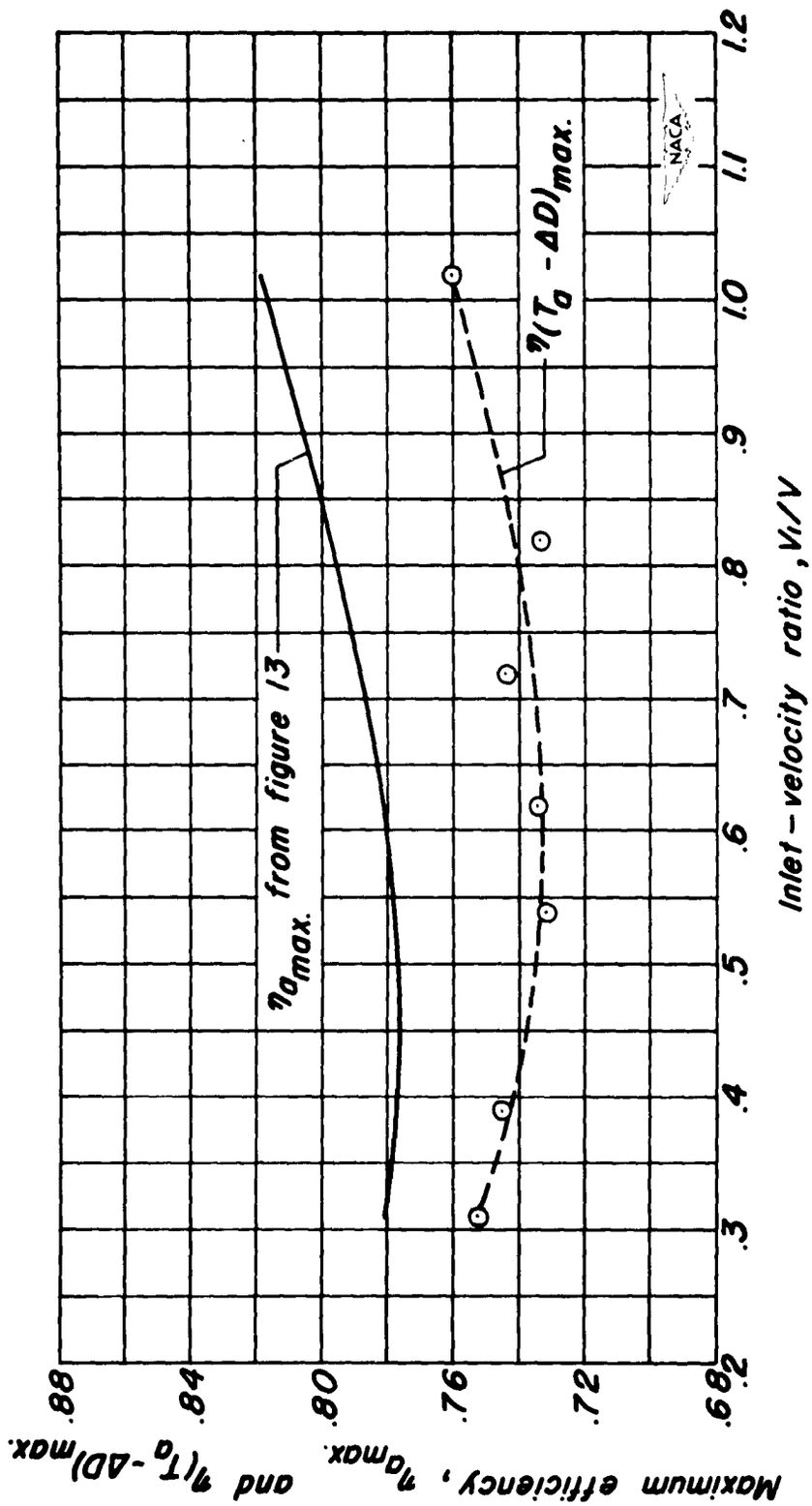

Figure 27.— Comparison of the efficiency of the propeller based on the apparent thrust and the efficiency based on the difference between the apparent thrust and the increase in pressure drag of the cowling due to operation of the propeller. M_d, 0.79; β, 60°; ideal juncture.

NACA-Langley - 4-13-53 - 325